UNIVERSITY OF CALIFORNIA

Los Angeles

Dynamics of sugar/H^+ symport proteins of the major facilitator superfamily

A thesis submitted in partial satisfaction

of the requirements for the degree Doctor of Philosophy

in Molecular, Cellular and Integrative Physiology

by

Junichi Sugihara

2016

ABSTRACT OF THE DISSERTATION

Dynamics of sugar/H^+ symport proteins of the major facilitator superfamily

by

Junichi Sugihara

Doctor of Philosophy

in Molecular, Cellular and Integrative Physiology

University of California, Los Angeles, 2016

Professor Howard R. Kaback, Chair

A variety of integral membrane proteins have evolved to transport biologically important molecules across phospholipid membranes, and a majority of membrane proteins encoded in the human genome is transporters. The major facilitator superfamily (MFS) is arguably the largest group of secondary active transporters present in the kingdoms of life, yet only three X-ray crystal structures have been obtained for human members of the superfamily. Thus, many inferred structures of eukaryotic transporters have been derived from homology modeling using prokaryotic transporters with known structures, and studies on prokaryotic transporters have become exceedingly important. Furthermore, current structural information is insufficient to achieve a comprehensive understanding of the

dynamics of these proteins, and application of biochemical and biophysical methods is vital for understanding of their mechanisms of action.

This thesis focuses on investigating dynamics of various MFS transporters, mainly L-fucose/H^+ and sucrose/H^+ symporters of *Escherichia coli* (FucP and CscB, respectively). FucP is a MFS transporter that catalyzes cotransport of L-fucose and H^+ across the cytoplasmic membrane. Although its crystal structure in an outward (periplasmic)-open conformation has been reported, nothing is known about its conformational dynamics. In addition, CscB, another MFS member, catalyzes sucrose/H^+ symport across the cytoplasmic membrane. The structural organization of key residues involved in sugar binding in CscB appears to be similar to that of the lactose permease of *E. coli* (LacY), arguably the best studied MFS member, which is highly specific for galactopyranosides. However, the determinants for sugar specificity in CscB, as well as structural dynamics, are unclear.

Conformational changes induced by sugar binding in FucP and CscB are analyzed by monitoring the fluorescence of Trp residues located on the walls of hydrophilic cavities in both symporters. The unique location of Trp residues provides a novel method for studying structural dynamics of membrane proteins purified in detergent. Also, the dynamics of FucP embedded in the native bacterial membrane is analyzed by examining site-directed alkylation of Cys-replacement mutants with the fluorescent alkylating agent, tetramethylrhodamine-5-maleimide. This method reveals sugar-induced changes in reactivity/accessibility of Cys replacements at given positions.

The dissertation of Junichi Sugihara is approved.

Hui Sun

Pascal Francois Egea

George Sachs

Ernest M. Wright

Howard R. Kaback, Committee Chair

University of California, Los Angeles

2016

Table of Contents

Acknowledgements

I would like to express my deepest appreciation to my advisor Dr. H. Ronald Kaback, who continually and convincingly conveyed a spirit of adventure in regard to research, and an excitement in regard to teaching. This dissertation would not have been possible without his guidance and unflagging support.

I would also like to thank my doctoral committee members, Dr. Ernest Wright, Dr. George Sachs, Dr. Hui Sun, and Dr. Pascal Egea, for their generous comments and warm encouragement.

In addition, I am deeply grateful to Dr. Vladimir Kasho and Dr. Irina Smirnova for the long discussions that helped me sort out myriad technical details of my work. They have always been there to listen and give advice.

I would also like to acknowledge Dr. Nieng Yan, Linfeng Sun and Meng Ke for lively discussions on related topics that helped me improve my knowledge of the area.

I am also grateful to the current and former members of the laboratory of Dr. Kaback for their many forms of support during my graduate study.

Finally, I would like to thank the UCLA Graduate Division for their financial support granted through fellowships, which made my research possible.

Vita

Junichi Sugihara was born in Kasugai, Aichi, Japan. After completing his schoolwork at Haruhigaoka high school in Japan, Junichi entered the University of California, Los Angeles (UCLA). He received a Bachelor of Science with a major in Molecular, Cellular, and Developmental Biology in June 2004. During the following 6 years, he was employed as a research associate at the David Geffen School of Medicine at UCLA. After receiving a Master of Science in Integrative Biology and Physiology at UCLA in 2012, he entered the doctoral program in Molecular, Cellular and Integrative Physiology at UCLA.

Chapter 1

Background

1.1 Membrane transport proteins

1.1.1 Cell and biological membrane

All organisms are made of cells, and not only do diverse forms of life exist as simple single-celled organisms like bacteria and protozoa but more complex organisms are comprised of numerous types of cells with specialized functions. For example, erythrocytes or red blood cells, carry oxygen to the body tissues and collect carbon dioxide from the tissues as a waste product through the use of hemoglobin. Myocytes or muscle cells, are found in muscle tissues whose functions range from producing motion and maintaining posture to generating electrical impulses that control the heart rate. These unique properties define cells the organism's basic units of function.

Many common structures are found throughout animal and plant cells as well as in prokaryotic cells. One marked feature of such cell structures common to all organisms is that the interior of a cell is separated from the outside environment by a biological membrane, preventing molecules from moving freely into and out of cells. Nonetheless, while maintaining differences between the composition of the extracellular fluid and that of the cytoplasm, the membrane must allow import of essential nutrients into the cell and excretion of waste products or toxic substances out of the cell. Therefore, it is crucial that the cell membrane serves not only as a chemical barrier that separates the cytoplasm

from the periplasm and its surroundings, but also as a selectively permeable barrier that controls the movement of molecules in and out of cells.

The cytoplasmic membrane consists of a bilayer of phospholipids, yielding hydrophobic interior and two hydrophilic surfaces, with embedded proteins whose functions range diversely from cell adhesion and environmental sensing to signal transduction and cell communication. One of the most notable functions of membrane proteins is to permit selective transport of diverse small molecules, ions, and water between cytoplasmic and periplasmic spaces. Without such membrane-embedded transport proteins, the membrane would be permeable only to a few gases and uncharged small molecules that can readily diffuse across a phospholipid membrane, and ions, amino acids, sugars, and other water-soluble molecules would lack the capacity to enter or leave a cell. Movement of such solutes across the membrane is vital for the cell growth and homeostasis, as molecules transported across the membrane include glucose, amino acids, and other cellular nutrients.

1.1.2. Membrane proteins and disease

All membrane proteins together comprise approximately one third of the proteins encoded in the human genome, in which more than 800 genes are predicted to encode transport proteins [1]. Additionally, approximately 1000 genes are assumed to encode transporter-related accessory proteins, such as regulatory proteins and interacting partners [1], thereby emphasizing the significance of membrane transport proteins in life. In addition, because a great

variety of biologically significant molecules are transported across the membrane by transport proteins, it is not surprising that altered function or expression of membrane transport proteins is linked to various human diseases. For example, cystic fibrosis is associated with the malfunction of a cytidine monophosphate-regulated chloride transport protein encoded by the *CFTR* gene, and more than 70% of all mutations causing cystic fibrosis are accounted for by deletion of a Phe residue at position 508 in the gene [2]. Also, hereditary nephrogenic diabetes insipidus, a kidney disorder involving regulation of water balance, is caused by mutations in the *AQP2* gene encoding aquaporin-2 that moves water across the apical cell membrane of the principal cells of the collecting duct in the kidney [3].

Despite their physiological importance, determining the structure and function of membrane transport proteins has been particularly challenging. With the exception of certain ATP-driven ion pumps, the majority of membrane transport proteins is scarce and requires recombinant overexpression for analysis. Furthermore, the hydrophobic nature of transport proteins embedded in phospholipid bilayers makes them difficult to overexpress and resistant to structure determination by traditional means.

1.1.3 Types of membrane transport proteins

The major types of membrane transport proteins are channels and primary or secondary transport proteins. Channels provide energy-independent pathways, which allow relatively small solutes to flow down their activity gradients. Primary

transport proteins convert chemical energy (e.g., hydrolysis of ATP or oxidation) or light into work in the form of a concentration gradient. Most secondary transport proteins transduce the energy stored in one concentration gradient into another concentration gradient (e.g., symporters and antiporters).

(1) Channels

Channels are membrane-spanning proteins, that allow water, ions or other relatively small molecules to be translocated across a membrane with an electrochemical gradient, and they are sometimes gated so as to require activation (Fig. 1.1A). Since both sides are open, channels generally exhibit high rates of substrate translocation. A widely known species of channels conserved from bacteria to mammals and plants is the aquaporins, which function as water channels promoting rapid movement of water across cellular membranes. While many types of aquaporins are specifically permeable to water, some also translocate other small uncharged molecules such as glycerol or urea [4-6].

(2) Primary active transporters

Primary active transporters include ATPases that utilize energy released from ATP hydrolysis to move small molecules or ions across the membrane against a concentration or electrical potential gradient (Fig. 1.1B). Major classes of primary active transporters are the ATP-binding cassette (ABC) superfamily as well as ion pumps that are further classified into P-, F-, and V-classes depending on function, structure, and types of ions transported. ABC transporters, the largest class of primary active transporters, bind and hydrolyze ATP for the transport of a variety of substances including ions, carbohydrates, lipids, and

drugs [1, 7]. Ion-transporting pumps hydrolyze ATP to actively pump ions such as H^+, Na^+, K^+, Cl^+ or Cu^+ [8-10]. These primary active transporters contribute to generation of as well as maintenance of electrochemical ion gradient across the membrane, which in turn is utilized by secondary active transporters to drive uphill transport of various substrates across the membrane.

In some bacteria, transport of certain sugars or sugar alcohols is catalyzed by vectorial phosphorylation via the PEP-dependent carbohydrate: phosphotransferase system (PTS). Thus, the PTS catalyzes transport and concomitant phosphorylation of substrate so that transport across the membrane and the first step in metabolism are accomplished simultaneously (Fig. 1.1C). The PTS is a multicomponent system composed of cytoplasmic proteins with no specificity for substrate and a transmembrane protein that is highly specific. Three cytoplasmic proteins are involved as phosphate carriers. HPr (Heat-stable Protein) is phosphorylated by Enzyme I (EI), which transfers the phosphoryl group from PEP, the high-energy phosphate donor for the system. Subsequently, when substrate is present in environment, the phosphoryl group is transferred from HPr to Enzyme IIA (EIIA) and then to membrane-bound Enzyme IIBC (EIIBC), which phosphorylates substrate in a highly specific manner as it is transported. The PTS is found only in bacteria and not present in other species.

Other sources of energy for primary active transporters include light and respiration. For example, proteins involved in photosynthesis use the energy from trapped photons to create an electrochemical H^+ gradient. Also, mitochondrial and bacterial electron transport chains use the energy produced

from oxidation of NADH and other electron donors to generate an electrochemical H^+ or Na^+ gradient.

(3) Secondary active transporters

Secondary active transports utilize the energy stored in an electrochemical gradient of ions, mainly H^+ or Na^+, to drive transport against a concentration gradient (Fig. 1.1D). After binding a substrate molecule, the transporter undergoes a conformational change that allows access of the binding site to either side of the membrane (an alternating access mechanism).

Secondary active transporters catalyze two types of substrate translocation: symport and antiport. Symporters (cotransporters) transport substrate with an ion, the ion flowing down its electrochemical gradient and the substrate against a concentration gradient. Antiporters (exchangers) catalyze translocation of substrate and an ion or another substrate molecule in the opposite direction (Fig. 1.1D).

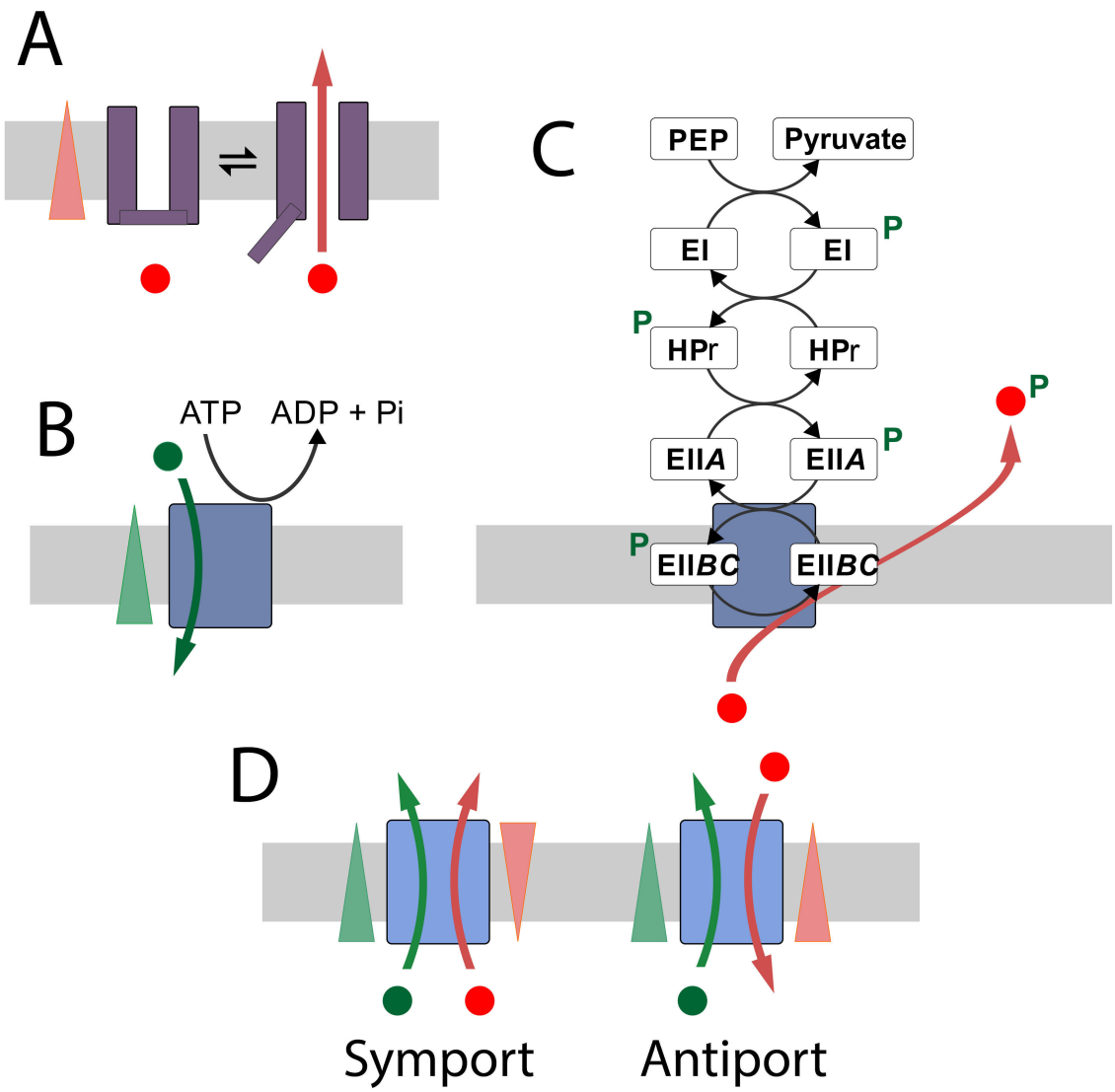

Fig. 1.1. Major types of membrane transport proteins. (A) Channels, when open, allow consecutive flow of substrate molecule down their concentration or electric potential gradient. (B) Primary active transporters utilize energy released from ATP hydrolysis to translocate substrates against a chemical concentration or electric potential gradient. (C) Glucose transport by phosphotransferase system (PTS) in *E. coli*. EI and HPr are common to all sugar substrates while EIIA and EIIBC are specific to glucose. (D) Secondary active transporters translocate substrates against concentration gradients by exploiting electrochemical ion gradient. Circles indicate transport substrates. Triangles indicate chemical gradients of the substrates.

1.1.4 The major facilitator superfamily (MFS)

Proteins are classified into a family or cluster based on the degree of sequence similarity, function, and topology or three-dimensional structure, and a superfamily is comprised of families of proteins that share a common ancestry. The largest superfamily of evolutionally-related secondary active transporters present in all kingdoms of life is the major facilitator superfamily (MFS), which includes over 70 subfamilies and 10,000 sequenced members to date [11-13]. MFS members are transmembrane single-polypeptides catalyzing uniport, symport or antiport, and the number of MFS transporters identified is growing rapidly as the number of sequenced genomes and three-dimensional structures increase.

Substrates transported by MFS proteins are diverse and include simple sugars, oligosaccharides, amino acids and peptides, lipids, nucleosides, drugs, and various anions and cations [14]. Due to this wide variety of substrates, MFS transporters are involved in numerous processes that are physiologically important. For example, up-regulation of glucose transporters GLUT1 and GLUT3 is often exhibited in malignant tumors as their high rates of glycolysis require increased glucose transport [15]. Also, a deficiency of GLUT1 causes low glucose concentrations in the cerebrospinal fluid leading to early-onset epilepsy, developmental delay, and a complex movement disorder [16, 17], and Fanconi-Bickel Syndrome is a glycogen storage disorder caused by a mutation in the *GLUT2* gene encoding the facilitative glucose transporter in the pancreas and the liver [18-20]. Furthermore, genetic defects in a urate transporter GLUT9 lead to a

metabolic syndrome characterized by early-onset nephropathy associated with increased uric acid levels [21].

1.1.5 Structural features shared by MFS transporters

The majority of MFS transporters have 400-600 amino acid residues in length organized into 12 transmembrane helices with both the N and C termini located on the cytoplasmic side of the membrane. They are organized into two domains, each consisting of 6 transmembrane helices, and the two domains display a two-fold pseudosymmetry. Moreover, the first and second triplets in each 6-helix domain have a high degree of structural homology but are in an inverse orientation [22].

Despite their physiological significance, structures of eukaryotic MFS transporters are limited to the GLUTs [23-27]. However, X-ray crystal structures of about 20 bacterial MFS transporters have been reported, and many inferred structures of eukaryotic transporters have been derived from homology modeling.

1.1.6 The lactose permease of *E. coli* (LacY)

The most intensively studied secondary active transporter is the lactose permease of *Escherichia coli* (LacY), a galactoside/H^+ symporter belonging to the MFS. LacY catalyzes the obligatory coupled translocation of a galactoside and an H^+ across the cytoplasmic membrane by transducing free energy stored in an electrochemical H^+ gradient into a galactoside concentration gradient. As a well-studied chemiosmotic model of a sugar/H^+ symporter, LacY is a paradigm for

secondary active transporters, and it has been studied extensively by using a wide variety of experimental techniques.

LacY is encoded by *lacY* gene, the second of the three structural genes in the *lac* operon. The other two genes in the operon, *lacZ* and *lacA*, encode cytoplasmic enzymes β-galactosidase and galactoside transacetylase, respectively. β-Galactosidase catalyzes cleavage of the disaccharide lactose into galactose and glucose. The enzyme also converts lactose into allolactose, the physiological inducer of the operon [28]. Binding of allolactose to the *lac* repressor allows RNA polymerase to bind to *lac* promoter and initiate transcription of the operon. The transacetylase utilizes acetyl-CoA to acetylate the 6-*O*-methyl position of a variety of galactopyranosides [29]. However, its biological role is unclear.

The *lacY* gene was the first gene encoding a membrane transport protein to be cloned into a recombinant plasmid [30], overexpressed, and sequenced [31]. Overexpressed LacY has been solubilized from the membrane, purified to homogeneity, reconstituted into proteoliposomes in a fully functional state [32-36]. It then took over 20 years to obtain the first X-ray crystal structure [37].

1.1.7 Galactoside/H^+ symport by LacY

The chemiosmotic hypothesis of Peter Mitchell [38-41] stipulates that accumulation of galactosides against concentration gradient by LacY is driven by an electrochemical H^+ gradient across the cytoplasmic membrane ($\Delta\tilde{\mu}_{H^+}$), which is composed of an electrical potential ($\Delta\psi$; interior negative) and/or a pH gradient

(ΔpH; interior alkaline). In the presence of $\Delta\tilde{\mu}_{H^+}$, LacY, functioning as a monomer [42], utilizes the free energy released from downhill translocation of H^+ to drive accumulation of galactosides against a concentration gradient (Fig. 1.2A). In the absence of $\Delta\tilde{\mu}_{H^+}$, LacY catalyzes the converse reaction, utilizing free energy released from downhill translocation of galactoside to drive uphill translocation of H^+ with the generation of $\Delta\tilde{\mu}_{H^+}$, the polarity of which depends upon the direction of sugar concentration gradient (Fig. 1.2B & C).

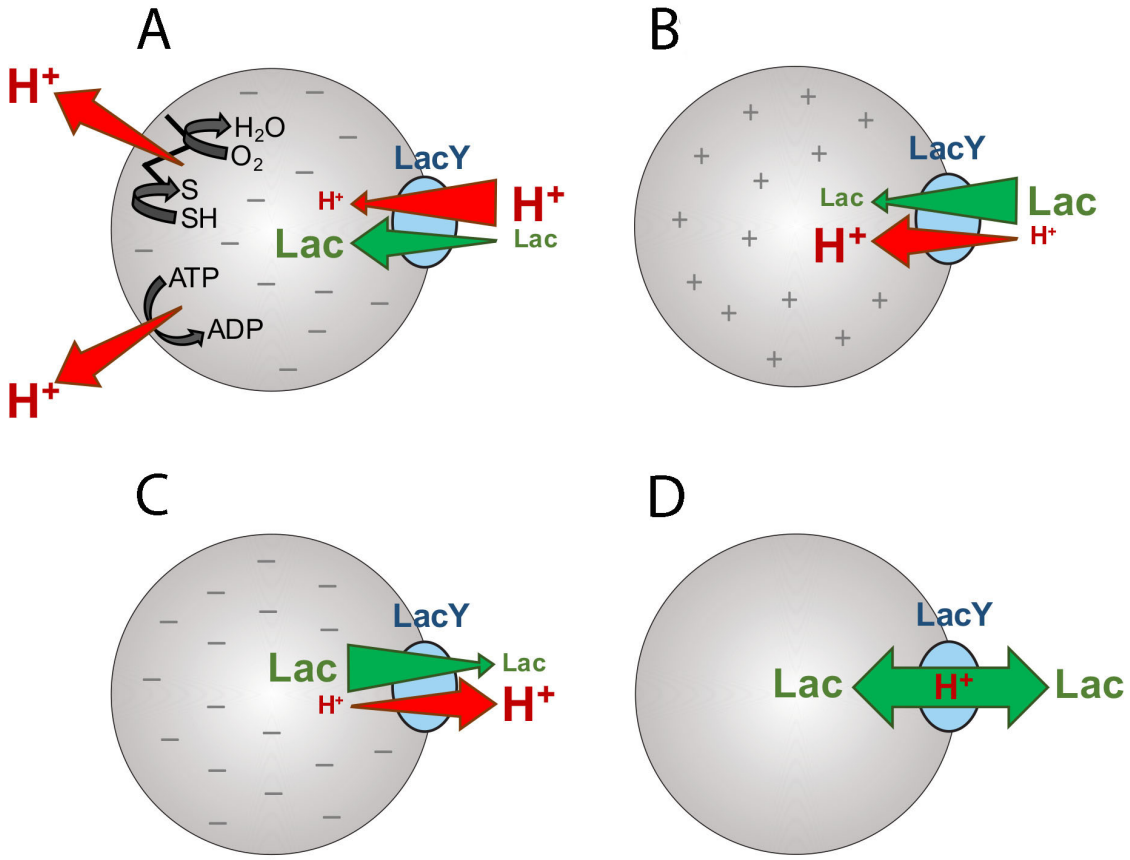

Fig. 1.2. Lactose/H^+ symport. (A) An electrochemical ion gradient is generated by the action of various cation-motive pumps. Free energy released from the downhill movement of H^+ is coupled to the uphill accumulation of lactose. LacY molecule is colored as blue. (B) Influx and (C) Efflux: Substrate gradients generate electrochemical H^+ gradients, the polarity of which depends upon the direction of the substrate concentration gradient. (D) Equilibrium exchange:

Protonated LacY catalyzes lactose exchange across the membrane at equal intra- and extra-cellular lactose concentrations.

A plethora of experimental evidence [reviewed in 43] strongly indicates that the mechanism of galactoside/H^+ symport is explained by the kinetic scheme depicted in Fig. 1.3. Starting from the outward-facing conformation, Influx is initiated with protonation of LacY (step 1) followed by binding of lactose (step 2). This triggers a conformational change to an occluded state (step 3) and subsequently to the inward-facing conformation (step 4). Once lactose is released into the cytoplasm (step 5), LacY deprotonates (step 6) to form an apo-occluded intermediate (step 7), which opens to the periplasm (step 8) and the cycle is re-initiated.

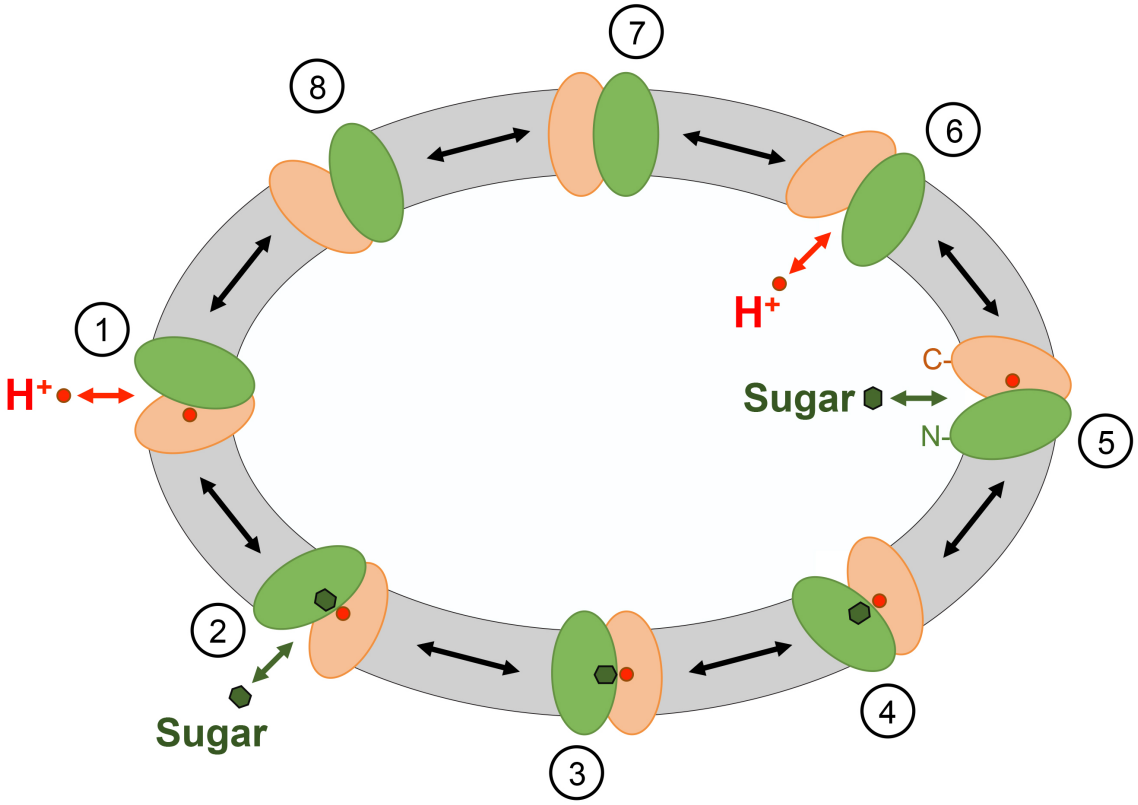

Fig. 1.3. Kinetic scheme and alternating access mechanism of sugar/H^+ symport in LacY. The cartoon representations for the N- and C-terminal domains of LacY molecule are colored as green and orange, respectively. Sugar and H^+ bind at the middle of the molecule, and LacY moves around the binding sites to release the symported substrates on either side of the membranes, as indicated by the arrows. Exchange and counterflow involve steps 2 to 5.

LacY also catalyzes another mode of translocation [44, 45]. At equal internal and external lactose concentrations, protonated LacY catalyzes equilibrium exchange of internal radiolabeled lactose for external unlabeled lactose in a manner that is independent of $\Delta\tilde{\mu}_{H^+}$ (Fig. 1.2D). Similarly, entrance counterflow, the reverse of equilibrium exchange, is independent of $\Delta\tilde{\mu}_{H^+}$. Equilibrium exchange or entrance counterflow involves only steps 2 through 5.

1.1.8 Residues involved in sugar-binding and H^+ translocation in LacY

LacY is composed of 417 amino acid residues with a molecular mass of 46,517 Da and contains twelve, mostly irregular transmembrane helices [37, 46]. X-ray crystal structures of WT LacY and the conformationally-restricted C154G mutant exhibit two pseudosymmetrical six-helix bundles surrounding a large hydrophilic cavity open only to the cytoplasm, an inward-facing conformation [37, 47-49] (Fig. 1.4). As shown by Cys-scanning and site-directed mutagenesis, only six amino acyl side chains in LacY are absolutely irreplaceable with respect to active transport – Glu126 (helix IV), Arg144 (helix V), Glu269 (helix VIII), Arg302 (helix IX), His322 and Glu325 (helix X) [50]. Trp151 (helix V) can be replaced with Tyr or Phe with corresponding decreases in affinity, but an aromatic side chain is obligatory [51]. Similarly, Asn272 (helix VIII) can be replaced with Gln with little or no effect on activity, but other replacements are inactive [52]. Interestingly, Tyr236 (helix VII) cannot be replaced with Phe, but mutants with Ala or Cys in place of Tyr236 exhibit significant transport activity [50, 53].

As demonstrated both biochemically [54-57] and structurally [58, 59], the specificity of LacY is directed solely towards the galactopyranosyl ring of the substrate, and the non-galactosyl moiety increases affinity particularly if it is hydrophobic. Thus, the monosaccharide galactose is the most specific substrate for LacY, but it has very poor affinity, which is increased by 3 orders of magnitude by attaching a nitrophenyl group in the α position to the C1-OH group.

The residues involved in sugar-binding/recognition and H^+ translocation are located near the apex of the hydrophilic cavity in the approximate middle of

the molecule [58, 59] (Fig. 1.4C). Glu269 is the acceptor of hydrogen bonds from the C4-OH group of the galactopyranosyl ring, making it the likely candidate for a primary role in specificity. The η1 NH_2 group of Arg144 donates a hydrogen bond to O5 in the ring and also is within hydrogen-bond distance to C6-OH. The η2 NH_2 group of Arg144 donates hydrogen bonds to C2'-OH of β-D-galactopyranosyl-1-thio-β-D-galactopyranoside (TDG) and to Glu126 Oε2. Glu126 acts as hydrogen bond acceptor from the C2'-OH of TDG. His322 acts as a hydrogen-bond donor/acceptor between the εNH of the imidazole ring and the C3-OH of TDG and is stabilized by a hydrogen-bond donor/acceptor with the δNH of the imidazole and the OH of Tyr236. Also, Asn272 (helix VIII) likely donates a hydrogen bond to the C4-OH of TDG. Glu325 and Arg302 are directly involved in coupled H^+ translocation. Neutral replacement of either residue yields mutants that are defective in all transport reactions that involve lactose/H^+ symport but catalyze equilibrium exchange and/or counterflow as well as or better than WT [60, 61]. It is also highly relevant that galactoside binding exhibits an apparent pK of ~10.5, indicating that protonation of LacY precedes sugar binding at physiological pH [62-64].

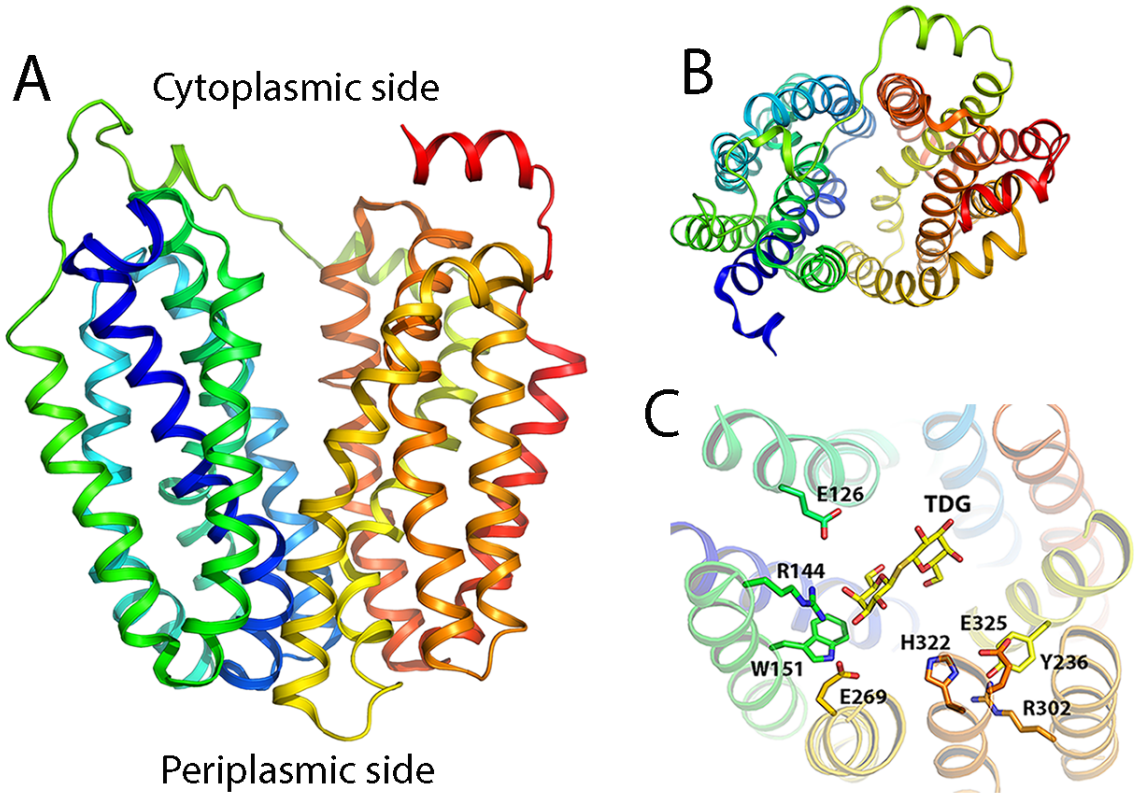

Fig. 1.4. X-ray crystal structure of LacY C154G (PDB code: 1PV7). Crystal structures of wild-type LacY as well as the conformationally restricted C154G and single-Cys mutants exhibit an inward-facing conformation. In the ribbon representations, the 12 transmembrane helices are colored from the N-terminus in blue to the C-terminus in red. The structure is displayed by using Pymol 1.4. (A) View parallel to the membrane. (B) Cytoplasmic view. (C) Detailed view from the cytoplasm showing residues in sugar- and H^+-binding sites. Residues in sugar- and H^+-binding sites are shown as sticks.

1.1.9 The alternating access mechanism

The alternating access mechanism postulates that the overall conformational change in LacY leading to transport involves alternating accessibility of sugar- and H^+-binding sites to either side of the membrane. LacY is highly dynamic, and hydrogen/deuterium exchange of backbone amide protons in WT LacY occurs at a remarkably rapid rate [65-67]. Furthermore, sugar binding by LacY is mostly entropic in nature [68], inducing widespread

conformation changes [reviewed in 69]. In addition, multiple independent biochemical and spectroscopic studies, which include thiol cross-linking [70-77], site-directed alkylation [77-83], single molecule fluorescence resonance energy transfer [84], double electron-electron resonance [85], and Trp fluorescence quenching [86-88], demonstrate that the periplasmic and cytoplasmic cavities in LacY open and close reciprocally. Comparison of two X-ray structures of LacY show that G46W/G262W mutant structure with an occluded galactoside molecule is related to WT apo LacY by an approximate 30° rotation of one domain against the other about an axis perpendicular to the membrane plane [58].

As indicated, in addition to the conformations open to either side of the membrane, evidence for an occluded intermediate in the transport cycle of LacY has been obtained. X-ray crystal structures of LacY mutant G46W/G262W exhibit either of two occluded galactosides with a narrow periplasmic opening and a tightly sealed cytoplasmic face [58, 59].

Indirect evidence for alternating access is also provided by structures of other MFS transporters. X-ray structures of the D-xylose/H^+ symporter XylE show ligand-bound outward-facing and partially occluded conformations [89, 90]. In addition, a ligand-free outward-open conformation is observed with the L-fucose/H^+ symporter FucP [91]. These and other structures appear to represent several distinct conformations that occur during the transport cycle. However, conformations depicting all stages of the transport cycle have not been observed with any given MFS transporter, making current structural information insufficient for a comprehensive understanding of transporter dynamics. Thus, application of

biochemical and spectroscopic methods is vital for understanding of the mechanism of action for any given transporter.

In this thesis, biochemical and biophysical approaches are utilized to delineate the dynamics of FucP and sucrose permease of *E. coli* (CscB) belonging to the MFS. Although these transporters are thought to function by an alternating access mechanism like LacY, their dynamics have not been examined.

Chapter 2

Determinants for substrate recognition in CscB

2.1 Introduction

Bacterial sugar transporters homologous to LacY belong to the oligosaccharide/H^+ symporter sub-family (OHS) of the MFS [92], and LacY is the best characterized member. Like LacY, other members of the OHS are believed to catalyze the coupled translocation of a sugar and an H^+ (sugar/H^+ symport). These proteins are also likely to have a structure similar to that of LacY [93, 94] with twelve, mostly irregular transmembrane α-helices that transverse the membrane in a zigzag fashion connected by hydrophilic loops with both N- and C-termini on the cytoplasmic face and a large water-filled cavity facing the cytoplasm [37, 47-49].

The second most well studied member of the OHS is CscB of *E. coli*, encoded by the *cscB* gene, which transports sucrose, but not lactose or other galactopyranosides [95, 96]. Another OHS symporter, the melibiose permease of *Enterobacter cloacae* (MelY), which has a high degree of sequence similarity with LacY, does not transport methyl 1-thio-β-D-galactopyranoside, a good substrate for LacY [97], while both proteins recognize melibiose and lactose as substrate. In any case, CscB exhibits 28% sequence identity with LacY and an overall level of homology of 51% [13, 93]. Most of the irreplaceable residues in LacY with respect to activity are conserved in CscB, and site-directed mutagenesis confirms their importance [94, 98, 99]. Moreover, homology threading of CscB with the LacY crystal structure as a template (Fig. 2.1), as well

as functional studies of site-directed mutants in CscB, predicts similar organization of the sugar- and H^+-binding sites [93, 94]. Glu126 (helix IV), Arg144 (helix V) and Trp151 (helix V) in LacY, which are directly involved in sugar binding, are homologous with Asp129, Arg147 and Tyr154 in CscB. Although Glu270 is one helix turn closer to the cytoplasmic side of CscB than the homologous residue Glu269 (helix VIII) in LacY, the functional role appears to be the same [94]. In addition, the spatial organization of the residues involved in H^+ translocation in LacY is almost identical in CscB, as judged from homology modeling [93, 94].

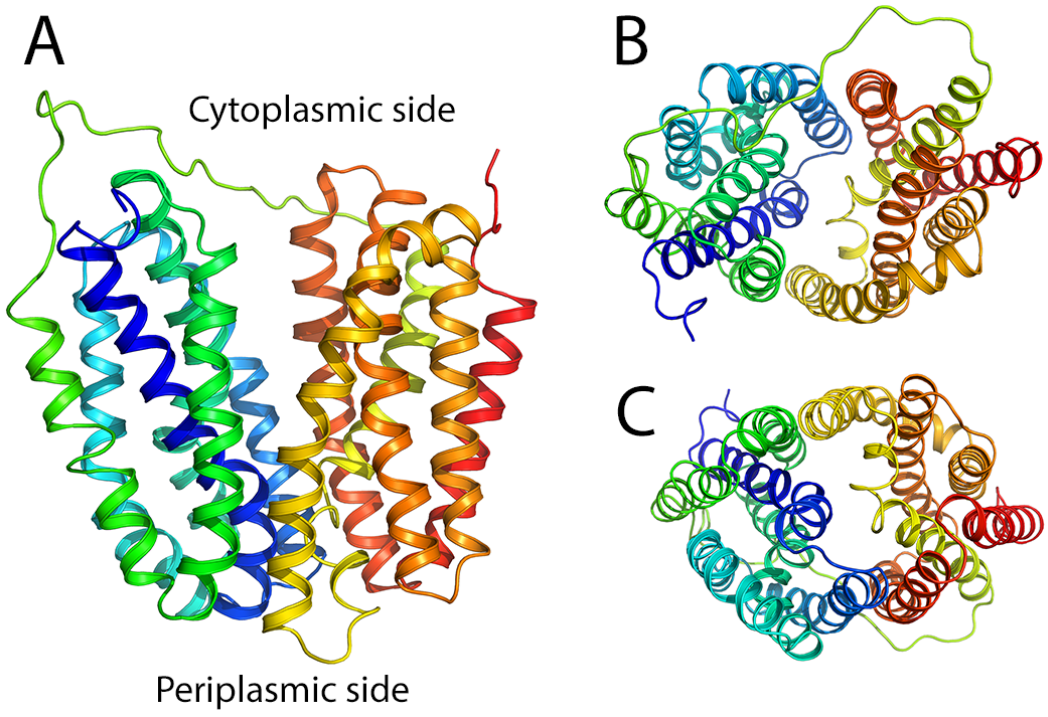

Fig. 2.1. CscB threaded into LacY structure (PDB code: 1PV7). Transmembrane helices are depicted as ribbons colored from blue (helix I) to red (helix XII). CscB structure is displayed by using Pymol 1.4. (A) View parallel to the membrane. (B) Cytoplasmic view. (C) Periplasmic view.

There are many bacterial genes encoding proteins that are significantly similar to LacY and CscB, although their expression and transport specificities have yet to be studied [93]. LacY specifically recognizes D-galactose and the D-galactopyranosyl moiety of its disaccharide substrates, but has no affinity for D-glucopyranosides or D-glucose [54-57]. Therefore, it was assumed that the specificity of CscB would be directed at the D-glucopyranosyl moiety of sucrose. To test this notion, I identified several sugars that might hypothetically be transported by CscB and found that CscB catalyzes transport of not only sucrose but also lactulose and fructose (Fig. 2.2). Moreover, D-glucopyranoside has no detectable affinity for CscB. Thus, the specificity of CscB appears to be directed toward the fructofuranosyl ring of sucrose and not the glucopyranosyl moiety. In addition, the C3-OH group on the fructofuranosyl ring appears to be important for recognition. Finally, lactulose is an excellent substrate for LacY, as predicted from its specificity for the galactopyranosyl moiety of its multiple substrates.

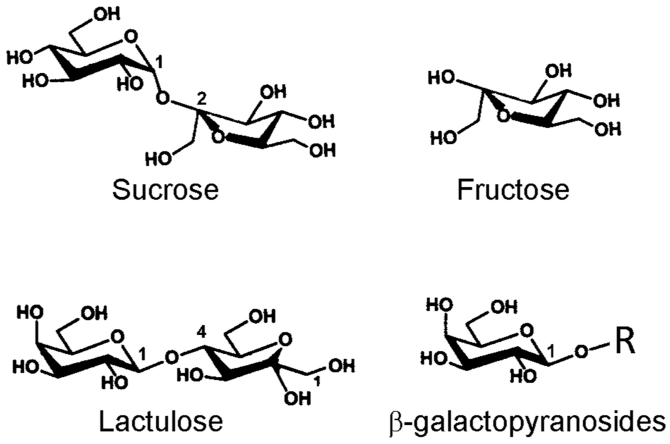

Fig. 2.2. Chemical structures of sucrose, fructose, lactulose and β-galactopyranosides. R represents different anomeric moieties (e.g., in galactose, R is H; in lactose, R is glucose).

2.2 Results

2.2.1 Sucrose or fructose transport by CscB

E. coli cells overexpressing CscB catalyze transport of either sucrose or fructose, while cells transformed with a vector devoid of CscB exhibit essentially no transport of either sugar (Fig. 2.3A & C). Transport of sucrose by cells expressing CscB increases at a rapid rate for ~5 min and reaches a steady-state level of ~140 nmol/mg of protein within ~20 min (Fig. 2.3A). In contrast, the same cells catalyze the transport of fructose at a relatively low rate to a steady-state level of ~20 nmol/mg (Fig. 2.3C). Right side-out (RSO) membrane vesicles expressing CscB exhibit transport of sucrose in a similar manner (Fig. 2.3E). Rates of transport as a function of sucrose or fructose concentration follow a hyperbolic relationship with a K_m for sucrose of 6.7 mM and a V_{max} of 110 nmol/min·mg protein (Fig. 2.3B); fructose transport exhibits a K_m of 36 mM and a V_{max} of 60 nmol/min·mg protein (Fig. 2.3D). Transport of neither sucrose nor fructose by cells overexpressing LacY is observed (Fig. 2.3A & C, filled triangles).

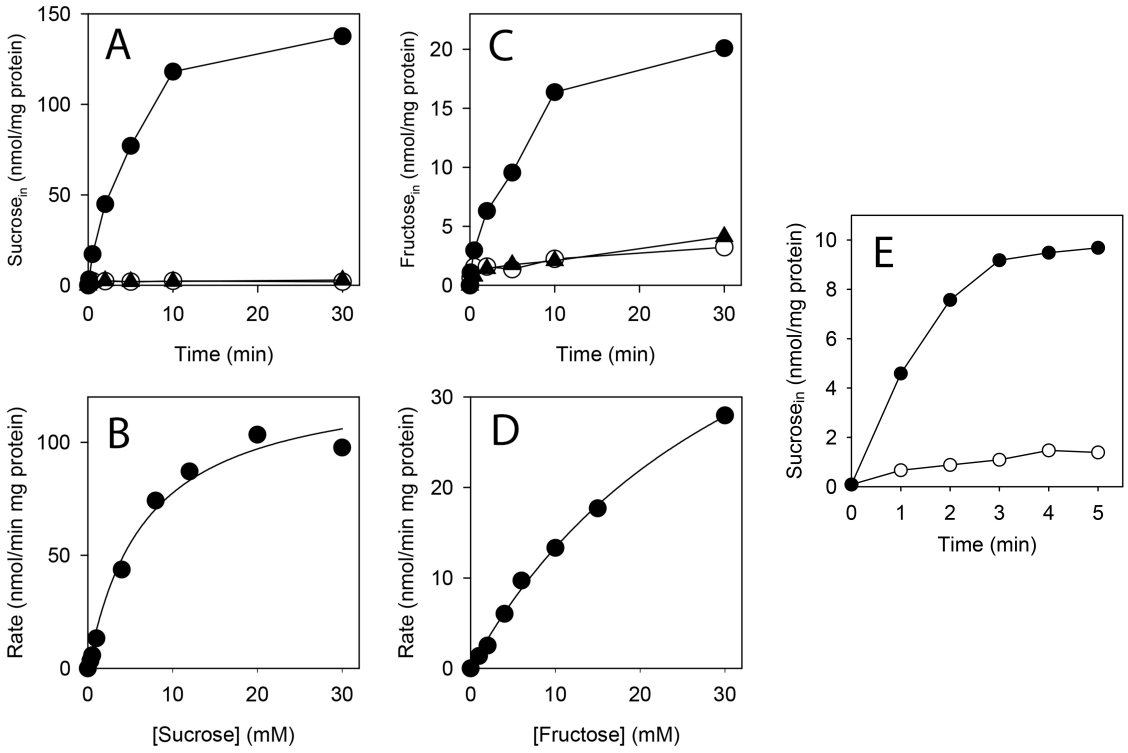

Fig. 2.3. Transport activity of CscB. (A) Time courses of accumulation of [^{14}C]sucrose (0.5 mCi/mmol) by *E. coli* T184 cells expressing CscB (●), LacY (▲) or no permease (○) were measured at 4 mM sucrose as described in *Materials and Methods*. (B) Concentration dependence of the initial rates of accumulation of sucrose by *E. coli* T184 cells expressing CscB measured as described in *Materials and Methods.* Hyperbolic fit shown as a solid line with estimated kinetic parameters: K_m = 6.7 ± 1.3 mM, and V_{max} = 110 nmol/min·mg protein. (C) Time courses of accumulation of 6 mM [^{14}C]fructose (0.3 mCi/mmol) were measured and presented as described for panel A. (D) Kinetic analysis of the transport of fructose by CscB conducted as described for panel B with the following estimated kinetic parameters for fructose: K_m = 36 ± 4 mM, and V_{max} = 60 nmol/min·mg protein. (E) Time courses of fructose accumulation by RSO membrane vesicles expressing CscB (●) and no permease (○).

2.2.2 Effect of various sugars on the transport of sucrose by CscB

Transport of sucrose by CscB is not inhibited to any degree whatsoever by glucose since kinetic parameters of transport remain unchanged even in the presence of 30 mM glucose (Fig. 2.4). Moreover, sugars devoid of a fructose moiety, which include galactose, lactose, melibiose, mannose, rhamnose or

ribose, have no effect on sucrose transport (data not shown). The results indicate that the specificity of CscB is directed toward the fructofuranosyl ring of substrate. To further evaluate the importance of the fructose moiety, different fructofuranosides were tested for their ability to inhibit the transport of sucrose by CscB (Fig. 2.5). The sugars tested include turanose (3-*O*-α-D-glucopyranosyl-D-fructose), lactulose (4-*O*-β-D-galactopyranosyl-D-fructose), and palatinose (6-*O*-α-D-glucopyranosyl-D-fructose). While 10 mM palatinose or lactulose inhibits sucrose transport, albeit relatively weakly, turanose does not have any effect on the transport, thereby providing suggestive evidence that the C3-OH group on the fructofuranosyl ring may be important for recognition by CscB. Detailed analysis reveals that fructose is a competitive inhibitor of sucrose transport with a K_i of 30–50 mM (Fig. 2.5B), which is in the same range as the K_m for fructose transport (Fig. 2.3D).

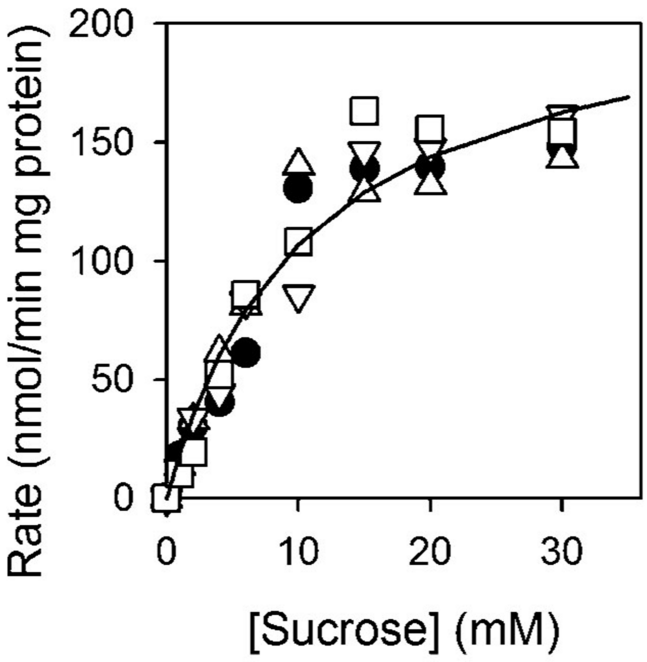

Fig. 2.4. Effect of glucose on the transport of sucrose by CscB. Initial rates of accumulation of [^{14}C]sucrose by *E. coli* T184 cells expressing CscB were measured and fitted as described in the legend of Fig. 2.3B in the absence of glucose (●) or in the presence of 10 (△), 20 (▽), or 30 mM glucose (□).

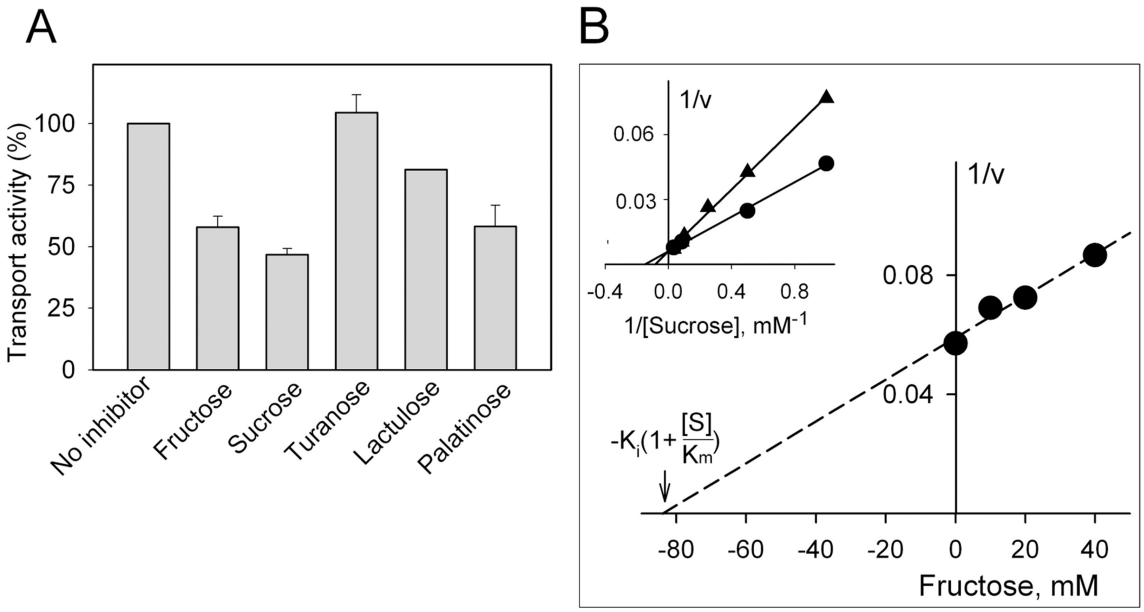

Fig. 2.5. Effect of fructofuranosides on the transport of sucrose by CscB. (A) Testing of different sugars for their ability to inhibit the transport of sucrose. Accumulation of [^{14}C]sucrose (4 mM) by *E. coli* T184 expressing CscB was

measured as described in the legend of Fig. 2.3A for 10 min without additions (100% activity) or in the presence of 10 mM unlabeled fructose, sucrose, turanose, lactulose, or palatinose. (B) Concentration dependence of fructose inhibition. Initial rates of [^{14}C]sucrose transport (30 sec) were measured as in panel A at various concentrations of unlabeled fructose (10, 20, or 40 mM). The inset demonstrates competitive inhibition of the transport of [^{14}C]sucrose by 20 mM fructose (▲) with an estimated K_i of ~30 mM and an unchanged V_{max} of 160 nmol/min·mg protein. A Dixon plot exhibits a linear fit of the data (broken line) with an estimated K_i of ~50 mM.

2.2.3 Transport of lactulose by CscB or LacY

E. coli cells overexpressing CscB catalyze transport of lactulose (Fig. 2.6). Accumulation of this disaccharide occurs at a relatively slow rate and does not reach steady state even by 60 min at 20 mM lactulose. In contrast, *E. coli* cells overexpressing LacY catalyze the transport of lactulose at a rapid rate to a steady-state level of ~85 nmol/mg protein in approximately 3 min (Fig. 2.7A). Kinetic parameters for lactulose transport by LacY estimated from concentration dependence of initial rate (Fig. 2.7B) are: K_m = 0.24 mM and a V_{max} = 49 nmol/min·mg protein. These values are similar to those obtained for transport of lactose by LacY [100].

As shown previously by substrate protection against alkylation of Cys148 in LacY, galactose or lactose exhibit apparent affinities of 50 or 9 mM, respectively [56], while TDG or 4-nitrophenyl-α-D-galactopyranoside (α-NPG), exhibit apparent affinities of 0.85 or 0.03 mM, respectively [62]. By using the same method, the apparent affinity of LacY for lactulose (K_d^{app}) is ~8 mM (Table 2.1), a value approximately the same as that observed for lactose.

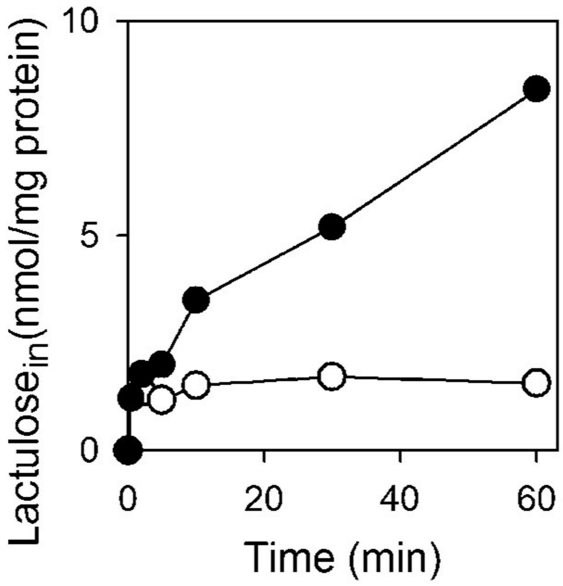

Fig. 2.6. Lactulose transport activity of CscB. Time courses of lactulose accumulation by *E. coli* T184 expressing CscB (●) or no permease (○) were measured at 20 mM [^{3}H]lactulose (0.1 mCi/mmol) as described in *Materials and Methods*.

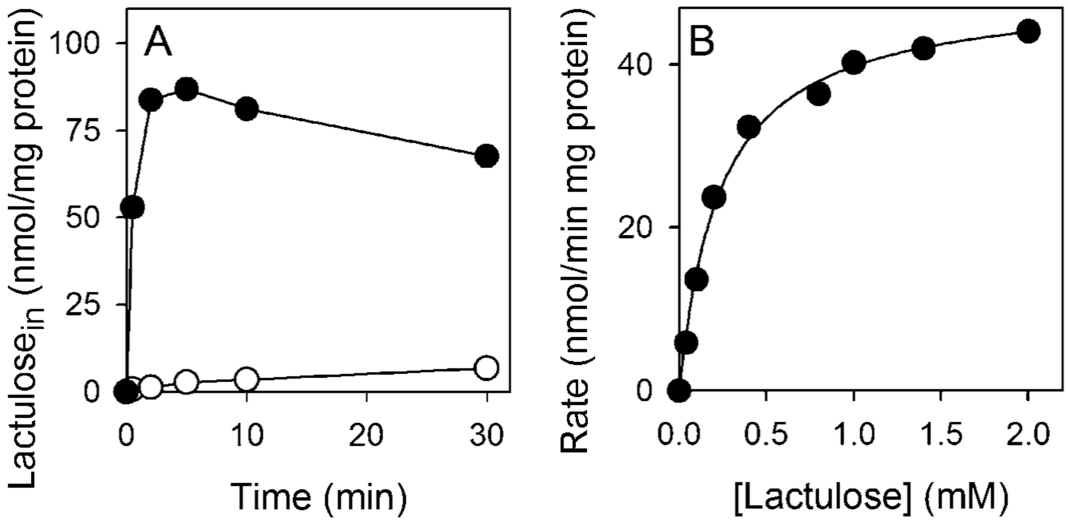

Fig. 2.7. Lactulose transport activity of LacY. (A) Time courses of lactulose accumulation by *E. coli* T184 cells expressing LacY (●) or no permease (○) were measured at 0.4 mM [^{3}H]lactulose (5 mCi/mmol) as described *in Materials and Methods*. (B) Concentration dependence of initial rates of lactulose accumulation measured as described in *Materials and Methods*. A hyperbolic fit is shown as a solid line with estimated kinetic parameters K_m = 0.24 ± 0.02 mM and V_{max} = 49 nmol/min·mg protein.

Sugar	K_d^{app}, mM
Galactose	**50**[a]
Lactose	**9**[a]
Lactulose	**8**[c]
TDG	**0.85**[b]
α-octylgalactoside	**0.05**[c]
α-NPG	**0.03**[b]

Table 2.1. Sugar binding affinity to LacY. Apparent K_ds for galactosidic sugars measured by substrate protection of Cys148 against alkylation by 2-(4'-maleimidylanilino)naphthalene-6-sulfonic acid (MIANS) as the effect of sugar concentration on the initial rate of MIANS labeling.

(a) Wu, J. & Kaback, H.R. (1994) *Biochemistry 33*, 12166-12171.
(b) Smirnova, I., Kasho, V. et al (2008) *Proc Natl Acad Sci USA 105*, 8896-8901.
(c) Current study

2.3 Discussion and conclusions

Although there is a clear similarity in the structural organization of key residues involved in sugar binding in LacY and CscB [93, 94], as shown here, there is an unexpected and surprising difference in substrate recognition between the two symporters. Thus, CscB catalyzes transport of sucrose, fructose or even lactulose, but exhibits no recognition of glucopyranosides, glucose in particular, as evidenced by the inability of glucose to inhibit sucrose transport. Taken together, the results lead to the conclusion that the specificity of CscB is directed toward the fructofuranosyl moiety of sucrose. In contrast, extensive studies demonstrate that the specificity of LacY is directed toward the galactospyranosyl moiety of substrate, and the C4-OH plays the predominant role by far in recognition and binding [57, 101]. The monosaccharide galactose

is the most specific substrate for LacY, although it binds with very low affinity [54, 55, 101], while galactopyranosides in the α configuration with anomeric substitutions, particularly those that are hydrophobic, exhibit increased affinity with little or no effect on specificity [57, 101].

Asp129 and Arg147 in CscB, which are positioned similarly to Glu126 and Arg144 in LacY respectively, probably also play a direct role in sugar recognition and binding, and Tyr154 in CscB, which is homologous to Trp151 in LacY, likely stacks hydrophobically with the fructofuranosyl ring of sucrose [93, 94]. Glu270 in CscB, although positioned one helix turn closer to the cytoplasmic side of CscB than Glu269 in LacY, is essential and is probably also important for substrate recognition and binding. Although replacement of Ser151 (homologous to Cys148 in LacY) with Cys causes CscB to become highly sensitive to *N*-ethylmaleimide in a manner similar to that of LacY, substrate affords no protection whatsoever against inactivation of transport or alkylation with CscB [98]. Thus, the overall architecture of the substrate binding sites appears to be conserved in CscB and LacY, but there are important differences in detailed interactions, and the fructofuranosyl moiety of sucrose likely occupies a position homologous to that of the galactopyranosyl moiety of lactose in LacY (Fig. 2.8).

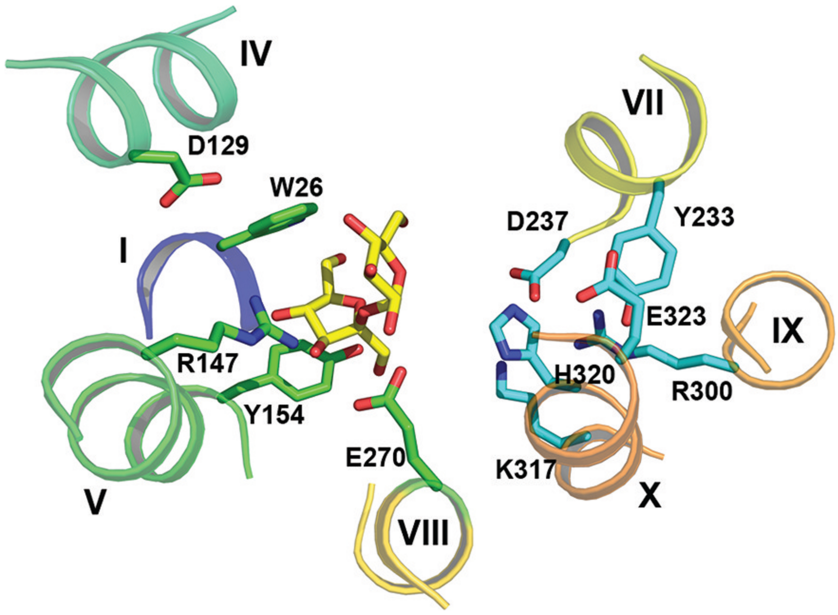

Fig. 2.8. Sucrose molecule modeled in the putative sugar-binding site of CscB. The sugar-binding site of CscB is viewed from the cytoplasmic side with a sucrose molecule docked according to the findings presented in this paper. The fructofuranosyl moiety is in close contact with amino acid residues essential for sugar binding [94], which are in the N-terminal 6-helix bundle and presented as green sticks. Residues important for H^+ translocation are located in C-terminal 6-helix bundle and shown as cyan sticks. Transmembrane helices are numbered with Roman numerals. The CscB model was build by homology modeling using the X-ray structure of LacY (PDB code: 1PV7) as template [93]. The sucrose molecule (coordinates from PDB code 1IW0) is presented as yellow sticks. The figure was generated with Pymol 1.4.

Inhibition studies with several fructofuranosides (Fig. 2.5) provide some evidence that the C3-OH of the fructose moiety in sucrose is important for binding. In lactulose and palatinose, the galactose moiety is attached to the C4 and C6 atoms of the fructose moiety, respectively. These fructofuranosides partially inhibit sucrose transport by CscB, suggesting that the C4-OH and C6-OH groups are not important. On the other hand, in turanose, the galactose moiety is attached to the C3 atom of fructose moiety, and turanose does not

inhibit sucrose transport, thereby suggesting that the C3-OH is likely an important player in the interaction of the fructose moiety with CscB.

Transport of lactulose is catalyzed by CscB, but at a low rate. In complex with sugar binding proteins, lactulose is in an extended, planar conformation with respect to the galactose and fructose moieties, which are in the β-configuration [102]. In contrast, sucrose is in a bent conformation with the glucose and fructose rings positioned at approximately a right angle (PDB codes: 1AF6, 1PT2, 1IW0). Therefore, in order for the C3-OH group of the fructose moiety in a disaccharide to be maximally accessible in the sugar-binding site of CscB, the anomeric ring may need to be attached to fructose moiety in such a manner that the C3-OH is readily accessible. With lactulose, the galactose ring may sterically interfere with the accessibility of the C3-OH of the fructose moiety, making it a relatively poor substrate for CscB.

In contrast to CscB, lactulose is an excellent substrate for LacY. In lactulose, the galactose moiety is bonded to fructose by a β-1,4 glycosidic bond, making the OH groups at each position on the galactose moiety as accessible as in lactose. Moreover, both protein-bound lactose (PDB codes: 1DLL, 1ULC) and lactulose are in extended conformations. Although the C4-OH is the major determinant for recognition and binding by LacY, each OH group makes a contribution to binding affinity [57]. Thus, it is not surprising that lactulose is a good substrate for LacY.

Chapter 3

Functional and structural comparison of FruP of *E. coli*, a putative fructose transporter, with LacY and CscB

3.1 Introduction

Fructose is an important energy source for bacteria as glycolysis occurs in nearly all organisms. Although a well-known mechanism that mediates fructose transport across the cytoplasmic membrane of many bacterial species is PTS, a fructose utilization system independent of PTS has been identified in the soil bacterium *Bacillus megaterium* [103]. A genetic locus involved in the system, designated *fru*, contains three genes: *fruP*, *fruA*, and *fruR*. FruP encoded by *fruP* gene is a putative non-PTS sugar permease mediating translocation of fructose across the membrane, and *fruA* gene encodes β-fructosidase that catalyzes the hydrolysis of sucrose and raffinose [103]. A transcriptional repressor encoded by *fruR* gene regulates transcription of *fruPA* genes by interacting with the *fruP* promotor region [103].

Analysis of its sequence suggests that FruP of *B. megaterium* is closely related to sugar/H^+ symport proteins of the MFS, although its sugar transport activity has not been demonstrated [93, 103]. Furthermore, a gene that possesses high sequence homology with *fruP* of *B. megaterium* is present in *E. coli*. This *fruP* gene of *E. coli* is assumed to encode a putative fructose transporter FruP, yet its sugar transport activity has not been reported.

Sequencing of *fruP* gene of *E. coli* reveals its product shares a high degree of similarity with LacY and other members of the OHS of the MFS (42%

identity and 60% similarity with LacY sequence). Homology threading of FruP protein sequence with the structure of LacY as template suggests that FruP is likely to have twelve transmembrane domains organized into pseudo-symmetrical six-helix bundles (Fig. 3.1). In this chapter, experiments demonstrating substrate specificity of FruP is presented and the structural and functional characteristics of FruP based on its similarity with LacY and CscB are described. As previous mutational analysis of LacY has elucidated the interaction between the amino acid residues at sugar-binding site and its substrates [reviewed in 104], site-directed mutagenesis was used to demonstrate the significance of conserved residues at a putative sugar-binding site of FruP.

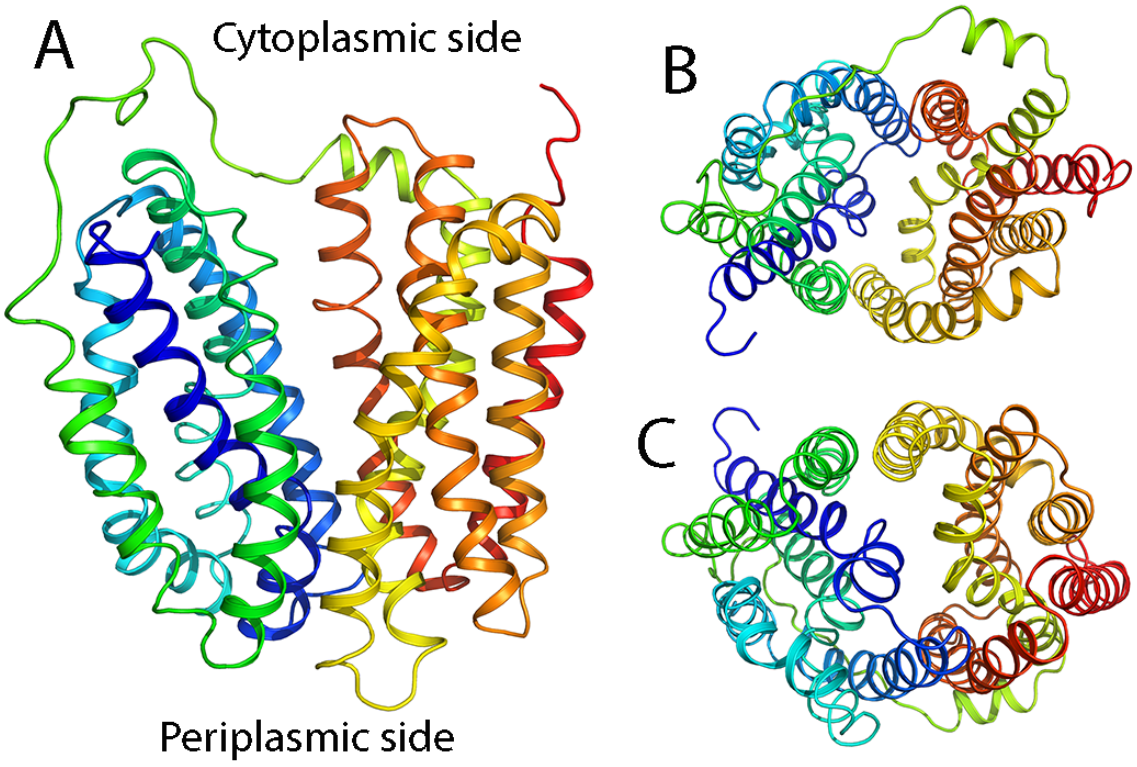

Fig. 3.1. FruP of *E. coli* threaded into LacY structure (PDB code: 1PV7). Transmembrane helices are depicted as ribbons colored from blue (helix I) to red

(helix XII). The cytoplasmic side is at the top and the periplasmic side is at the bottom. FruP structure is displayed by using Pymol 1.4. (A) View parallel to the membrane. (B) Cytoplasmic view. (C) Periplasmic view.

3.2 Results

3.2.1 Fructose or sucrose transport by FruP

The accumulation of fructose occurs at a high rate for 10 min and reaches a steady-state level of 140 nmol/mg protein (Fig. 3.2A), and immunoblots of membrane fractions of FruP probed with antibody against a C-terminal 6-His tag revealed a single protein with an apparent M_r of approximately 33 kDa (Fig. 3.2C). Also, similar accumulation of fructose is exhibited in RSO membrane vesicles expressing FruP (Fig. 3.2D). In addition, FruP catalyzes the transport of sucrose although the accumulation does not occur at as high rate as that of fructose (Fig. 3.2B).

In order to determine substrate affinity for transport in FruP, the kinetic values for fructose and sucrose transports were determined (Fig. 3.2E & F). *E. coli* T184 cells expressing *fruP* gene accumulate fructose with K_m of approximately 9.1 mM and V_{max} of 41 nmol/min/mg protein (Fig. 3.2E). In contrast, even though transport of sucrose is observed in FruP, the low rate of sucrose transport precludes reliable kinetic studies (Fig. 3.2F).

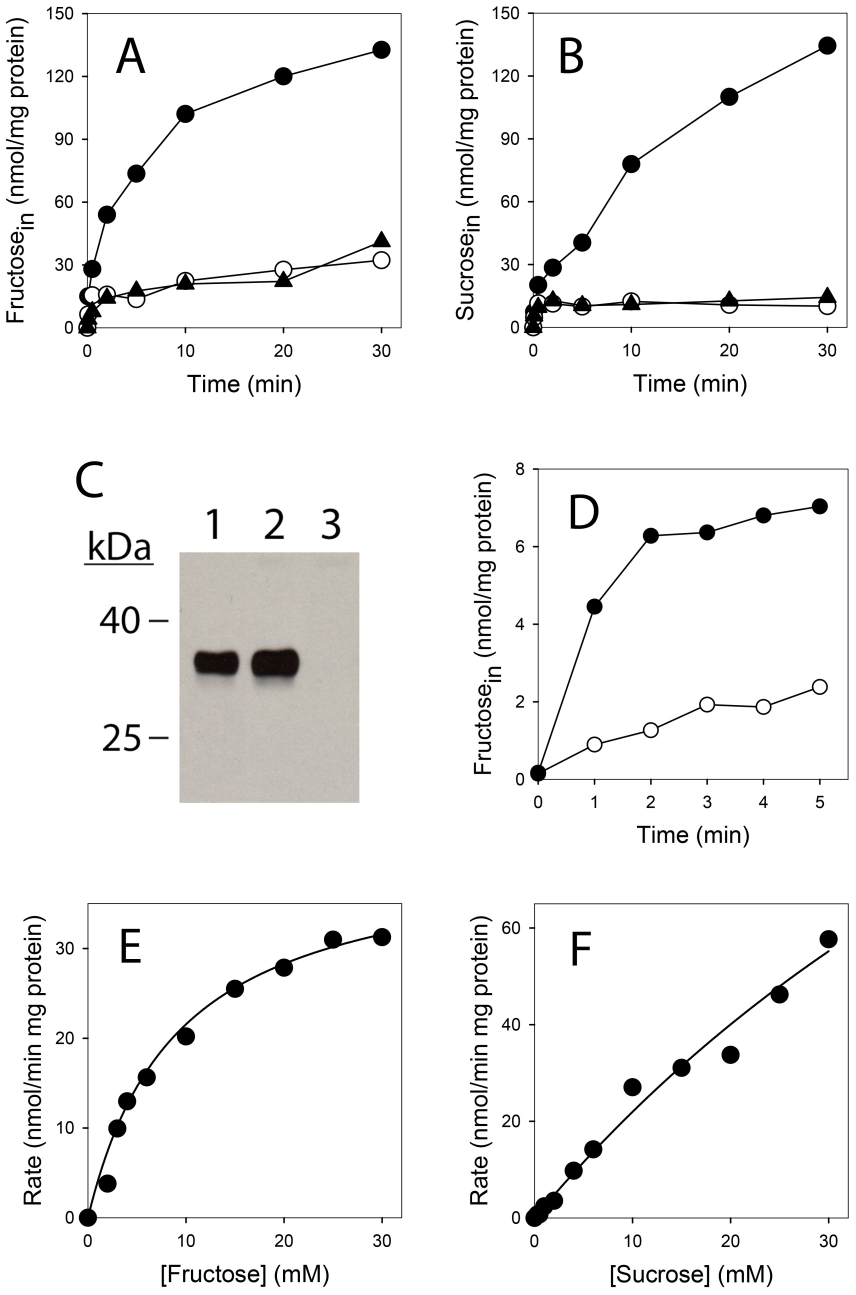

Fig. 3.2. Transport activity of FruP. Time courses of fructose (A) and sucrose (B) accumulation by *E. coli* T184 cells expressing FruP (●), LacY (▲), and no permease (○) were measured in 50 µl aliquots of cell suspensions containing 70 µg of total protein and 6 mM of [^{14}C]fructose or 4 mM of [^{14}C]sucrose as described in *Materials and Methods*. (C) Expression of FruP as determined by Western blotting. Lane 1, FruP; Lane 2, LacY; Lane 3, no permease. (D) Time courses of fructose accumulation by RSO membrane vesicles expressing FruP (●) and no permease (○). Also, kinetic analysis of fructose and sucrose transport by *E. coli* T184 expressing FruP was assayed for fructose (E) and sucrose (F) transport. Concentration dependence of the initial rates of accumulation of

fructose or sucrose by *E. coli* T184 cells expressing FruP was measured as described in *Materials and Methods.* Hyperbolic fit shown as a solid line with estimated kinetic parameters for fructose: K_m = 9.1 ± 2.4 mM, and V_{max} = 41 nmol/min·mg protein. Kinetic parameters for sucrose were not determined due to low rate of sucrose transport.

3.2.2 Effect of various sugars on the transport of fructose by FruP

Fructose transport by FruP is not inhibited by glucose, which has no effect on kinetic parameters of fructose transport (Fig. 3.3). Also, inhibition of fructose transport is not observed with any other sugars that do not contain furanosidic ring, including galactose, lactose, melibiose, maltose, mannose, rhamnose, and ribose (data not shown). Together with the observation that cells expressing *fruP* gene accumulate fructose and sucrose, these studies confirm the conclusion that the specificity of FruP directed toward the furanosidic ring of the substrate.

In order to further evaluate importance of fructose moiety of substrate, various fructofuranosides including turanose (3-*O*-α-D-glucopyranosyl-D-fructose), lactulose (4-*O*-β-D-galactopyranosyl-D-fructose), and palatinose (6-*O*-α-D-glucopyranosyl-D-fructose) were tested for their ability to inhibit the transport of fructose by FruP (Fig. 3.4A). While 10 mM palatinose or lactulose weakly inhibit fructose transport, turanose has no effect on fructose transport, suggesting that the C3-OH group on the fructofuranosyl ring may be important for recognition by FruP. Furthermore, analysis using Lineweaver-Burk and Dixon plots demonstrates that sucrose is a competitive inhibitor of fructose transport with a K_i of 50–60 mM (Fig. 3.4B)

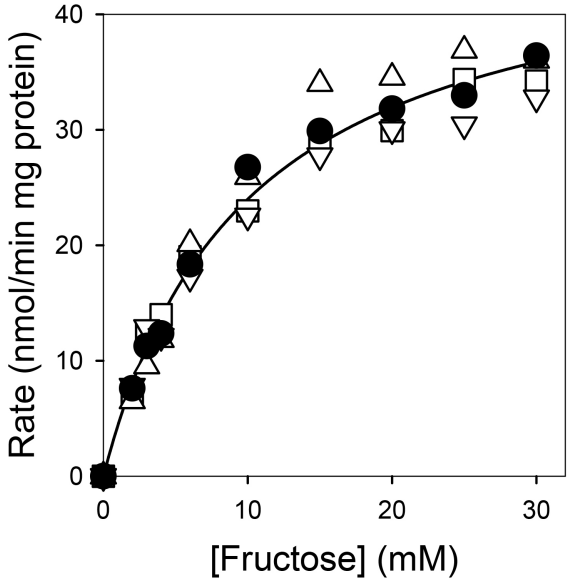

Fig. 3.3. Effect of glucose on the transport of fructose by FruP. Initial rates of accumulation of [^{14}C]fructose by *E. coli* T184 cells expressing FruP were measured and fitted as described in the legend of Fig. 3.2E in the absence of glucose (●) or in the presence of 10 (△), 20 (▽), or 30 mM glucose (□).

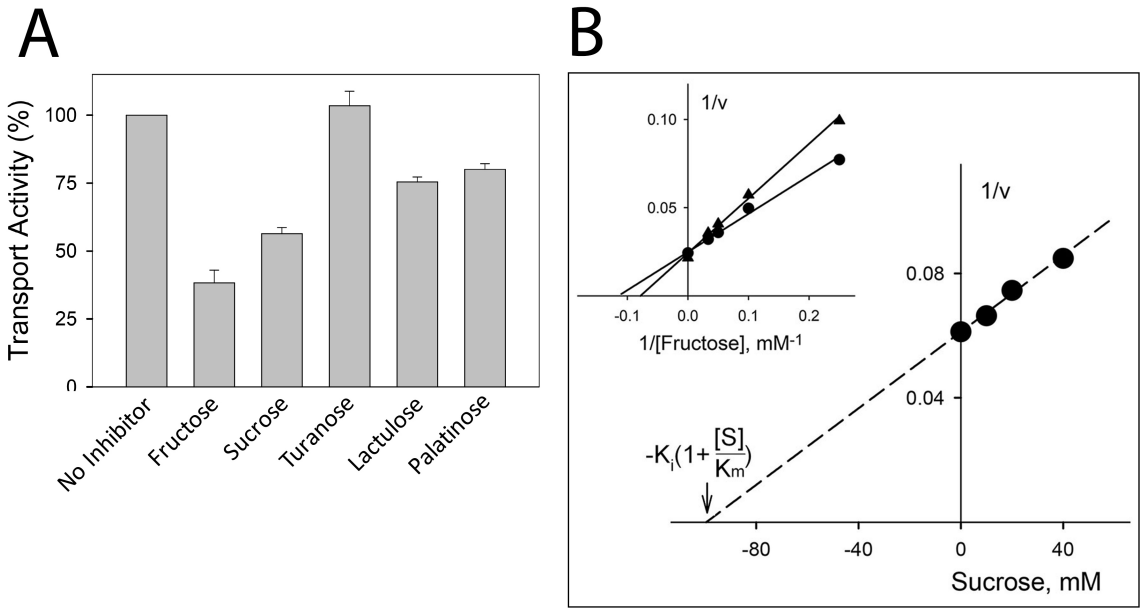

Fig. 3.4. Effect of fructofuranosides on fructose transport by FruP. Various fructofuranosides were tested for their ability to inhibit transport of fructose. Accumulation of [^{14}C]fructose (6 mM) by *E. coli* T184 cells expressing FruP was measured as described in Fig. 3.2A for 10 min without additions (100% activity)

or in the presence of 10 mM unlabeled fructose, sucrose, turanose, lactulose, or palatinose. (B) Concentration dependence of sucrose inhibition. Initial rates of [^{14}C]fructose transport (1 min) were measured as in panel A at various concentrations of unlabeled fructose (10, 20, or 40 mM). The inset demonstrates competitive inhibition of the transport of [^{14}C]sucrose by 20 mM fructose (▲) with an estimated K_i of ~50 mM and an unchanged V_{max} of 40 nmol/min·mg protein. A Dixon plot exhibits a linear fit of the data (broken line) with an estimated K_i of ~60 mM.

3.2.3 Residues involved in sugar binding

Sequencing of the *fruP* gene reveals a high degree of similarity with LacY, and many of the irreplaceable residues for substrate binding and H^+ translocation in LacY are conserved in FruP. As revealed by site-directed and Cys- and Gly-scanning mutagenesis approaches, LacY contains four residues that are critical with respect to the binding of lactose: Glu126, Arg144, Trp151, and Glu269 [reviewed in 43, 104].

Glu125 and Arg143 of FruP are homologous to Glu126 and Arg144 of LacY, which are likely charge-paired [63, 105-108]. As shown in Fig. 3.5A, replacements of Glu125 or Arg143 of FruP reduce fructose transport activity in a manner similar to those observed with the replacement of Glu126 or Arg144 in LacY [105]. E125D catalyzes active fructose transport at a relatively slow rate to an almost same steady-state level of accumulation as the WT. Also, markedly decreased transport activities are observed in mutants E125Q, R143A, and R143K.

Glu269 in LacY is a critical residue for sugar recognition and binding. Any replacements of Glu269 in LacY, with exception of Asp, completely abolish lactose transport [109-111]. Although three-dimensional model shows Glu267 in

FruP is positioned one helical turn closer to the cytoplasmic face of the membrane than Glu269 in LacY, replacement of Glu267 in FruP with Asp, Ala, or Gln exhibit a dramatic decrease in the transport of fructose, indicating the functional importance of Glu267 in fructose transport (Fig. 3.5B).

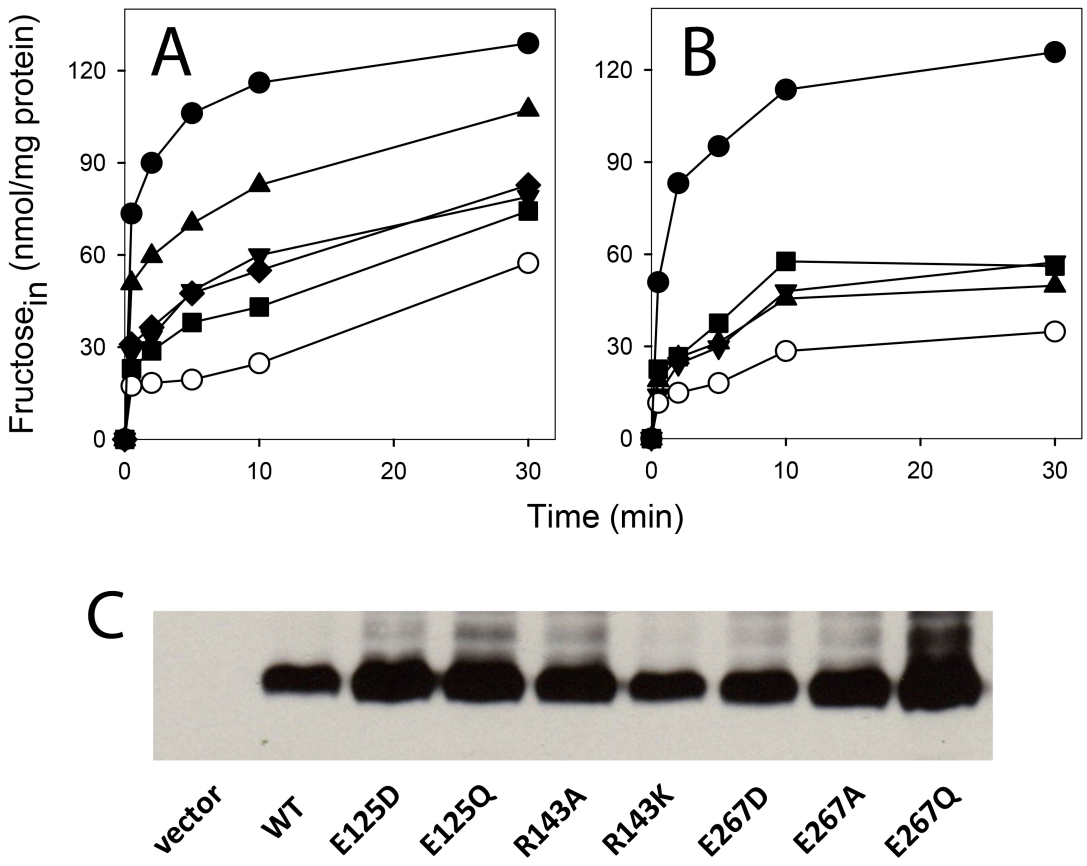

Fig. 3.5. Functional significance of putative sugar binding site residues E125, R143, and E267 in FruP. (A) Time courses of fructose accumulation by *E. coli* T184 expressing WT FruP (●), no permease (○) or FruP mutants: E125D (▲), E125Q (▼), R143A (■), and R143K (◆) were obtained as described for Fig. 3.2. (B) Time courses of fructose accumulation by *E. coli* T184 expressing wild-type FruP (●), no permease (○) or FruP mutants: E267D (▲), E267A (▼), and E267Q (■) were obtained as described for Fig. 3.2. (C) Expression of FruP mutants as determined by Western blotting. WT FruP and mutants are expressed to similar levels in the membrane of *E. coli*.

Trp150 of FruP is in the homologous position as Trp151 of LacY, which hydrophobically interacts with galactoside substrates [51, 112]. However, in FruP, the replacement of Trp150 with Ala or Tyr has no effect on the fructose transport activity (Fig. 3.6A). W150A and W150Y exhibit the similar rate of active fructose transport and steady-state level of accumulation to those of WT, indicating no involvement of Trp150 in the activity of substrate transport. Instead, the replacement of Trp23, situated adjacent to Trp150, with Ala significantly decreases the transport activity (Fig. 3.6B). Because W23Y catalyzes active fructose transport as WT, the hydrophobic moiety situated at this position appears to be important for fructose transport.

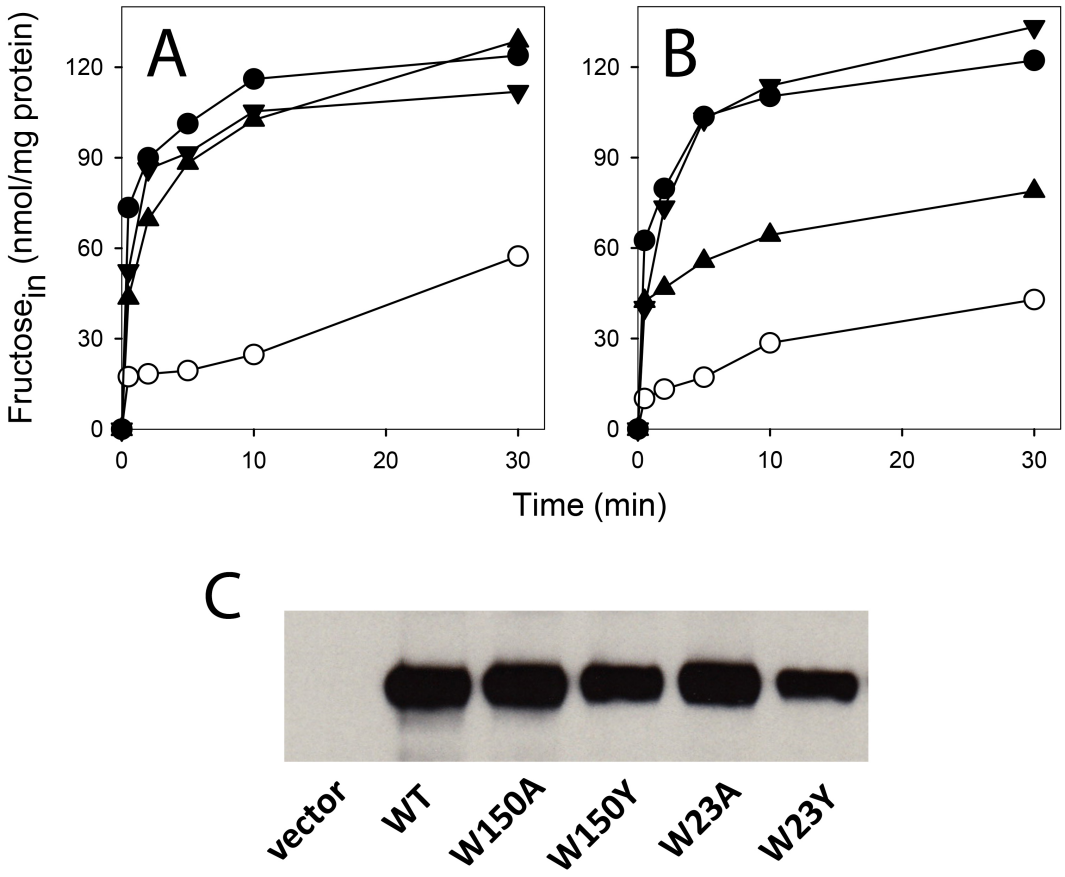

Fig. 3.6. Functional significance of putative sugar binding site residues W150 and W23 in FruP. (A) Time courses of fructose accumulation by *E. coli* T184 expressing wild-type FruP (●), no permease (○) or FruP mutants: W150A (▲), W150Y (▼) were obtained as described for Fig. 3.2. (B) Time courses of fructose accumulation by *E. coli* T184 expressing wild-type FruP (●), no permease (○) or FruP mutants: W23A (▲) and W23Y (▼) were obtained as described for Fig. 3.2. (C) Expression of FruP mutants as determined by Western blotting. WT FruP and mutants are expressed to similar levels in the membrane of *E. coli*.

4.3 Discussion and conclusions

MFS transporters are divided into over 70 subfamilies in the Transporter Classification Database (TCDB: #2.A.1) but many of the subfamilies are of unknown or only putative functions have been proposed. A putative fructose transporter FruP of *E. coli* exhibits high level of sequence homology with OHS members of the MFS, yet its function has not been investigated. However,

intensive studies on lactose/H^+ symport of LacY and other MFS transporters provide a framework for understanding functional and structural characteristics of FruP.

As characteristics of MFS proteins, FruP is likely to contain twelve transmembrane helices organized into two pseudosymmetrical domains. However, despite the structural similarities between FruP and LacY, their substrate specificities are strikingly different. LacY is selective for disaccharides containing a D-galactopyranosyl ring, as well as D-galactose, and has no interaction with D-glucopyranosides or D-glucose [54-57]. In contrast, FruP is selective for fructose and disaccharides containing a D-fructofranosyl ring and has no affinity for D-glucopyranosides or D-glucose (Fig. 3.2 & 3.3). Moreover, kinetic analysis elucidates the affinity of FruP for different substrates; FruP has higher affinity for the transport of fructose than for that of any other furanosides (Fig. 3.2). In FruP, because the substrates with furanosidic ring are transported with higher affinity in the form of monosaccharide than that of disaccharide, the size of substrate may be critical for the determination of transport affinity in FruP.

Furthermore, inhibition studies with various fructofuranosides suggest that the C3-OH of fructose moiety in sugar substrate is crucial for interaction with FruP (Fig. 3.4). Fructose transport by FruP is inhibited by sucrose, lactulose, and palatinose, in which glucose or galactose moiety is attached to the C2, C4, and C6 atoms of the fructose moiety, respectively. On the other hand, turanose, which contains galactose moiety at the C3 atom of its fructose moiety, has no effect on fructose transport. These suggest that the C3-OH of fructose moiety is

likely a key player in interacting with FruP. Interestingly, as shown in the previous chapter of this thesis, the same determinant for substrate specificity is seen in CscB where specificity is also directed toward the fructofuranosyl moiety of sucrose.

Site-directed mutagenesis analysis of the putative sugar-binding site of FruP elucidates its similarities and differences with that of LacY. Mutations at Glu125 and Arg143 of FruP lead to decreased transport activity in a manner similar to that observed in LacY with mutations of corresponding residues (Fig. 3.5A). E125D exhibits relatively slow rate of fructose transport and replacement of Glu125 or Arg143 with neutral amino acyl side chains significantly lowers the rate of substrate transport.

A marked difference between FruP and LacY is the position of hydrophobic moiety that interacts with substrate. Replacement of Trp150 in FruP has little or no effect on the transport activity (Fig. 3.6A). W150Y and W150A have the same rate of fructose transport and steady-state level of fructose accumulation as WT, indicating that Trp150 is not involved in FruP transport. This is contrary to the homologous residue Trp151 in LacY, where the aromatic ring hydrophobically interacts with the galactosidic ring of substrate [51, 112]. However, removal of aromatic ring at Trp23 in FruP, situated adjacent to Trp150, significantly lowers transport activity (Fig. 3.6B), suggesting its interaction with substrate. Moreover, the finding that replacement of this residue with Tyr rescues active transport indicates that an aromatic side chain at this position plays an

important role in substrate binding and may interact hydrophobically with substrate.

Also, Glu267 in FruP, which is homologous to irreplaceable Glu269 in LacY, is important for fructose transport. Glu269 of LacY is the acceptor of hydrogen bonds from the C4-OH group of the galactopyranosyl ring [58, 59]. Although threading of FruP shows that Glu267 is positioned one helical turn closer to the cytoplasm than Glu269 in LacY, its replacement with Asp, Ala, or Gln shows significantly decreased level of fructose transport (Fig. 3.5B). However, in FruP, because the involvement of Trp150 in sugar binding is not observed and the homology threading shows large distance between Glu267 and Trp23, Glu267 may be involved in the translocation of H^+, not in the binding of sugar substrate (Fig. 3.7).

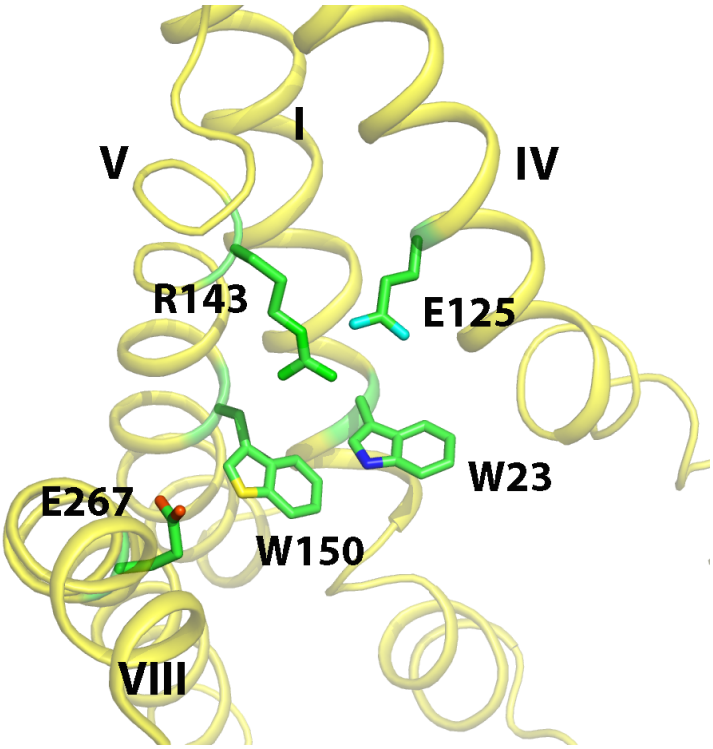

Fig. 3.7. Cytoplasmic view of putative sugar-binding site of FruP. Transmembrane helices are numbered with Roman numerals. The FruP model was build by homology modeling using the X-ray structure of LacY (PDB code: 1PV7) as template. The figure was generated with Pymol 1.4.

Chapter 4

Dynamics of FucP and CscB purified in detergent

4.1 Introduction

L-Fucose (6-deoxy-L-galactose) is a naturally occurring methylpentose found in mammalian cells as a major component of N- and O-linked glycans and glycolipids [113, 114]. In addition, L-fucose, which is present in bacterial polysaccharides, is needed for adhesion and localization and is also utilized by a variety of microorganisms as a carbon and energy source [115, 116]. In *E. coli*, transport of L-fucose is mediated by the transmembrane protein FucP, which is encoded by *fucP*, one of the genes of the *fuc* regulon that is responsible for the catabolism of L-fucose [117-119]. FucP consists of 438 amino acids (47,773 Da) and is an L-fucose/H^+ symporter belonging to the fucose-galactose-glucose/H^+ symporter (FGHS) subfamily of the MFS [13, 120, 121]. FucP catalyzes symport of L-fucose and H^+ across the cytoplasmic membrane by transducing free energy stored in the electrochemical H^+ gradient into a substrate concentration gradient [13, 117, 120].

FucP shares limited sequence homology with other sugar/H^+ symporters [120], but the X-ray crystal structure reveals many characteristics observed in other MFS transporters [91]. Thus, FucP contains 12 transmembrane α-helical domains arranged into two pseudo-symmetrical 6-helix bundles surrounding a deep water-filled cavity with the N and C termini on the cytoplasmic side of the membrane (Fig 4.1). However, unlike other MFS transporters, FucP is in an outward-facing conformation; the cavity is open on the periplasmic side and

tightly sealed on the cytoplasmic side. Although it is likely that FucP functions by an alternating access mechanism like LacY [reviewed in 69], nothing is known about its functional dynamics.

Out of a total of six Trp residues, FucP contains two – Trp38 (helix I) and Trp278 (helix VII) – that are on opposing walls of the open periplasmic cavity ~16 Å across from each other (Fig. 4.1). If FucP functions by an alternating access mechanism, sugar binding might cause closure of the periplasmic cavity. In order to test this notion, Trp fluorescence of purified FucP in the detergent dodecyl-β-D-maltopyranoside (DDM) was studied. Remarkably, binding of L-fucose and other sugar substrates induces ~20% quenching, and it is demonstrated that these two Trp residues are responsible for the effect. Moreover, evidence is presented indicating that these Trp residues play a role in the transport mechanism, possibly as components of the sugar-binding site.

Furthermore, the unique location of Trp residues provides a novel method for analyzing structural dynamics of not only FucP but also CscB that contains multiple Trp residues on the walls of the hydrophilic cavity. Thus, quenching of Trp fluorescence is elicited in CscB by addition of its substrates in a concentration-dependent manner while non-substrates have relatively small effects.

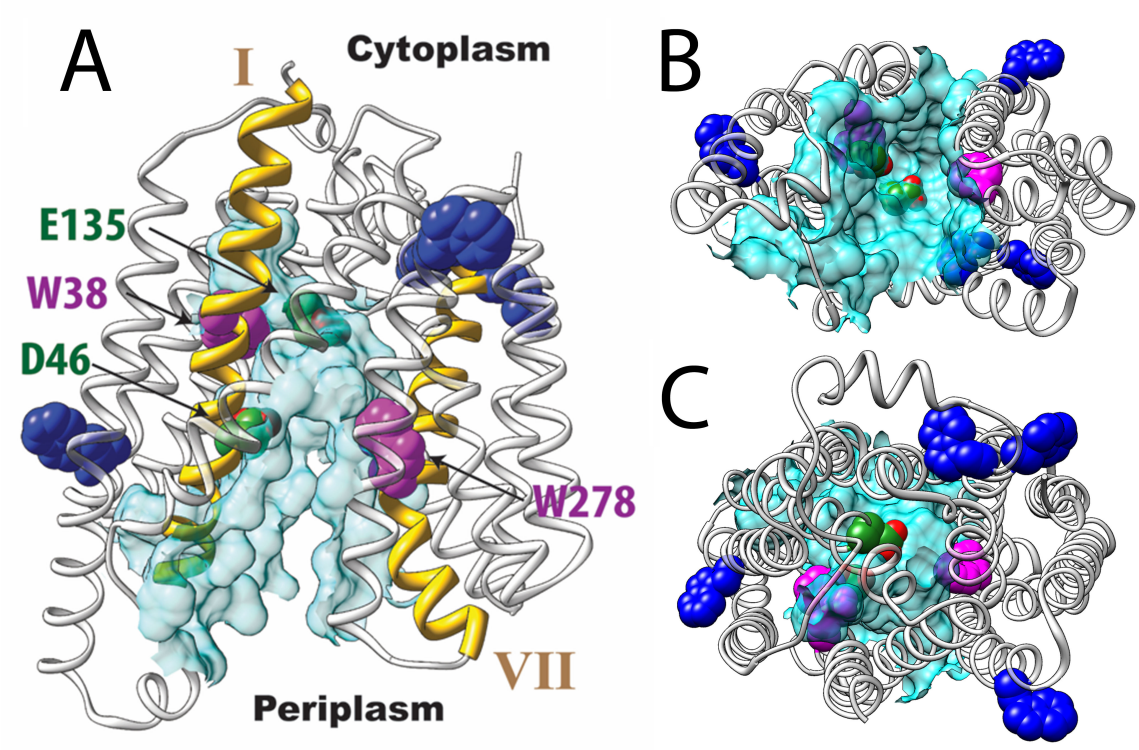

Fig. 4.1. Two Trp residues on the surface of cavity walls of FucP. (A) Side view. W38 (helix I) and W278 (helix VII) are shown as pink spheres, and the distance between them is approximately 16 Å. The other 4 Trp residues are shown as blue spheres. Two acidic residues, D46 (helix I) and E135 (helix IV), are shown as green spheres. Helices I and VII are shown in gold, and water-accessible surface of cavity is shown in light blue. (B) Periplasmic view. (C) Cytoplasmic view. The figures were prepared using UCSF Chimera and the water-accessible surface was calculated using CASTp webtool with a probe size of 1.4 Å.

4.2 Results

4.2.1 Overexpression of *fucP* gene

In order to identify the *fucP* gene product, plasmids carrying the gene were engineered with C-terminal 8-histidine tag. Immunoblots of membrane fractions of wild-type FucP probed with antibody against histidine tag revealed a single protein with an apparent M_r of approximately 35 kDa (Fig. 4.2). Like most hydrophobic membrane proteins, FucP migrates faster on PAGE than its actual mass of 47,773 Da due to excess dodecyl sulfate binding [122].

Although the *fucP* gene was initially placed under pET21b expression vector, the level of FucP protein expression in the membrane was relatively low as detected by Western blot analysis (Fig. 4.2A, lanes 1 and 3). In order to optimize expression, the *fucP* gene with C-terminal histidine tag was placed under the L-arabinose promoter of pBAD expression vector, which resulted in markedly higher expression level of the protein after induction with 0.02 % L-arabinose (Fig. 4.2A, lanes 2 and 4). Also, expression of pBAD/*fucP*/His8 was tested in various *E. coli* strains. The protein was expressed to approximately equal levels in the membrane of *E. coli* XL-1 Blue and T-184 cells while BL21 cells exhibited slightly lower level of its expression (Fig. 4.2B).

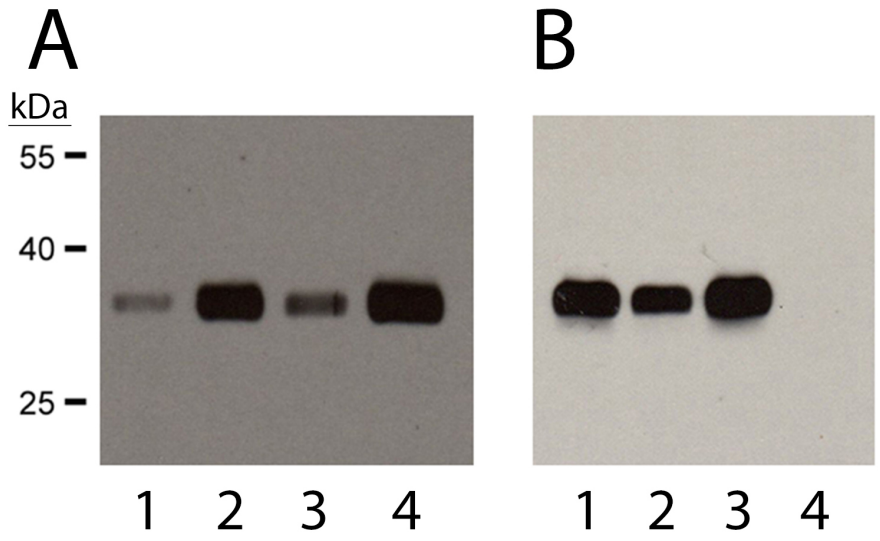

Fig. 4.2. Expression of FucP detected by Western blotting. (A) pET21b/*fucP*/His8 (lanes 1 and 3) or pBAD/*fucP*/His8 (lanes 2 and 4) expressed in 2 µg (lanes 1 and 2) or 4 µg (lanes 3 and 4) of the membranes from *E. coli* XL-1 Blue cells. Cells harboring pET21b/*fucP*/His8 or pBAD/*fucP*/His8 were induced for 2 hours with 1mM isopropyl β-D-1-thiogalactopyranoside (IPTG) or 0.02% L-arabinose, respectively. (B) Expression of FucP from plasmid pBAD/*fucP*/His8 in various *E. coli* strains. FucP expressed in 4 µg of the membranes of T184 (lane 1), BL21 (lane 2), or XL-1 Blue (lane 3) cells is shown. pBAD without permease in XL-1 Blue cells is shown in lane 4.

4.2.2 Active transport of radiolabeled L-fucose by FucP

Transport activity of L-fucose by FucP was analyzed using *E. coli* T184 cells harboring plasmid pBAD/*fucP*/His8. The cells accumulate L-[5,6-^{3}H]fucose to a significant level, in contrast to cells transformed with vector devoid of *fucP* exhibiting only negligible accumulation of the sugar (Fig. 4.3A). The transport of L-fucose increased at a rapid rate for ~40 sec and reached a steady-state level of ~85 nmol/mg protein, and similar accumulation of L-fucose was also observed in RSO membrane vesicles expressing FucP (Fig. 4.3C). In addition, rates of transport as a function of L-fucose concentration follow a hyperbolic relationship with a K_m of 71.4 μM and a V_{max} of 120 nmol/min·mg protein (Fig. 4.3B).

Moreover, addition of excess non-radiolabeled L-fucose to the cells caused rapid release of accumulated radiolabeled L-fucose (Fig. 4.3A, arrows). As a result, approximately 80% of the accumulated L-fucose was recovered from the cells, demonstrating that metabolization of L-fucose occurs relatively slowly in cells overexpressing FucP.

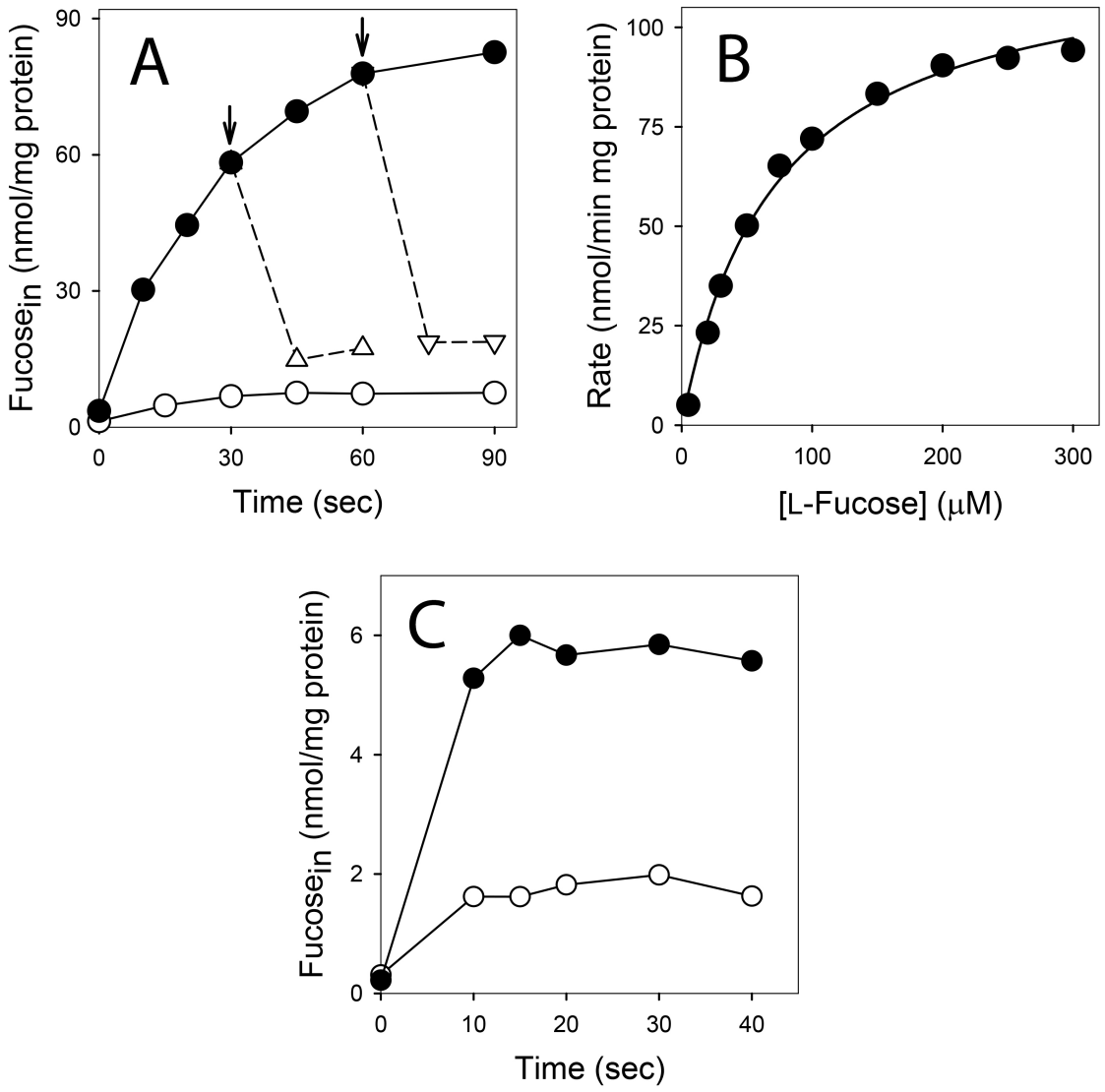

Fig. 4.3. Transport activity of FucP. (A) Time courses of accumulation of L-[5,6-^{3}H]fucose by *E. coli* T-184 cells harboring plasmid pBAD/*fucP*/His8 (●) or pBAD without permease (○) were measured at 0.4 mM L-fucose as described in *Materials and Methods*. Arrows indicate the time of addition of 20 mM non-radiolabeled L-fucose: at 30 sec (△, broken line) or 60 sec (▽, broken line). (B) Concentration dependence of the initial rates of accumulation of L-fucose by *E. coli* T-184 cells expressing FucP measured as described in *Materials and Methods*. The hyperbolic fit is shown as a solid line with the following estimated kinetic parameters: K_m = 71.4 ± 4.8 μM, and V_{max} = 120 nmol/min·mg protein. (C) Time courses of accumulation of L-[5,6-^{3}H]fucose by RSO membrane vesicles expressing pBAD/*fucP*/His8 (●) or pBAD without permease (○) were measured as described in panel A.

4.2.3 Purification of FucP

FucP was solubilized in DDM and purified to the homogeneity by cobalt affinity chromatography (Fig. 4.4). Fraction eluted with 200 mM imidazole (peak 3 fraction in Fig. 4.4A) yielded a single band on SDS-PAGE when stained with a highly sensitive silver procedure (Fig. 4.4B, lanes 7 and 8). The purified protein has an apparent M_r of ~35 kDa, which is in agreement with the M_r of FucP determined by Western blot analysis (Fig. 4.2).

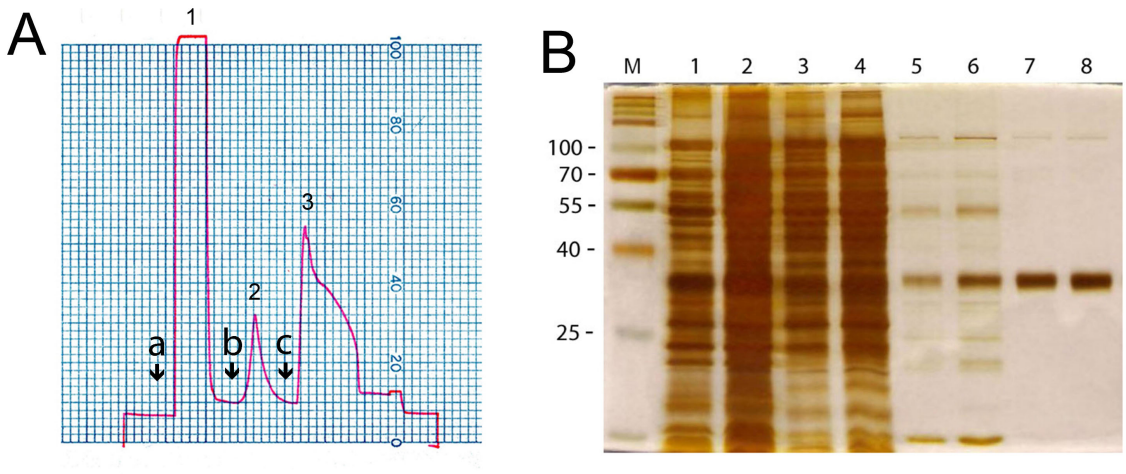

Fig. 4.4. Purification of His-tagged FucP by cobalt affinity chromatography. (A) Purification profile of chromatography. Membrane fraction solubilized with DDM was applied to 5-ml bed of cobalt resin in 50 mM NaP_i buffer (pH 7.5, with 0.01% DDM) (*arrow* a). 30 mM Imidazole was applied to remove impurities bound to resin nonspecifically (*arrow* b). 200 mM Imidazole was applied to elute FucP (*arrow* c) (B) Silver-stained SDS-PAGE gel of various fractions collected during purification of FucP. Lane 1, marker; lanes 2 and 3, DDM extract of membrane fraction (0.4 µl and 0.8 µl, respectively); lanes 4 and 5, flowthrough sample (0.4 µl and 0.8 µl of peak 1 fraction in panel A, respectively); lanes 5 and 6, wash (5 µl and 10 µl of peak 2 fraction in panel A, respectively); lanes 7 and 8, FucP purified in DDM (0.2 µg and 0.4 µg of protein, respectively).

4.2.4 Trp Fluorescence of FucP

Emission spectra of purified WT FucP with excitation at 295 nm in the absence or presence of different sugars are shown in Fig. 4.5. Addition of L-

fucose clearly induces quenching without shifting the λ_{max} at 327 nm, and the magnitude of the effect is dependent on the L-fucose concentration (Fig. 4.5A). Trp quenching is also observed upon the addition of D-arabinose, a substrate for FucP, although the effect of sugar concentration is less dramatic (Fig. 4.5B). In contrast, D-galactose, L-arabinose, sucrose and lactose exhibit a relatively small, non-specific effect (Fig. 4.5C & D; Fig. 4.6). The results are consistent with the substrate specificity of FucP [91, 117, 120].

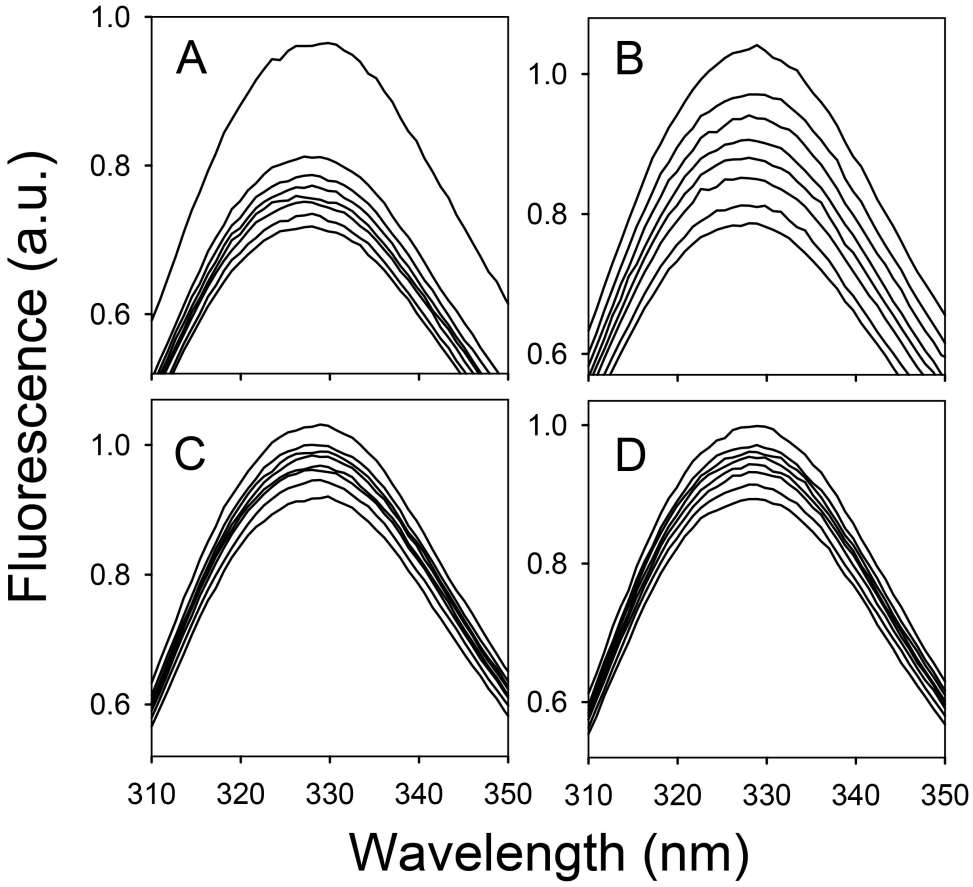

Fig. 4.5. Fluorescence emission of WT FucP. Emission spectra of purified, detergent-solubilized WT FucP was measured in the absence or presence of L-fucose (A), D-arabinose (B), D-galactose (C), and L-arabinose (D) at different concentrations (beginning at the top of the traces: 0, 0.5, 1, 2, 3, 5, 10, and 15

mM final concentration) as described in *Materials and methods*. The λ_{exc} was 295 nm.

4.2.5 Sugar affinities of FucP

The apparent affinity of FucP for substrate (K_d^{app}) was determined from the concentration of sugar that produces half-maximum quenching of Trp fluorescence (Fig. 4.6). WT FucP exhibits a K_d^{app} of 0.20 ± 0.01 mM for L-fucose, close to the K_d obtained by isothermal calorimetry [91], and a K_d^{app} of 1.85 ± 0.27 mM for D-arabinose. Thus, FucP has ~9-fold higher affinity for L-fucose than for D-arabinose. In contrast, the small degree of quenching observed with L-arabinose, D-galactose, sucrose and lactose is clearly non-specific, as these sugars are not substrates for FucP.

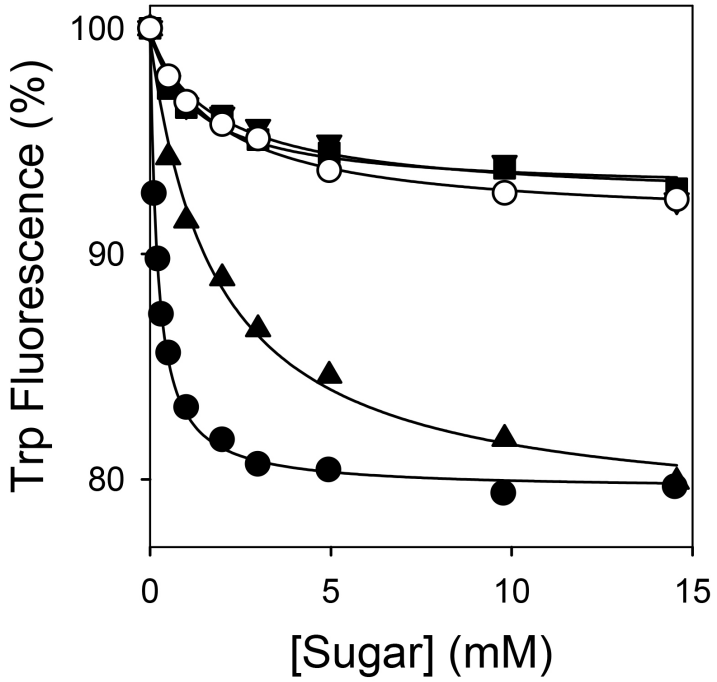

Fig. 4.6. Trp quenching with different sugars. Changes in Trp fluorescence (λ_{max} at 327 nm) in response to addition of L-fucose (●), D-arabinose (▲), D-galactose (▼), L-arabinose (■), sucrose or lactose (○) are plotted as a function of sugar concentration. The curves represent the average of two independent

measurements. The K_d^{app} values of WT FucP for L-fucose and D-arabinose observed in this experiment are 0.20 ± 0.01 and 1.85 ± 0.27 mM respectively. The change in Trp fluorescence observed in the presence of D-galactose, L-arabinose, sucrose and lactose is due to a nonspecific effect of these sugars, which are not substrates for FucP.

Trp fluorescence quenching in FucP is also induced by the addition of various fructosides (Fig. 4.7). Among fructosides tested, the addition of fructose induced the most evident Trp fluorescence quenching, although the effect of concentration is not as marked as that of L-fucose. WT FucP exhibits a K_d^{app} of 1.51 ± 0.41 mM for fructose. Quenching was also induced by the addition of turanose (3-*O*-α-D-glucopyranosyl-D-fructose), lactulose (4-*O*-β-D-galactopyranosyl-D-fructose), or palatinose (6-*O*-α-D-glucopyranosyl-D-fructose), but their affinities were too low to accurately determine of K_d values. In contrast, a small, non-specific effect was exhibited by sucrose (2-*O*-α-D-galactopyranosyl-D-fructose) as observed with L-arabinose. These results demonstrate that substrates of FucP include various fructosides except sucrose and suggest that the C2-OH group on the fructofuranosyl ring plays the predominant role in recognition and binding of fructosides.

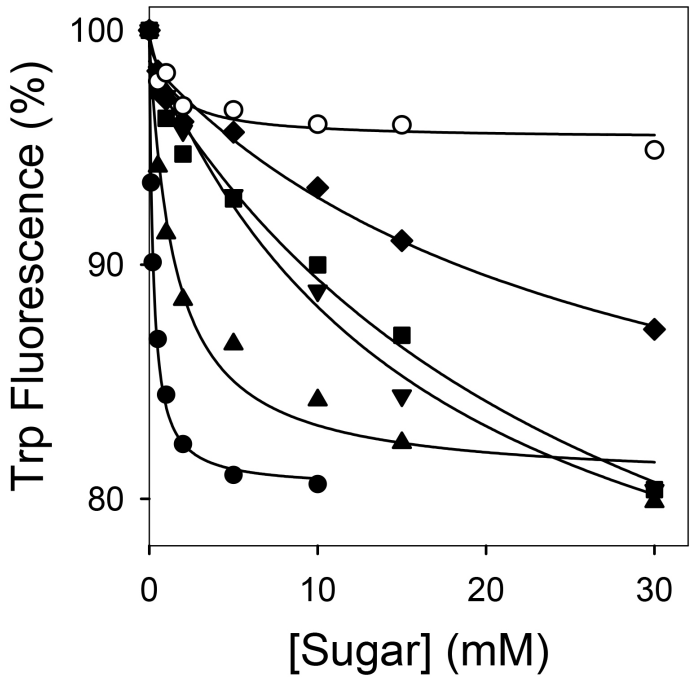

Fig. 4.7. Trp quenching with different fructosides. Changes in Trp fluorescence (λ_{max} at 327 nm) in response to addition of L-fucose (●), fructose (▲), palatinose (▼), lactulose (■), turanose (◆), and sucrose or L-arabinose (○) are plotted as a function of sugar concentration. The curves represent the average of two independent measurements. The K_d^{app} value of WT FucP for fructose observed in this experiment is 1.51 ± 0.41 mM.

4.2.6 Role of Trp38 (helix I) and Trp278 (helix VII) in quenching

FucP contains six Trp residues, and in order to identify which are involved in sugar-induced quenching, the two located on the walls of the outward-facing cavity – Trp38 and Trp278 – were replaced with Tyr or Phe by site-directed mutagenesis, and the effect of L-fucose on quenching was monitored (Fig. 4.8). As described above, quenching induced by L-fucose is dramatic with WT FucP yielding a K_d^{app} of 0.20 ± 0.01 mM, but markedly reduced with mutant W38Y, which manifests a K_d^{app} of 6.2 ± 1.1 mM. With mutant W38F, quenching is abrogated, and a K_d^{app} could not be determined. Trp quenching is less severely

reduced with mutant W278Y, which exhibits a K_d^{app} of 4.7 ± 0.8 mM, and with W278F a K_d^{app} of 0.31 ± 0.04 mM that is comparable to the K_d^{app} for WT FucP. Thus, Trp38 is clearly the major player in the quenching phenomenon. In any case, when Trp38 and Trp278 are both replaced with Tyr or Phe, almost no significant quenching is induced by L-fucose. The results demonstrate that both Trp residues – but predominantly Trp38 – are involved in sugar-induced quenching, while the remaining four Trp residues in FucP play little or no role in the phenomenon. It is also notable that with the exception of mutant W38F, which exhibits essentially no quenching, each of the other Trp mutants shows a marked decrease in apparent affinity for L-fucose.

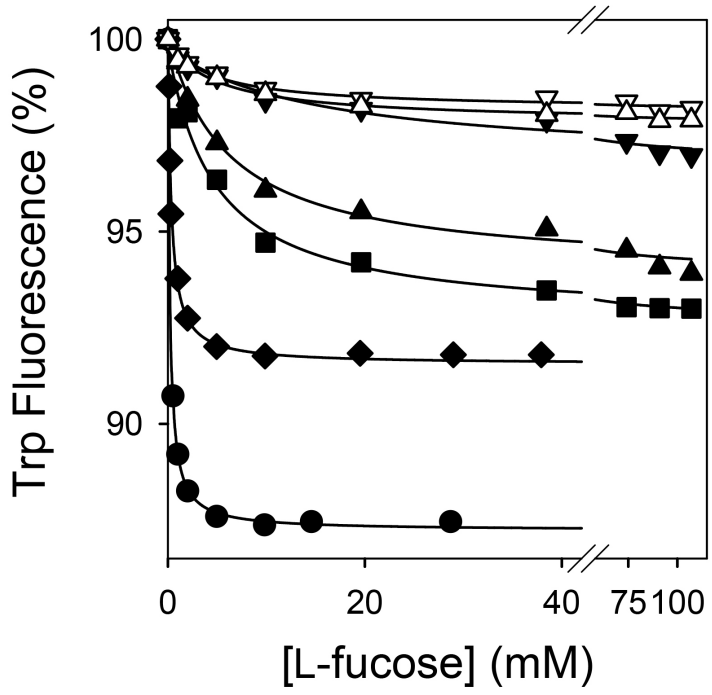

Fig. 4.8 Trp quenching by Trp38 and Trp278 mutants. Trp fluorescence of purified Trp38 or Trp278 mutants was measured at a λ_{em} of 327 nm in the absence or presence of L-fucose at given concentrations as in Fig. 4.6 and plotted after correction for fluorescence quenching for the non-specific quenching by L-arabinose. The curves represent the average of two independent

measurements. (●) WT; (▲) W38Y; (▼) W38F; (■) W278Y; (◆) W278F; (△) W38Y/W278Y; (▽) W38F/W278F.

4.2.7 Active transport of W38 or W278 mutants (uphill L-fucose/H^+ symport)

E. coli T184 cells expressing WT FucP catalyze accumulation of 40 μM L-fucose at a rapid rate for ~20 s to a steady-state level of ~7 nmol/mg of protein within 30 s (Fig. 4.9). In contrast, mutants W38Y, W38F and W38I exhibit decreased rates of L-fucose transport to steady-state levels of 20-50% of WT (Fig. 4.9A). Mutant W278I transports ~70% as well as WT, while mutants W278Y and W278F transport L-fucose at reduced rates to essentially the same steady state as WT (Fig. 4.9B), Finally, replacing both Trp residues at position 38 and 278 with Tyr, Phe or Ile appears to yield the averaged activity of the individual Trp38 and Trp278 mutants (Fig. 4.9C).

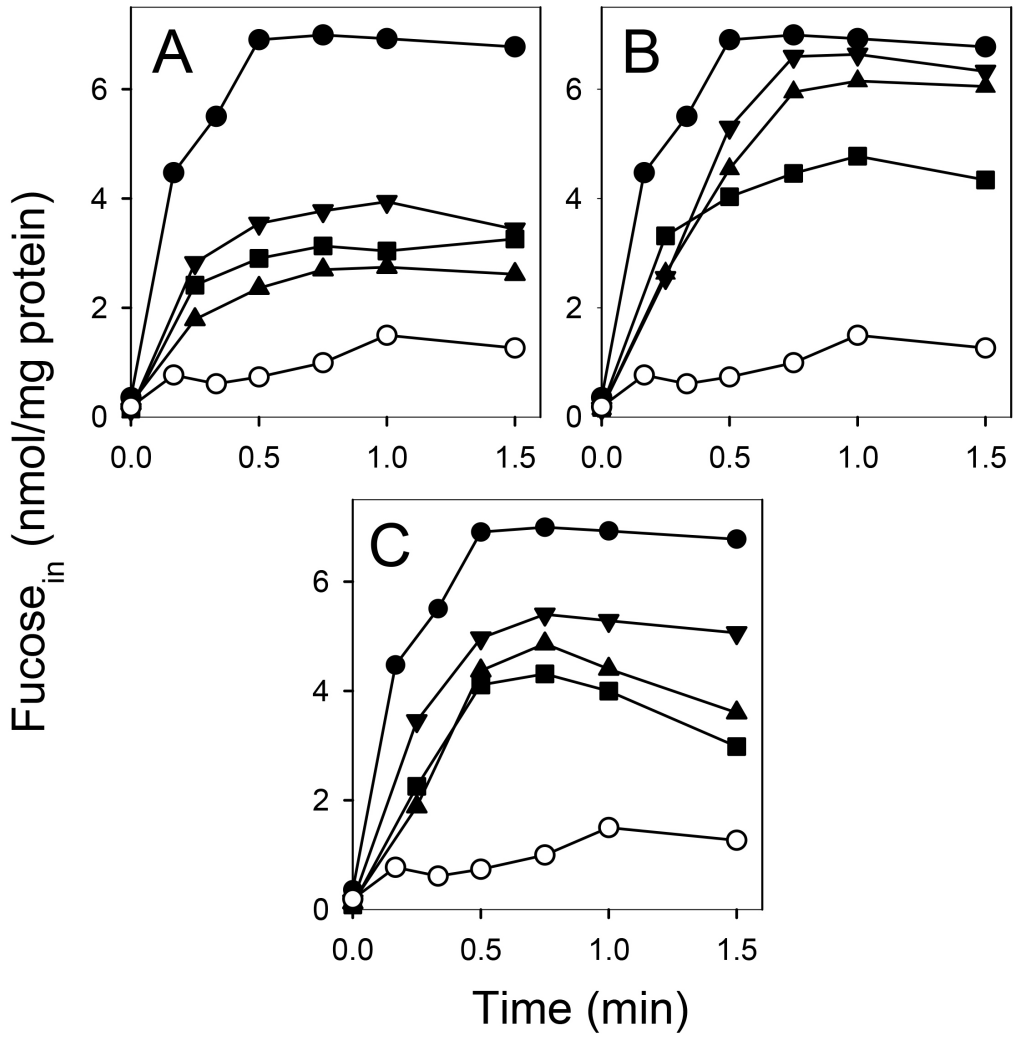

Fig. 4.9. L-Fucose transport of W38 or W278 mutants. T184 cells transformed with plasmid encoding WT FucP or mutants were grown and assayed as described in *Materials and Methods*. (A) Time courses of accumulation of 40 μM L-fucose by cells expressing WT (●), W38Y (▲), W38F (▼), W38I (■), or no permease (○). (B) Time courses of accumulation of 40 μM L-fucose by cells expressing WT (●), W278Y (▲), W278F (▼), W278I (■), or no permease (○). (C) Time courses of accumulation of 40 μM L-fucose by cells expressing WT (●), W38Y/W278Y (▲), W38F/W278F (▼), W38I/W278I (■), or no permease (○).

4.2.8 Asp46 and Glu135

Based on mutagenesis studies, Dang et al. [91] suggested that both Asp46 and Glu135 are involved in H^+ translocation. Therefore, the effect of mutations at these positions on Trp quenching was tested (Fig. 4.10). Since

Glu135 mutants do not bind L-fucose [91], it is not surprising that mutants E135Q or E135D exhibit little or no L-fucose-induced quenching. In contrast, Asp46 is apparently an 'uncoupled' mutant that binds L-fucose well and catalyzes counterflow, but is unable to catalyze uphill L-fucose/H^+ symport. Mutant D46E quenches Trp fluorescence like WT with a K_d^{app} of 0.50 ± 0.05 mM (i.e., ~twice the K_d^{app} of WT), and mutant D46N is somewhat less effective but has a K_d^{app} of 0.43 ± 0.06 mM, close to the K_d^{app} of WT FucP. Clearly, Asp46 is not involved in the conformational change that leads to quenching of Trp fluorescence.

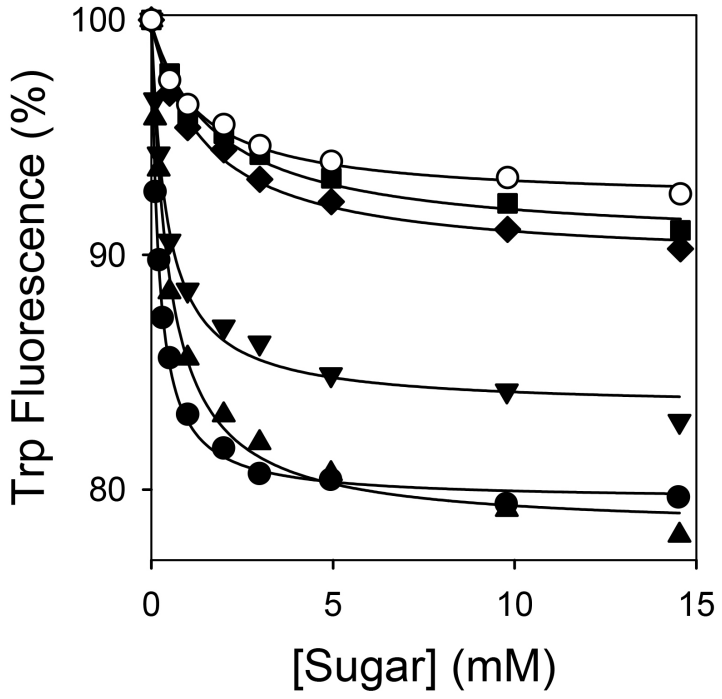

Fig. 4.10. Trp quenching by Asp46 or Glu135 mutants. Trp fluorescence of purified Asp46 or Glu135 mutants was measured at a λ_{em} of 327 nm in the absence or presence of L-fucose at given concentrations as in Fig. 4.6. The curves represent the average of two independent measurements. (●) WT; (▲) D46E; (▼) D46N; (■) E135D; (◆) E135Q. The K_d^{app} values for D46E and D46N are 0.50 ± 0.05 or 0.43 ± 0.06 mM, respectively. Titration of Trp fluorescence of WT FucP with L-arabinose (○) is shown as a control.

4.2.9 Double-Trp or tetra-Trp mutants of FucP

Alignment of LacY sequence with sequences of homologous MFS transporters revealed conservation of residues important not only for sugar binding and H^+ translocation but also for structural flexibility [93]. One of the structural elements conserved among MFS transporters is the position of certain Gly residues. As Gly does not have a side chain and provides high flexibility in the polypeptide chain, it is often found in regions where the polypeptide chain makes a sharp turn. Because the presence of turns at certain positions is a characteristic of a unique fold of a protein structure, conservation of Gly residues is often exhibited in protein families. In addition, paired Gly residues in opposing helices allow the helices to pack more tightly [123].

In LacY, tight interaction between N- and C-terminal six helix bundles on the periplasmic side is facilitated by two pairs of Gly residues; one pair with Gly46 on helix II and Gly370 on helix XI and the other with Gly159 on helix V and Gly262 on helix VIII. Double Gly → Trp mutants (G46W/G262W and G159W/G70W) do not catalyze sugar/H^+ transport, but sugar binding is more rapid in the mutants [123]. Furthermore, the X-ray crystal structure of G46W/G262W mutant, obtained only in the presence of a galactoside, is almost occluded and narrowly open to the periplasm while the cytoplasmic end is tightly sealed [58, 59]. A simple explanation for the behavior of the mutants is that in the absence of sugar, the periplasmic pathway in the mutant is sufficiently open to allow access of TDG to the binding site. But when binding occurs and the mutant attempts to transition into an occluded state, it cannot do so completely because

the bulky Trp residues at positions 46 and 262 block complete closure. Thus, the mutant is able to bind sugar and initiate transition into an occluded state, which it cannot complete. Therefore, the mutant is completely unable to catalyze transport of any type across the membrane.

A LacY mutant with replacement of four Gly with Trp (G46W/G159W/G262W/G370W) was constructed and sugar binding by the tetra-Trp mutant was analyzed by Trp → α-NPG FRET. α-NPG, a high affinity substrate for LacY, acts as a FRET acceptor from Trp151, a component of sugar-binding site that stacks hydrophobically with the galactopyranosyl ring of sugar substrate [112, 124, 125].

Even though decrease in Trp fluorescence of LacY is observed upon addition of α-NPG as expected, it is due not only to Trp → α-NPG FRET effect but also to an nonspecific filter effect of α-NPG absorbing irradiated excitation light at 295 nm [125]. In order to isolate Trp → α-NPG FRET from the total change in Trp fluorescence, displacement of α-NPG bound to LacY with melibiose, a non light-absorbing substrate, was measured. The increase in Trp fluorescence observed upon addition of melibiose represents a specific Trp → α-NPG FRET effect. Fig. 4.11 shows the increase in Trp fluorescence upon addition of saturating concentration of melibiose after incubation with α-NPG at different concentrations. The apparent affinity for α-NPG (K_d^{app}), determined as the concentration of α-NPG that produces half-maximal fluorescence increase, is calculated to be 5.64 ± 0.95 μM, which is close to the value obtained for WT

LacY (19 μM) [125], indicating that sugar binding remains unaffected in the tetra-Trp mutant.

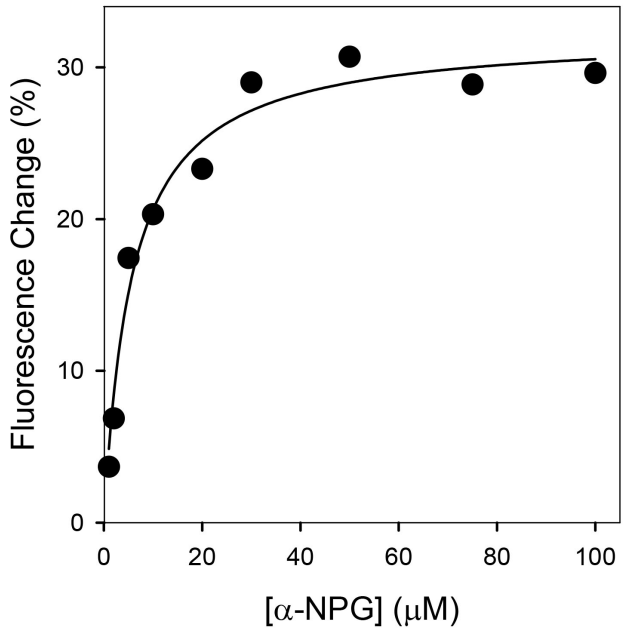

Fig. 4.11. Binding of tetra-Trp LacY detected by Trp → α-NPG FRET. Affinity of G46W/G159W/G262W/G370W for α-NPG was measured by displacement with melibiose. The relative changes in fluorescence induced by addition of 30 mM melibiose (final concentration) are plotted as a function of α-NPG concentration. The solid line shows the hyperbolic fit to the data with an estimated K_d^{app} = 5.64 ± 0.95 μM.

The paired double-Gly motif on the periplasmic side of LacY and other MFS transporters is conserved in FucP. Gly64 (helix II), Gly173 (helix V), Gly303 (helix VIII), and Gly402 (helix XI) of FucP are found at the positions corresponding to Gly46, Gly159, Gly370, and Gly262, respectively, in LacY (Fig. 4.12). As shown in Fig. 4.13A, dual replacements of G64/G303 or G173/G402 with Trp significantly reduce L-fucose transport activity, and simultaneous replacements of these four Gly residues similarly lead to low level of transport activity, despite expression at a level comparable to WT FucP (Fig. 4.13B).

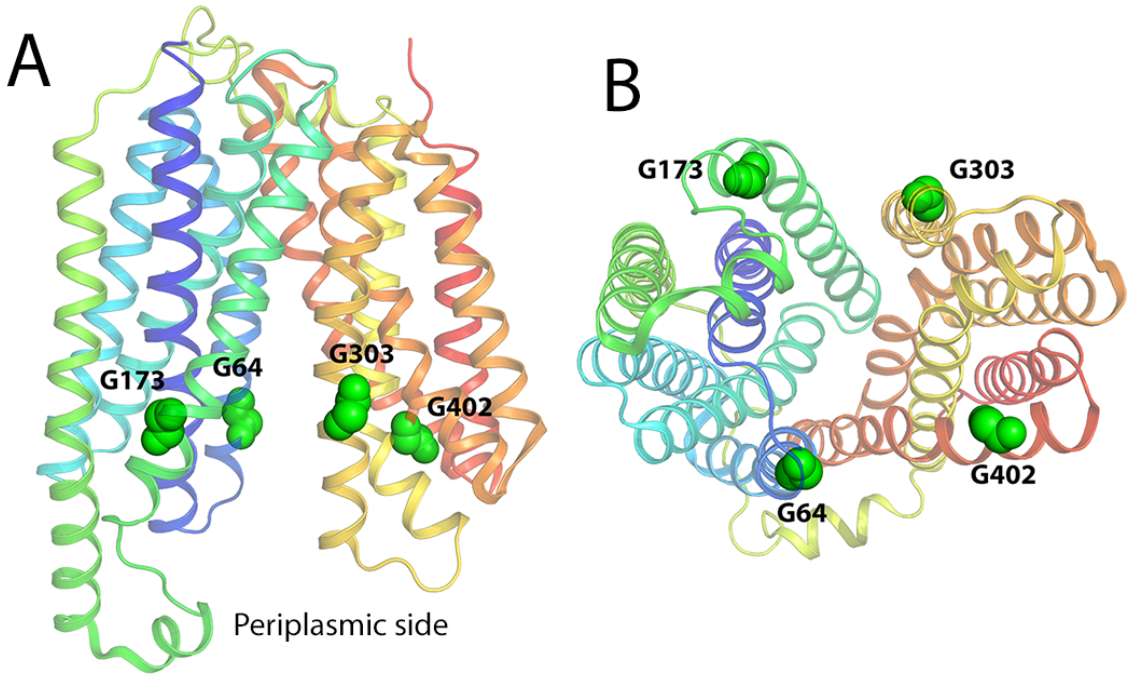

Fig. 4.12. Conserved Gly residues on the extracellular surface of FucP between the N and C-terminal six-helix bundles. Gly residues at position 64, 173, 303, and 402 are shown in spheres. Twelve transmembrane helices are colored from the N-terminus in blue to the C-terminus in red. FucP structure is displayed by using Pymol 1.4. (A) View parallel to the membrane. (B) Periplasmic view.

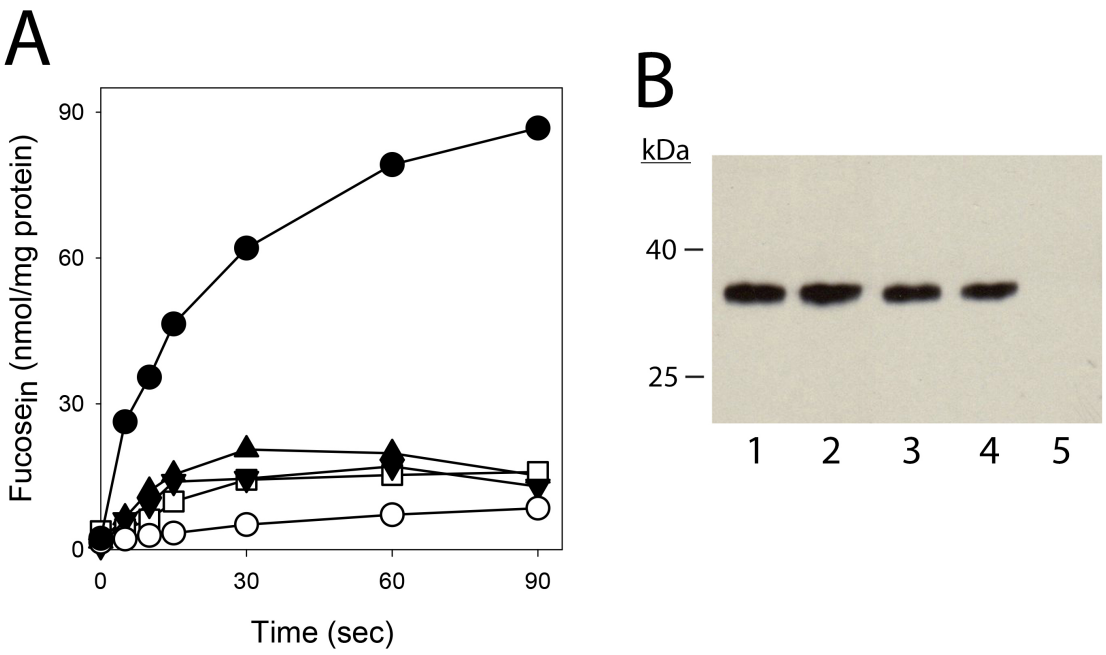

Fig. 4.13. Transport activity of FucP double- and tetra-Trp mutants. (A) Time courses of L-fucose accumulation by *E. coli* T184 cells expressing wild-type FucP (●), no permease (○) or FucP mutants: G64W/G303W (▲), G173W/G402W (▼), and G64W/G173W/G303W/G402W (□) were obtained as described in *Materials and Methods*. (B) Expression of wild-type FucP and mutants as determined by Western blotting. Lane 1, WT FucP; lane 2, G64W/G303W; lane 3, G173W/G402W; lane 4, G64W/G173W/G303W/G402W; lane 5, no permease.

Emission spectra of FucP mutants G64W/G303W, G173W/G402W, and G64W/G173W/G303W/G402W purified in detergent with excitation at 295 nm are shown in Fig. 4.14. Quenching of Trp fluorescence is induced by addition of L-fucose in both double-Trp mutants and no shift in λ_{max} is exhibited. Addition of L-fucose to the mutant G64W/G303W or G173W/G402W elicits ~18% or ~12% quenching of Trp fluorescence, respectively, while L-arabinose exhibits a smaller, non-specific effect (Fig 4.14A-F). Furthermore, ~15% quenching is observed with tetra-Trp mutant as well (Fig 4.14G-I). The findings indicate L-fucose binding with the mutants induces partial closing of the periplasmic cavity.

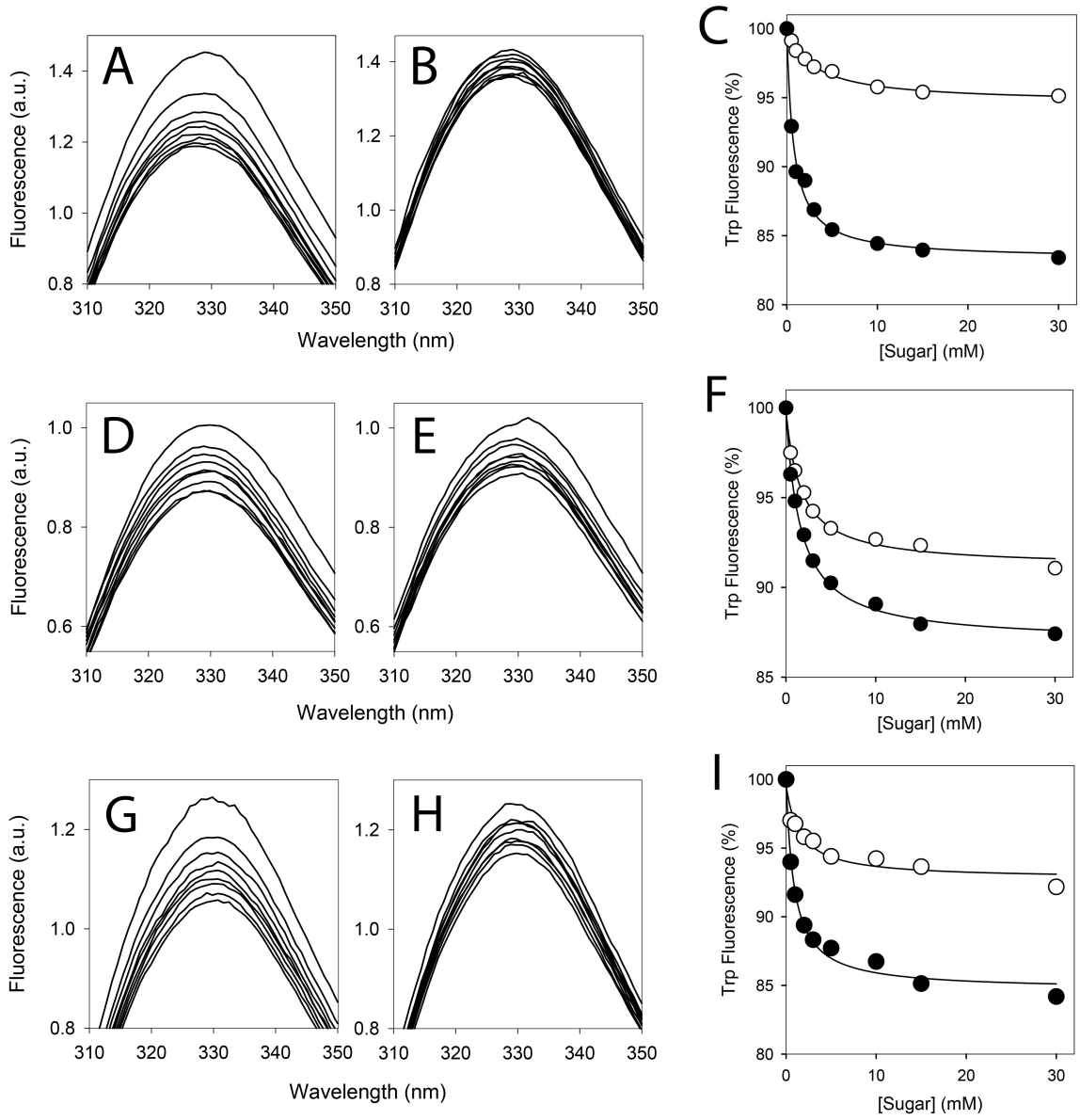

Fig. 4.14. Fluorescence emission and Trp quenching of double-Trp mutants, G64W/G303W (A-C), G173W/G402W (D-F), and tetra-Trp mutant G64W/G173W/G303W/G402W (G-I), of FucP. Emission spectra of purified, detergent-solubilized FucP mutants were measured in the presence of L-fucose (A and D) and L-arabinose (B and E) at different concentrations (beginning at the top of the traces: 0, 0.5, 1, 2, 3, 5, 10, and 15 mM final concentration) as described in *Materials and Methods*. The λ_{exc} was 295 nm. (C and F) Changes in Trp fluorescence (λ_{max} at 327 nm) in response to addition of L-fucose (●) or L-arabinose (○) are plotted as a function of sugar concentration.

4.2.10 Trp Fluorescence of CscB

Quenching of Trp fluorescence in CscB was also examined as the CscB model build by homology modeling with the X-ray structure of LacY as template shows three Trp residues on opposing walls of the open cytoplasmic cavity – Trp26, Trp30 on helix I, and Trp229 on helix VII (Fig. 4.15).

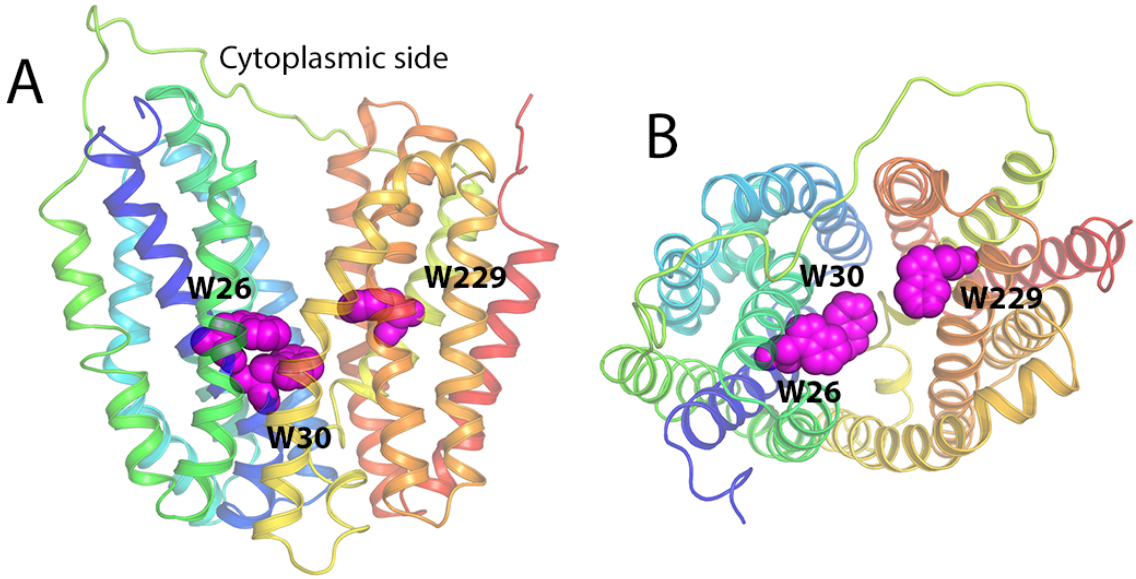

Fig. 4.15. Three Trp residues on the surface of cavity walls of CscB. Homology model of CscB threaded into LacY structure reveals Trp26, Trp30 (helix I), and Trp229 (helix VII) on the surface of cavity walls which are shown as magenta spheres. Twelve transmembrane helices are colored from the N-terminus in blue to the C-terminus in red. CscB structure is displayed by using Pymol 1.4. (A) View parallel to the membrane. (B) Cytoplasmic view.

CscB was solubilized in DDM and purified by cobalt affinity chromatography (Fig. 4.16). The fraction eluted with 150 mM imidazole (peak 3 fraction in Fig. 4.16A) yielded a single band at M_r of ~33 kDa on SDS-PAGE when stained with silver (Fig. 4.16B, lanes 5-8).

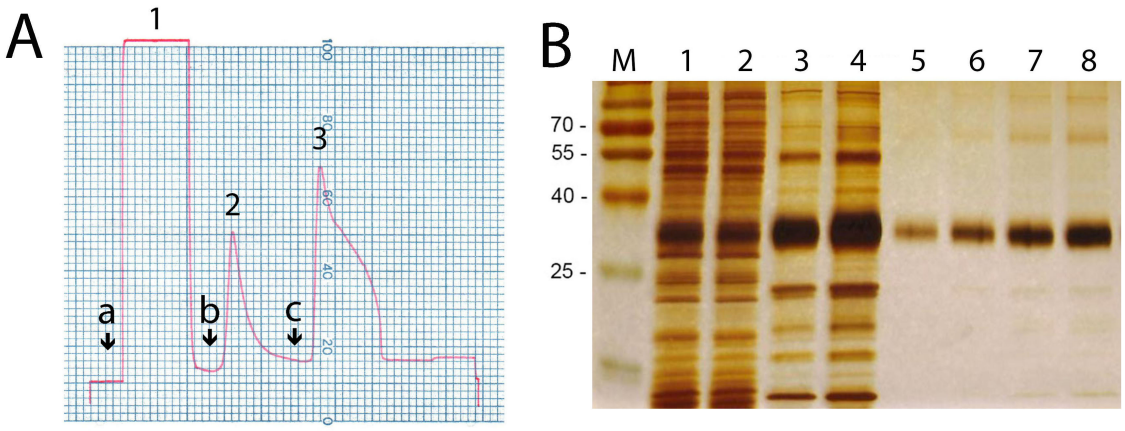

Fig. 4.16. Purification of His-tagged CscB by cobalt affinity chromatography. (A) Purification profile of chromatography. Membrane fraction solubilized with DDM was applied to 5-ml bed of cobalt resin in 50 mM NaP_i buffer (pH 7.5, with 0.01% DDM) (*arrow* a). 15 mM Imidazole was applied to remove impurities bound to resin nonspecifically (*arrow* b). 150 mM Imidazole was applied to elute CscB (*arrow* c) (B) Silver-stained SDS-PAGE gel of various fractions collected during purification of CscB. Lane 1, DDM extract of membrane fraction (0.4 µl); lanes 2, flowthrough sample (0.4 µl of peak 1 fraction in panel A); lanes 3 and 4, wash (5 µl and 10 µl of peak 2 fraction in panel A, respectively); lanes 5, 6, 7, and 8, CscB purified in DDM (0.1 µg, 0.2 µg, 0.4 µg, and 0.8 µg of protein, respectively).

Fig. 4.17 shows emission spectra of purified WT CscB with excitation at 295 nm in the absence or presence of different sugars. Addition of sucrose induces marked quenching without shifting the λ_{max} at 327 nm, and the magnitude of the effect is dependent on the sucrose concentration (Fig. 4.17A). Trp quenching is also observed upon the addition of fructose, another substrate for CscB, but the effect of sugar concentration is slightly less marked than that of sucrose (Fig. 4.17B). Addition of these substrates elicits ~15% of Trp fluorescence quenching, yielding K_d^{app} values of 0.57 ± 0.19 and 1.27 ± 0.35 mM for sucrose and fructose, respectively (Fig. 4.18). In contrast, glucose and TDG exhibit a markedly smaller effect that appears to be non-specific as they are not transport substrates of CscB (Fig. 4.17C; Fig. 4.18).

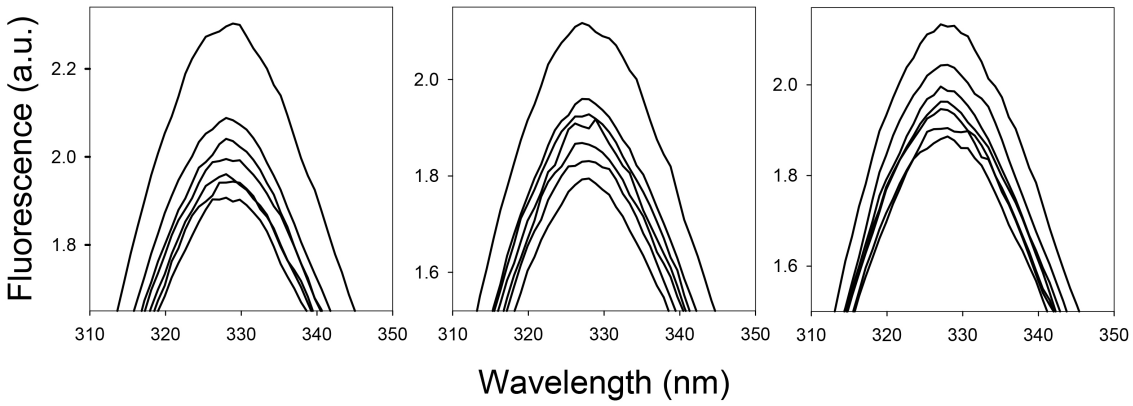

Fig. 4.17. Fluorescence emission of WT CscB. Emission spectra of purified, detergent-solubilized WT CscB was measured in the absence or presence of sucrose (A), fructose (B), and glucose (C) at different concentrations (beginning at the top of the traces: 0, 1, 2, 5, 10, 15, and 30 mM final concentration) as described in *Materials and methods*. The λ_{exc} was 295 nm.

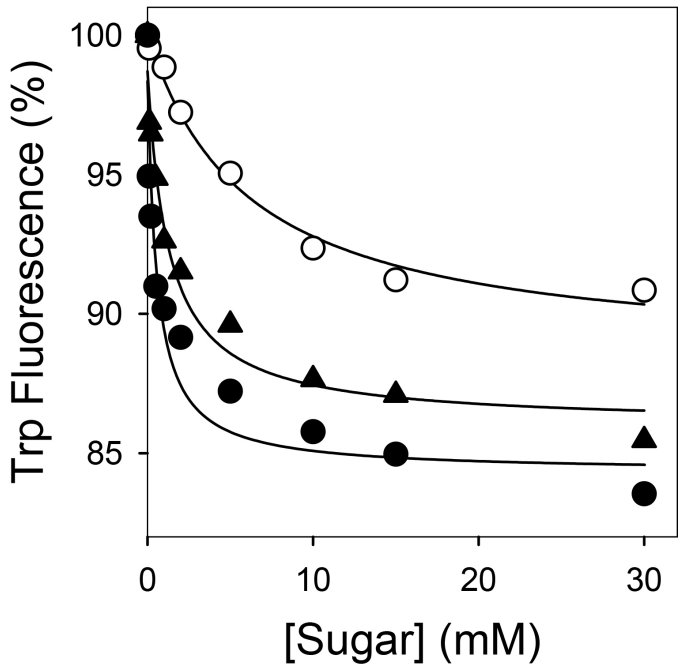

Fig. 4.18. Trp quenching of CscB with different sugars. Changes in Trp fluorescence (λ_{max} at 327 nm) in response to addition of sucrose (●), fructose (▲), and glucose or TDG (○) are plotted as a function of sugar concentration. The curves represent the average of two independent measurements. The K_d^{app} values of WT CscB for sucrose and fructose observed in this experiment are 0.57 ± 0.19 and 1.27 ± 0.35 mM, respectively. The change in Trp fluorescence

observed in the presence of glucose and TDG is due to a nonspecific effect of these sugars as they are not substrates for CscB.

4.3 Discussion and conclusions

According to the alternating access model of transport, studied most extensively with LacY [reviewed in 69], co-substrate-binding sites for sugar and H^+ in the middle of FucP becomes exposed alternatively to either side of the membrane due to reciprocal closing and opening of periplasmic and cytoplasmic cavities, respectively. The X-ray crystal structures of LacY [37, 47-49] exhibit a tightly closed periplasmic aspect with a cavernous, cytoplasmic opening, and site-directed alkylation studies indicate that the protein has a similar structure in the membrane [77, 83]. In contrast, the X-ray structure of FucP reveals the opposite — a wide-open periplasmic side with a tightly sealed cytoplasmic face [91]. However, little or nothing is known about the structure of FucP in the membrane or about its dynamics.

In polytopic membrane protein structures, Trp residues are preferentially localized at interfacial regions due to the favorable interaction of aromatic groups with the bilayer interface [126]. But less frequently, Trp residues are found in the interior of membrane proteins near carbohydrate binding sites, for example, where they interact hydrophobically with sugar substrates [51, 112, 125]. Fluorescence spectroscopy of endogenous Trp residues located in a substrate translocation pathway are useful for studying structural dynamics since the indole rings of Trp residues can be utilized as an intrinsic fluorophore. The amino acid sequence of FucP contains six Trp residues, two of which (Trp38 and Trp278)

are located on opposing faces of the outward-facing hydrophilic cavity (Fig. 4.1). This study demonstrates that the fluorescence of these two Trp residues is quenched specifically upon binding of L-fucose or D-arabinose, known substrates of the symporter.

The emission spectrum of purified WT FucP exhibits significant quenching of Trp fluorescence upon addition of L-fucose in a concentration-dependent manner with no change in λ_{max} (Fig. 4.5). Therefore, it is unlikely that the quenching phenomenon observed is due to a change in the local environment of the Trp residues. The phenomenon also mirrors the substrate specificity of FucP since L-fucose and D-arabinose, sugars known to be transport substrates of FucP [117, 120, 127], quench Trp fluorescence while other sugars, which are not substrates, have no effect (Fig. 4.6).

Sugar-induced quenching specifically involves the two Trp residues at positions 38 and 278 on opposing faces of the cavity walls. Replacing either residue — particularly Trp38 — with Tyr or Phe leads to decreased fluorescence quenching, and negligible fluorescence quenching is observed when both residues are replaced (Fig. 4.8). Thus, only the Trp residues at positions 38 and 278 are important, and other Trp residues located at interfacial regions are not involved in the phenomenon. Both Trp residues are located in the approximate middle of FucP ~16 Å apart from each other in outward-facing conformation (Fig. 4.1). Importantly, during the conformational change from outward-facing to occluded, helices I and VII are predicted to come together [91], and in all likelihood, it is these two Trp residues coming into closer opposition as the

outward-facing cavity closes that are responsible for sugar-induced quenching in FucP. In this regard, although the experiments presented here were carried out with purified FucP in detergent, the findings are consistent with the X-ray structure of FucP, which exhibits an outward-facing conformation devoid of substrate.

It is also highly likely that Trp38 and Trp278 comprise part of the sugar-binding site in FucP. Thus, replacement of either with Tyr or Phe causes a decrease in L-fucose-induced quenching with a significant decrease in affinity (i.e., an increase in K_d^{app}), and simultaneous replacement of both Trp residues abolishes sugar-induced quenching (Fig. 4.7). In addition, replacing either or both Trp residues with Tyr, Phe or Ile significantly inhibits L-fucose transport (Fig. 4.9) as expected if these residues are directly involved in binding. Given a scenario in which Trp38 and Trp278 are components of the sugar-binding site and sugar binding induces quenching because the two Trp residues come into close opposition, it seems reasonable to propose that the two Trp may sandwich the bound L-fucose. By this means, the interaction between the bound pyranose ring of L-fucose and the indole rings of the Trp residues, as well as the close proximity of the two Trp residues might be primarily responsible for quenching.

Isothermal calorimetry measurements provide evidence that Glu135 is directly involved in binding, and as demonstrated here (Fig. 4.10), mutants E135D or E135Q exhibit essentially no L-fucose-induced Trp quenching, which is consistent with this interpretation. However, there is no evidence for the proposal that Glu135 plays a role in H^+ translocation. In contrast, mutants D46E and D46N

exhibit L-fucose-induced quenching with near-WT binding, and the D46A mutant binds well calorimetrically (L. Sun & N. Yan, personal communication). Moreover, although mutant D46A does not catalyze uphill L-fucose/H^+ symport, it catalyzes counterflow [91]. In this respect, Asp46 has some of the main characteristics of Glu325 LacY mutants. Mutants with neutral replacements for Glu325 are unable to catalyze all translocation reaction that involve H^+ transport, but catalyze equilibrium exchange and counterflow. This and additional evidence [104, 128-130] indicate that Glu325 is directly involved in deprotonation of LacY [43]. Furthermore, exchange and counterflow involve the global conformational change central to the alternating access mechanism. Therefore, Asp46 mutants in FucP are expected to exhibit quenching.

Furthermore, FucP mutants with Gly residues at periplasmic positions 64/303 and/or 173/402 replaced with bulky Trp residues exhibit Trp fluorescence quenching upon binding L-fucose (Fig. 4.14) despite a marked defect in transport (Fig. 4.13). This suggests that although mutants are not capable of completing a transport cycle due to the presence of bulky Trp residues on their periplasmic side, the periplasmic cavity closes partially upon binding of L-fucose. Therefore, co-crystalization of these mutants with L-fucose may lead to a structure of FucP with bound sugar in a similar manner to that of the double-Trp LacY mutant.

CscB purified in detergent also exhibits Trp fluorescence quenching upon binding of substrate in a concentration-dependent manner without a shift in λ_{max} (Fig. 4.17). The phenomenon is induced by binding of fructose, a substrate for CscB, while quenching induced by non-substrates such as D-glucose or TDG is

smaller and non-specific. The Trp fluorescence quenching phenomenon was expected as the homology model to LacY exhibits multiple Trp residues on opposing walls of the hydrophilic cavity. Thus, as indicated with FucP, the phenomenon is likely due to the Trp residues coming into closer opposition as the inward-facing cavity closes upon binding of substrate.

In conclusion, the findings presented here demonstrate a direct interaction of FucP and CscB with their sugar substrates by utilizing Trp fluorescence spectroscopy. In FucP, sugar binding evokes quenching of specific Trp residues in a manner that clearly reflects a conformational change in FucP. Moreover, it is most probable that this structural change is due primarily closure of the outer-facing cavity to form an occluded state that may represent the high-energy conformation of the protein, as suggested for LacY [43, 131].

Chapter 5

Dynamics of FucP in the native bacterial membrane

5.1 Introduction

Most X-ray crystal structures of transporters were obtained using proteins purified in detergents in the absence of added phospholipids. However, lipid composition has been shown to play an essential role in the structure and function of many transport proteins [132-139], and little information on the role of lipids is provided by crystal structures obtained in the presence of detergents.

Site-directed alkylation of Cys has been utilized extensively to obtain information regarding both static and dynamic features of LacY embedded in the native bacterial membrane [77-83]. Among all amino acids, Cys is average in steric bulk and relatively hydrophobic, and importantly, it is amenable to highly specific modification. Thus, a library of constructs with a single-Cys residue at almost every position of LacY generated for Cys-scanning mutagenesis has been used in combination with biochemical and biophysical techniques and has provided a wealth of functional and structural information on the protein.

Alkylation of functional LacY with single-Cys residue at any given position of the molecule with membrane-permeant thiol reagents, such as fluorescent tetramethylrhodamine-5-maleimide (TMRM) or radiolabeled *N*-ethylmaleimide (NEM) (Fig. 5.1), reflects the accessibility and/or reactivity of the Cys replacement. Alkylation of a Cys replacement depends on the environment in the vicinity of the thiol side chain. In addition to physical accessibility of the thiol group in Cys to thiol reagents, its reactivity is influenced by exposure to water;

reactivity increases when pK_a (~9.1 for the ionizable thiol group in Cys in aqueous solution) is lowered due to increased exposure of the thiol group to water, while a Cys buried in a hydrophobic environment has an increased pK_a and decreased reactivity.

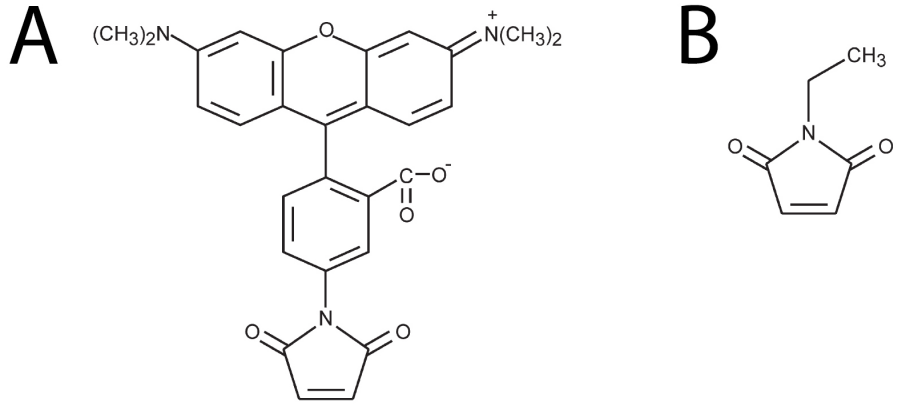

Fig. 5.1. Structures of (A) TMRM and (B) NEM.

With LacY, the accessibility/reactivity of single-Cys replacements is consistent with an alternating access mechanism. The accessibility/reactivity of single-Cys replacements located on the periplasmic side of the sugar-binding site is generally low in the absence of sugar and increases dramatically upon binding of a galactoside. In contrast, single-Cys replacements located on the cytoplasmic side generally exhibit the opposite accessibility/reactivity.

The spectroscopic analyses described in previous chapter demonstrated conformational changes in FucP triggered by direct interaction with sugar substrates with purified proteins in detergent micelles. In contrast, site-directed

alkylation presented in this chapter reveals dynamics of FucP embedded in the native bacterial membrane using right-side-out RSO membrane vesicles.

5.2 Results

5.2.1 Transport activity of Cys-less FucP

WT FucP contains eight Cys residues at positions 32, 133, 269, 277, 307, 339, 357, and 421 (Fig. 5.2). For site-directed alkylation studies, it is important to use FucP devoid of Cys (Cys-less FucP) to introduce a single-Cys at any given position to analyze its reactivity/accessibility. It is also essential that Cys-less FucP is an active protein. To construct Cys-less FucP, all eight Cys residues were simultaneously replaced with Ala by site-directed mutagenesis (C32A/C133A/C269A/C277A/C307A/C339A/C357A/C421A).

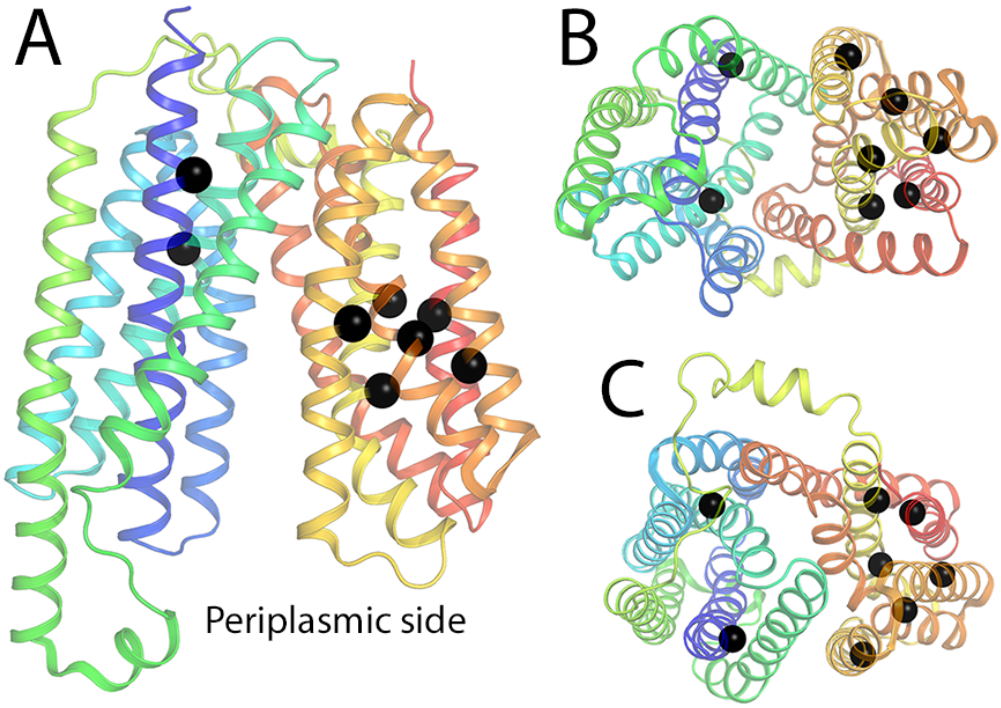

Fig. 5.2. Native Cys residues of FucP. The black spheres represent C_α atoms of native Cys residues where Ala substitutions were introduced to construct FucP devoid of Cys. Twelve transmembrane helices are colored from the N-terminus in blue to the C-terminus in red. FucP structure is displayed by using Pymol 1.4. (A) View parallel to the membrane. (B) Periplasmic view. (C) Cytoplasmic view.

5.2.2 TMRM labeling of WT FucP

In contrast to Cys-less LacY, which largely retains lactose transport activity, replacement of all Cys residues in FucP with Ala markedly reduced L-fucose transport activity (Fig. 5.3). However, as shown in Fig. 5.4, no labeling with TMRM was observed with WT FucP in the absence or presence of L-fucose, thereby demonstrating that none of the native Cys residues in FucP is accessible/reactive in the absence or presence of sugar.

As a control, labeling of WT LacY with TMRM was tested under the same experimental conditions. In the absence of sugar, WT LacY reacted strongly with TMRM, and no labeling was observed in the presence of α-NPG. It is long known

that the high reactivity of WT LacY with maleimides is due primarily to Cys 148 and that galactoside binding sterically protects the residue against alkylation [140, 141].

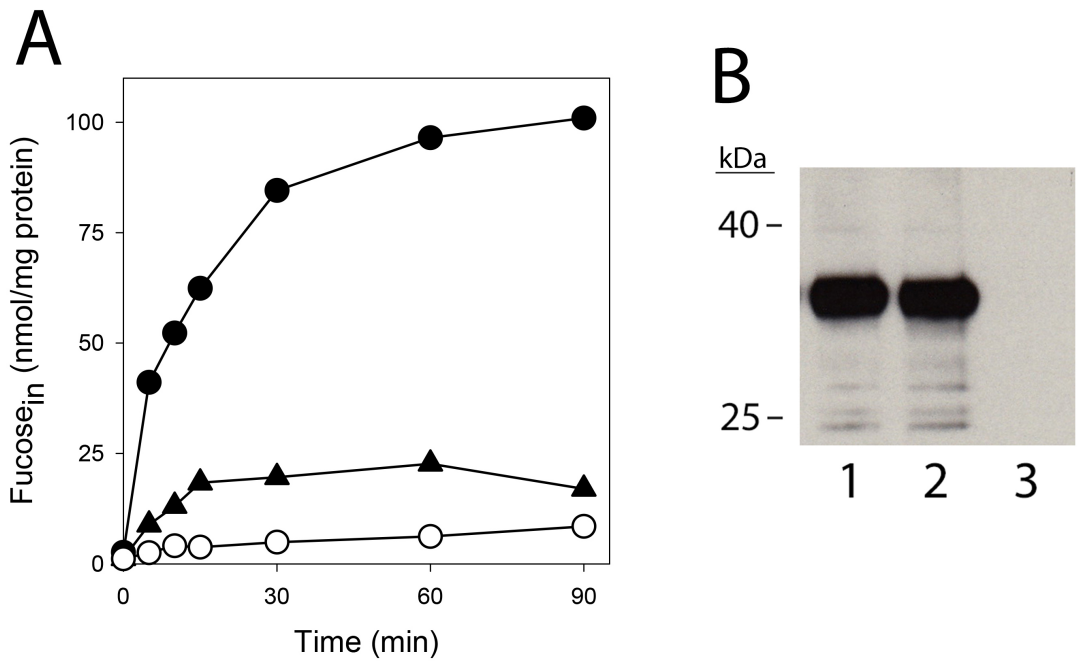

Fig. 5.3. Transport activity of Cys-less FucP mutant. (A) Time courses of L-[5,6-^{3}H]fucose accumulation by *E. coli* T184 cells expressing wild-type FucP (●), Cys-less FucP mutant (▲), or no permease (○) were obtained as described in *Materials and Methods*. (B) Expression of Cys-less FucP mutant as determined by Western blotting. Lane 1, WT FucP; lane 2, Cys-less FucP; lane 3, no permease.

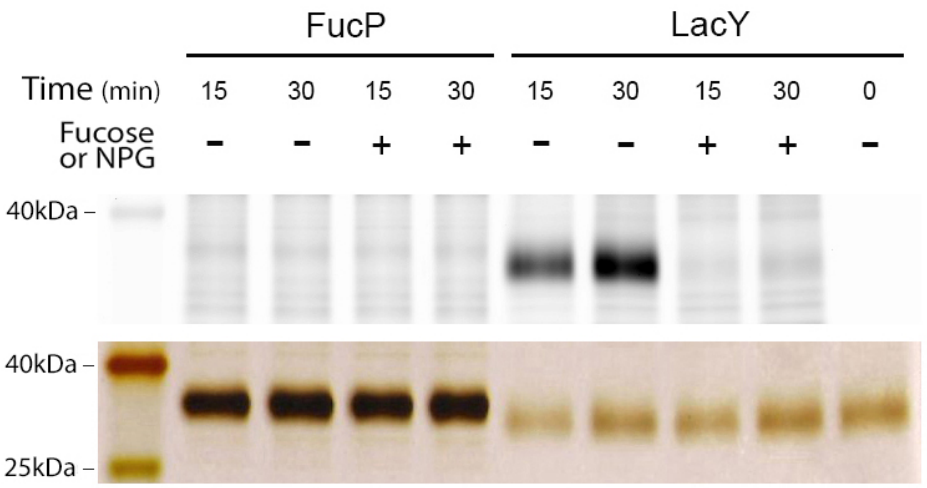

Fig. 5.4. TMRM labeling of WT FucP. RSO membrane vesicles (0.1 mg of protein in 50 µl) prepared from *E. coli* with WT FucP were incubated for 15 or 30 min at 0°C in the absence or presence of L-fucose with 40 µM TMRM. 2-Mercaptoethanol was added to terminate the reactions, and DDM was used to solubilize the membrane. His-tagged proteins were purified and subjected to SDS-PAGE. For 0 min, 2-mercaptoethanol was added prior to TMRM. TMRM-labeled (upper panel) and silver-stained (lower panel) bands corresponding FucP or LacY were imaged as described in *Materials and Methods*.

5.2.3 TMRM labeling of Cys-replacement mutants of FucP

To analyze dynamic aspects of FucP in the native bacterial membrane, Cys-replacement mutants on either the periplasmic or cytoplasmic side were constructed and TMRM labeling of the mutants was carried out in the absence or presence of L-fucose.

Eight positions within the widely open periplasmic cavity of WT FucP were chosen for site-directed alkylation (Fig. 5.5). T398C mutant is strongly labeled with TMRM in the absence of sugar substrate, but it barely reacts with TMRM in the presence of L-fucose. A similar decrease in TMRM reactivity is observed at positions 279 and 282 upon L-fucose binding. Q54 is the only position tested that exhibits increased reactivity with TMRM in the presence of L-fucose, and Cys

replacements at positions 53, 66, 166, and 298 show the same level of reactivity in the absence or presence of L-fucose. Thus, predominantly decreased reactivity is observed with Cys replacements located on the periplasmic side of the molecule in the presence of ligand.

Site-directed alkylation with TMRM was also carried out to probe the potential cavity on the cytoplasmic side of FucP (Fig. 5.5). Mutants L155C and S370C show strong TMRM reactivity in the absence of sugar substrate and clear decrease in the reactivity was caused by L-fucose binding. Similarly, decrease in TMRM reactivity was observed with mutants T380C and S384C. With T143C and H152C, reactivity with TMRM was observed only in the absence of L-fucose. Cys replacements at positions 138 and 387 exhibit the same level of reactivity in the absence or presence of L-fucose. Therefore, similarly to Cys replacements on the periplasmic side, decreased TMRM reactivity is exhibited with Cys replacements located on the cytoplasmic side in the presence of ligand.

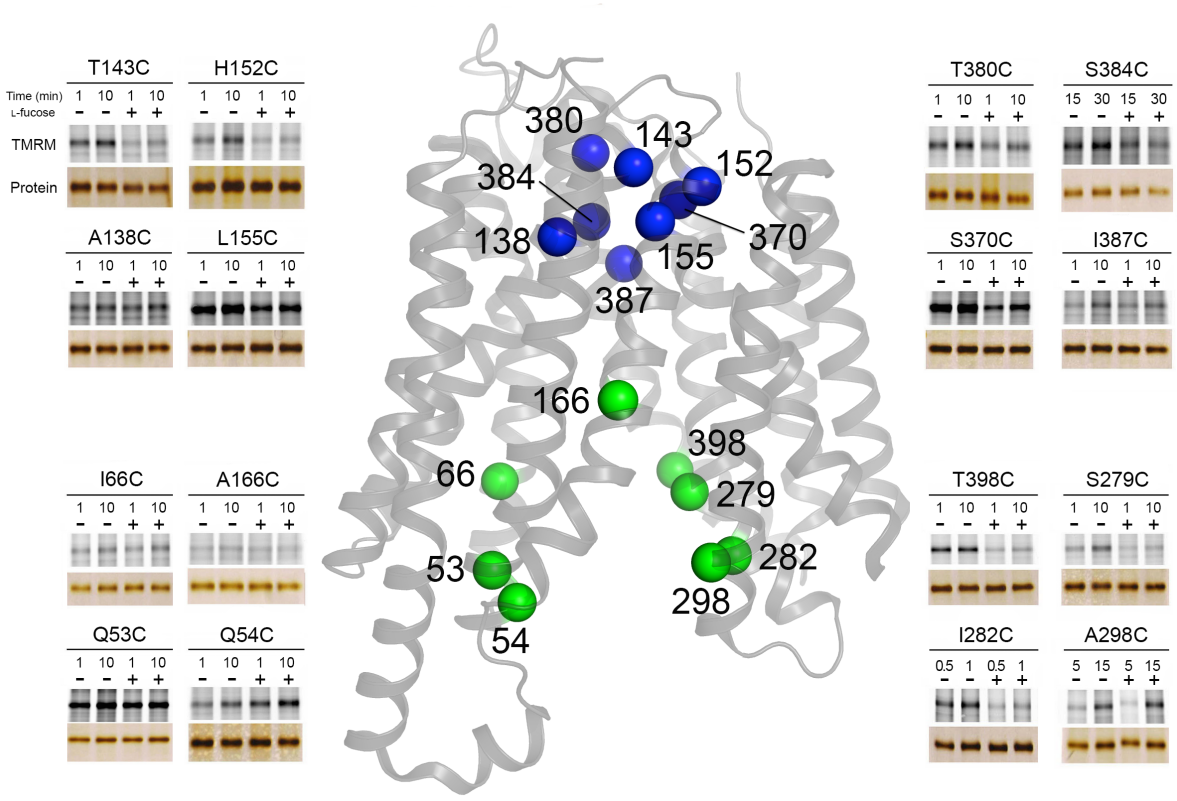

Fig. 5.5. Effect of L-fucose on TMRM reactivity of FucP Cys-replacement mutants. Cys-replacements in FucP were labeled with 40 μM TMRM for the time indicated at 0 °C in the absence or presence of 40 mM L-fucose. Purified proteins labeled with TMRM were subjected to SDS-PAGE, and then TMRM-labeled (upper panels) and silver-stained (lower panels) bands corresponding to FucP were imaged. C_α atoms of corresponding Cys replacements are shown as spheres. It is assumed that sugar-binding site is located in the middle of the molecule at the apex of the hydrophilic cavity opened to the periplasm.

5.3 Discussion and conclusions

Dynamic aspects of LacY have been extensively studied. Multiple independent biochemical and biophysical studies, including thiol cross-linking [70-77], site-directed alkylation [77-83], single molecule fluorescence resonance energy transfer [84], double electron-electron resonance [85], and Trp fluorescence quenching [88], demonstrate that the periplasmic cavity of LacY must open and close for transport to occur. Sugar-binding with LacY causes

transition to a high-energy intermediate occluded state that opens to either side of the membrane, which leads to increased probability of opening a hydrophilic cavity on the periplasmic side with reciprocal closing of the cytoplasmic cavity (the alternating access mechanism). By this means, the sugar and H^+ binding sites have alternating accessibility to either side of the membrane.

Site-directed alkylation studies of LacY with NEM or TMRM show that binding of a high affinity lactose analogue induces an increase in reactivity of single-Cys replacements in the tightly packed periplasmic domain, while decreased reactivity is observed on the cytoplasmic side [77-83]. The overall results are consistent with the alternating access model in which opening of a pathway for sugar on the periplasmic side of LacY is correlated with the closure of the cytoplasmic cavity.

Site-directed alkylation analysis on FucP presented in this chapter shows that binding of L-fucose induces a decrease in accessibility/reactivity of Cys replacements in a widely opened cytoplasmic cavity of FucP. Although this observation suggests closure of the periplasmic cavity upon binding of L-fucose, opening of a cytoplasmic, water-accessible cavity upon sugar binding was not observed. Surprisingly, the same pattern of decrease in reactivity of Cys replacements was exhibited in Cys replacements located in the periplasmic side of the molecule. Although the findings suggest the global conformational change occurring upon L-fucose binding, the findings suggest that sugar binding with FucP induces transition to a relatively long-lived occluded conformation.

Chapter 6

Future studies

To further delineate the dynamics of FucP, approaches used with LacY will be utilized.

6.1 Double electron-electron resonance (DEER)

One of effective methods to visualize ligand-induced conformational changes in transport proteins purified in detergent is double electron-electron resonance (DEER). The method uses nitroxide probes attached to pairs of Cys replacements and is highly sensitive to distance changes within the range of 20-60 Å in proteins, which is compatible with the distances in FucP.

Nitroxide-labeled paired-Cys replacements introduced at the ends of transmembrane helices on either the cytoplasmic or periplasmic side of FucP can be used for distance measurements in the absence or presence of L-fucose. If FucP functions by alternating access mechanism and exists in outward-facing conformation, as suggested by its X-ray crystal structure and Trp fluorescence spectroscopic analysis, it is anticipated that L-fucose binding induces decrease in distance on the periplasmic side and increase on the cytoplasmic side. With LacY, sugar binding causes conformational rearrangements on both sides of the molecule [85]. On the cytoplasmic side, nitroxide-labeled pairs exhibit decreased interspin distances ranging from ~4 to 21 Å. Conversely, on the periplasmic side, spin-labeled pairs show increased distances ranging from ~4 to 14 Å. These findings demonstrate sugar-induced closing of cytoplasmic cavity and opening of a cavity on the tightly packed periplasmic side in LacY, providing quantitative

evidence for the alternating access model. With FucP, distance changes opposite to those observed with LacY is anticipated, and DEER may provide support for alternating access model as well as inward-facing conformer of FucP purified in detergent.

6.2 Site-directed crosslinking

Site-directed crosslinking is a useful method to analyze dynamics of membrane transporters embedded in the native bacterial membrane. The X-ray crystal structure of FucP in outward-facing conformation shows that its helices IV and X from the N- and C-terminal six-helix bundles, respectively, participate in sealing the cavity on the cytoplasmic side [91]. Paired double-Cys replacements introduced in the interface between helices IV and X on the cytoplasmic side of FucP can be tested for crosslinking with flexible, homo-bifunctional thiol-reactive reagents varying from 5 to 25 Å in length. Then, crosslinked double-Cys mutants will be assessed for transport activity in RSO membrane vesicles.

In LacY, helices I/II and VII from the N- and C-terminal six-helix bundles, respectively, participate in sealing the cavity on the periplasmic side. Crosslinking paired double-Cys introduced in the interface between helices I/II and VII on the periplasmic side with flexible homo-bifunctional reagents shorter than 15 Å abolishes transport activity while they retain full or partial activity when crosslinked with reagents greater than ~15 Å in length [77]. This indicates that LacY involves opening and closing of a relatively large, water-filled periplasmic cavity. If FucP translocates its substrate across the membrane in a manner similar to LacY and sugar binding induces opening of the cytoplasmic cavity,

inactivation of L-fucose transport is expected to be dependent on the length of the crosslinking reagents.

Despite an increasing number of structures of membrane transporters, structural information is limited in achieving a comprehensive understanding of dynamics of these proteins. Integration of the findings with various MFS family members through application of biochemical and biophysical methods will develop greater insight into a general mechanism of action as well as coupling between sugar and H^+ translocation in MFS transporters.

Appendix

Materials and Methods

A1 Materials

L-Fucose, D-arabinose, D-galactose, fructose, glucose, sucrose, lactulose, turanose, and palatinose were obtained from Sigma-Aldrich (St. Louis, MO). L-Arabinose was from Gold Biotechnology (St. Louis, MO). All other materials were of reagent grade obtained from commercial sources. Octyl-α-D-galactopyranoside was from Carbosynth Limited (UK). All oligonucleotides were synthesized by Integrated DNA Technologies, Inc (Coralville, IA).

L-[5,6-^{3}H]Fucose was was purchased from American Radiolabeled Chemicals, Inc. (St. Louis, MO), [U-^{14}C]sucrose Perkin Elmer (Boston, MA), D-[U-^{14}C]fructose from Moravek Biochemicals (Brea, CA), and [galactose-6-^{3}H]lactulose from American Radiolabeled Chemicals, Inc (St. Louis, MO).

All nucleotides were synthesized by Integrated DNA Technologies, Inc. (Coralville, IA). Restriction endonuleases were from New England Biolabs, and T4 DNA ligase was from Promega (Madison, WI). QuickChange II kits were obtained from Stratagene (La Jolla, CA), and DNA plasmid purification kits and the penta-His antibody−horseradish peroxidase (HRP) conjugate were from Qiagen (Valencia, CA). Supersignal West Pico Chemiluminescent substrate kit was from Pierce Inc. (Rockford, IL). Dodecyl-β-D-maltopyranoside (DDM) was obtained from Anatrace (Maumee, OH) and Talon superflow resin was from BD Clontech (Palo Alto, CA).

Tetramethylrhodamine-5-maleimide (TMRM, T-6027) was obtained from Molecular Probes, Invitrogen Corp. (Carlsbad, CA). 4-Nitrophenyl α-D-galactopyranoside was obtained from Sigma-Aldrich (St. Louis, MO). All other materials were reagent grade and obtained from commercial sources.

A2 Methods

A2.1 Plasmid Construction

The *fucP* gene encoding wild-type FucP was isolated from pET21b/FucP using NcoI and HindIII restriction sites introduced by PCR at the 5' and 3' ends, respectively. The isolated *fucP* gene fragment was subcloned into the expression vector pBAD using T4 DNA ligase. The codon for Thr304 in FucP was modified from ACC to ACG in order to delete a native NcoI restriction site at this position. Plasmid pSP72/cscB was constructed as described [96]. The *fruP* gene from strain BEN2908 was amplified by PCR using a sense and antisense oligonucleotide primer with 5' and 3' overhangs containing a NcoI and a BglII restriction site, respectively. The PCR fragment was treated with NcoI and BglII and ligated to pCS19 vector.

All mutants were constructed by site-specific mutagenesis using a QuickChange II site-directed mutagenesis kit. Thirty- to 40-bp direct and reverse primers bearing the mutated triplet in the middle of the primer were designed using the Vector NTI 10 Suit program (Invitrogen, Carlsbad, CA). Mutagenic constructs were sequenced over the entire gene and through the restriction sites

to confirm the mutations introduced and to discard unwanted mutations. All constructs were engineered with a C-terminal His-tag.

A2.2 Expression Analysis

All constructs were engineered to encode the appropriate permease with a C-terminal His-tag to enable identification of protein expression by Western blot analysis. Protein concentrations were determined by Micro BCA protein assay, and their expression levels in the membrane of *E. coli* were detected by using penta-His HRP conjugated antibody and Supersignal West Pico Chemiluminescent substrate.

A2.3 Transport Assays

E. coli T184 [$lacI^{+}O^{+}Z^{-}Y^{-}(A)$, *rspL*, met^{-}, thr^{-}, *recA*, *hsdM*, *hsdR/F'* $lacI^{q}OZ^{D118}(Y^{+}A^{+})$] was transformed with the appropriate plasmids and grown aerobically overnight at 37 °C in Luria-Bertani culture medium containing 100 µg/ml of ampicillin. A ten-fold dilution of the culture was grown for 2 h before induction. Overexpression of FucP was induced with 0.02% L-arabinose and that of other permeases was induced with 1 mM IPTG. Following induction, growth was continued for further 2 h, after which the cells were harvested by centrifugation, washed with 100 mM potassium phosphate (KP_i; pH 7.0) containing 10 mM $MgSO_4$, and adjusted to an absorbance at 420 nm (A_{420}) of 15-20 (approximately 1.0-1.4 mg/ml of protein) for transport measurements. Transport was carried out at room temperature. Transport was initiated by

addition of 2 µl radiolabeled sugar to 50 µl aliquots of cells containing 50 µg of total protein and terminated by dilution followed by rapid filtration [98, 142, 143].

Rates of transport at various substrate concentrations were measured by mixing 50 µl aliquots of cells with 50 µl of radiolabeled sugars and stopped after incubation at room temperature for 1 min (CscB or FruP) or 15 sec (FucP). Total level of radioactivity was maintained constant in samples with different sugar concentrations. The rates of transport were estimated after correction for sugar uptake by cells carrying vector without permease. Data were analyzed by using the Michaelis-Menten equation and Sigmaplot 10 (Systat Software Inc., Richmond, CA).

A2.4 Preparation of right side-out (RSO) membrane vesicles

RSO membrane vesicles were prepared from 800 mL cultures of *E. coli* T184 cells expressing the appropriate permease by lysozyme-EDTA treatment and osmotic lysis [144, 145]. RSO membrane vesicles were resuspended to a protein concentration of 10–20 mg/mL in 100 mM KP_i (pH 7.5) containing 10 mM $MgSO_4$, frozen in liquid nitrogen and stored at −80°C until use.

A2.5 MIANS Labeling

The apparent affinity of purified LacY for galactosidic sugars was measured by substrate protection of Cys148 against alkylation by 2-(4'-maleimidylanilino)-naphthalene-6-sulfonic acid (MIANS) as the effect of sugar concentration on the initial rate of MIANS labeling as described previously [62,

146]. The change in fluorescence was monitored at room temperature using an SLM-Aminco (Urbana, IL) 8100 spectrofluorimiter modified by OLIS, Inc. (Bogart, GA) with excitation and emission wavelengths of 330 and 415 nm, respectively. Data fitting was conducted using Sigmaplot 10 (Systat Software Inc., Richmond, CA).

A2.6 Homology threading and tertiary structure analysis

CscB and FruP were threaded into the LacY structure by using the X-ray coordinates (PDB code: 1PV7) as a template on the web-based SWISSPROT modeling server [93, 147]. Three-dimensional structures obtained by homology threading were displayed using Pymol 1.4.

A2.7 Protein Purification

WT FucP or CscB and given mutants were purified from *E. coli* XL1-Blue cells (Stratagene, La Jolla, CA) transformed with plasmids harboring appropriate genes by using Co(II) affinity chromatography as described [148] with the following modifications. While overexpression of WT CscB and mutants were induced with 0.3 mM IPTG, that of WT FucP and mutants was induced with 0.02% L-arabinose. The urea wash step in the protocol was omitted. Proteins eluted from the Co(II)-Talon column were concentrated and washed with 50 mM sodium phosphate (NaP_i; pH 7.5)/0.01% DDM on an Amicon Ultra-15 concentrator with a 30K cut-off (Millipore, Billerica, MA). All protein preparations were at least 95% pure as judged by silver staining after SDS polyacrylamide gel

electrophoresis. Protein concentrations were determined by Micro BCA protein assay, and samples with protein concentrations at 5–10 mg/ml in 50 mM NaP_i buffer (pH 7.5)/0.01% DDM were frozen in liquid nitrogen and stored at –80°C.

A2.8 Fluorescence Measurements

Steady-state fluorescence was monitored at room temperature using SLM-Aminco 8100 spectrofluorimeter (Urbana, IL) modified by OLIS, Inc. (Bogart, GA) as described [125] with excitation and emission wavelengths at 295 nm and 310-400 nm, respectively. The purified proteins used for fluorescence measurements were adjusted to a concentration at which an approximately equal level of Trp fluorescence was observed in the absence of sugar (0.5 μM, final concentration). Titrations were recorded after sequential addition of a given sugar. Titration data were corrected for dilution. Data fitting was carried out by using SigmaPlot 10 (Systat Software Inc., Richmond, CA).

A2.9 α-NPG Binding to LacY

α-NPG binding measurements were made with an SLM-Aminco 8100 spectrofluorometer as described previously with minor modifications [125]. In a 1 cm x 1 cm cuvette, purified LacY mutant was diluted in 50mM NaP_i (pH 7.5) and 0.01% DDM to a final concentration of 1 μl in a volume of 2 ml. α-NPG was added to a given concentration, and then 30 mM (final concentration) melibiose was added to displace α-NPG. Changes in fluorescence resulting from Trp → α-α-NPG FRET were recorded while the sample was being constantly stirred and

corrected for dilution caused by addition of the ligand. Data fitting was carried out by using SigmaPlot 10 (Systat Software Inc., Richmond, CA).

A2.10 TMRM Labeling

Labeling experiments were carried out following the procedure described previously [83, 149]. RSO membrane vesicles [0.1 mg total protein in 50 µL 100 mM KP_i (pH 7.5) / 10 mM $MgSO_4$] containing WT FucP or a given Cys-replaced mutants were incubated with 40 µM TMRM in the absence or presence of 40 mM L-fucose at 0 °C. After adding 2-mercaptoethanol (40 mM, final concentration) at given times to stop the reaction, vesicles were solubilized with 1.0% DDM, diluted with 1 mL suspension buffer [50 mM NaP_i (pH 7.5), 0.2 M NaCl, 0.01% DDM, 5 mM Imidazole], and incubated with 100 µL Co(II)-Talon metal affinity resin for 20 min at room temperature. The mixture was loaded on to a mini column followed by washing with 3 mL of washing buffer [50 mM NaP_i (pH 7.5), 0.2 M NaCl, 0.01% DDM, 20 mM Imidazole] and FucP was eluted with 50 µL of elution buffer [50 mM NaP_i (pH 7.5), 0.01% DDM, 200 mM Imidazole]. Aliquots (10 µL out of 50 µL total of purified protein) were subjected to SDS-PAGE. The gels were immediately scanned by using Amersham Typhoon 9410 Workstation (λ_{ex} = 532 nm and λ_{em} = 580 nm for TMRM), and the protein bands were developed subsequently by silver staining.

References

1. Hediger, M.A., et al., *The ABCs of membrane transporters in health and disease (SLC series): introduction.* Mol Aspects Med, 2013. **34**(2-3): p. 95-107.
2. Boucher, R.C., *Evidence for airway surface dehydration as the initiating event in CF airway disease.* J Intern Med, 2007. **261**(1): p. 5-16.
3. Bichet, D.G., *Nephrogenic diabetes insipidus.* Adv Chronic Kidney Dis, 2006. **13**(2): p. 96-104.
4. Borgnia, M., et al., *Cellular and molecular biology of the aquaporin water channels.* Annu Rev Biochem, 1999. **68**: p. 425-58.
5. Hubert, J.F., et al., *Pore selectivity analysis of an aquaglyceroporin by stopped-flow spectrophotometry on bacterial cell suspensions.* Biol Cell, 2005. **97**(9): p. 675-86.
6. Pettersson, N., et al., *Aquaporins in yeasts and filamentous fungi.* Biol Cell, 2005. **97**(7): p. 487-500.
7. Borst, P. and R.O. Elferink, *Mammalian ABC transporters in health and disease.* Annu Rev Biochem, 2002. **71**: p. 537-92.
8. Dunbar, L.A. and M.J. Caplan, *The cell biology of ion pumps: sorting and regulation.* Eur J Cell Biol, 2000. **79**(8): p. 557-63.
9. Cox, D.W. and S.D. Moore, *Copper transporting P-type ATPases and human disease.* J Bioenerg Biomembr, 2002. **34**(5): p. 333-8.
10. Muller, V. and G. Gruber, *ATP synthases: structure, function and evolution of unique energy converters.* Cell Mol Life Sci, 2003. **60**(3): p. 474-94.
11. Reddy, V.S., et al., *The major facilitator superfamily (MFS) revisited.* FEBS J, 2012. **279**(11): p. 2022-35.
12. Marger, M.D. and M.H. Saier, Jr., *A major superfamily of transmembrane facilitators that catalyse uniport, symport and antiport.* Trends Biochem Sci, 1993. **18**(1): p. 13-20.
13. Pao, S.S., I.T. Paulsen, and M.H. Saier, Jr., *Major facilitator superfamily.* Microbiol Mol Biol Rev, 1998. **62**(1): p. 1-34.
14. Saier, M.H., Jr., et al., *The major facilitator superfamily.* J Mol Microbiol Biotechnol, 1999. **1**(2): p. 257-79.
15. Krzeslak, A., et al., *Expression of GLUT1 and GLUT3 glucose transporters in endometrial and breast cancers.* Pathol Oncol Res, 2012. **18**(3): p. 721-8.
16. De Vivo, D.C., et al., *Defective glucose transport across the blood-brain barrier as a cause of persistent hypoglycorrhachia, seizures, and developmental delay.* N Engl J Med, 1991. **325**(10): p. 703-9.
17. Klepper, J. and B. Leiendecker, *GLUT1 deficiency syndrome--2007 update.* Dev Med Child Neurol, 2007. **49**(9): p. 707-16.
18. Fanconi, G. and H. Bickel, *[Chronic aminoaciduria (amino acid diabetes or nephrotic-glucosuric dwarfism) in glycogen storage and cystine disease].* Helv Paediatr Acta, 1949. **4**(5): p. 359-96.

19. Santer, R., et al., *Mutations in GLUT2, the gene for the liver-type glucose transporter, in patients with Fanconi-Bickel syndrome.* Nat Genet, 1997. **17**(3): p. 324-6.
20. Santer, R., et al., *The mutation spectrum of the facilitative glucose transporter gene SLC2A2 (GLUT2) in patients with Fanconi-Bickel syndrome.* Hum Genet, 2002. **110**(1): p. 21-9.
21. Mueckler, M. and B. Thorens, *The SLC2 (GLUT) family of membrane transporters.* Mol Aspects Med, 2013. **34**(2-3): p. 121-38.
22. Radestock, S. and L.R. Forrest, *The alternating-access mechanism of MFS transporters arises from inverted-topology repeats.* J Mol Biol, 2011. **407**(5): p. 698-715.
23. Pedersen, B.P., et al., *Crystal structure of a eukaryotic phosphate transporter.* Nature, 2013. **496**(7446): p. 533-6.
24. Deng, D., et al., *Crystal structure of the human glucose transporter GLUT1.* Nature, 2014. **510**(7503): p. 121-5.
25. Parker, J.L. and S. Newstead, *Molecular basis of nitrate uptake by the plant nitrate transporter NRT1.1.* Nature, 2014. **507**(7490): p. 68-72.
26. Sun, J., et al., *Crystal structure of the plant dual-affinity nitrate transporter NRT1.1.* Nature, 2014. **507**(7490): p. 73-7.
27. Yan, N., *Structural Biology of the Major Facilitator Superfamily Transporters.* Annu Rev Biophys, 2015. **44**: p. 257-83.
28. Juers, D.H., B.W. Matthews, and R.E. Huber, *LacZ beta-galactosidase: structure and function of an enzyme of historical and molecular biological importance.* Protein Sci, 2012. **21**(12): p. 1792-807.
29. Roderick, S.L., *The lac operon galactoside acetyltransferase.* C R Biol, 2005. **328**(6): p. 568-75.
30. Teather, R.M., et al., *Amplification of the lactose carrier protein in Escherichia coli using a plasmid vector.* Mol Gen Genet, 1978. **159**(3): p. 239-48.
31. Buchel, D.E., B. Gronenborn, and B. Muller-Hill, *Sequence of the lactose permease gene.* Nature, 1980. **283**(5747): p. 541-5.
32. Newman, M.J. and T.H. Wilson, *Solubilization and reconstitution of the lactose transport system from Escherichia coli.* J Biol Chem, 1980. **255**(22): p. 10583-6.
33. Newman, M.J., et al., *Purification and reconstitution of functional lactose carrier from Escherichia coli.* J Biol Chem, 1981. **256**(22): p. 11804-8.
34. Foster, D.L., et al., *Lactose-proton symport by purified lac carrier protein.* Biochemistry, 1982. **21**(22): p. 5634-8.
35. Viitanen, P., M.L. Garcia, and H.R. Kaback, *Purified reconstituted lac carrier protein from Escherichia coli is fully functional.* Proc Natl Acad Sci U S A, 1984. **81**(6): p. 1629-33.
36. Viitanen, P., et al., *Purification, reconstitution, and characterization of the lac permease of Escherichia coli.* Methods Enzymol, 1986. **125**: p. 429-52.
37. Abramson, J., et al., *Structure and mechanism of the lactose permease of Escherichia coli.* Science, 2003. **301**(5633): p. 610-5.

38. Mitchell, P., *Chemiosmotic coupling in oxidative and photosynthetic phosphorylation.* Biol Rev Camb Philos Soc, 1966. **41**(3): p. 445-502.
39. Mitchell, P., *Translocations through natural membranes.* Adv Enzymol Relat Areas Mol Biol, 1967. **29**: p. 33-87.
40. Mitchell, P. and J. Moyle, *Chemiosmotic hypothesis of oxidative phosphorylation.* Nature, 1967. **213**(5072): p. 137-9.
41. Mitchell, P., *Performance and conservation of osmotic work by proton-coupled solute porter systems.* J Bioenerg, 1973. **4**(1): p. 63-91.
42. Sahin-Toth, M., M.C. Lawrence, and H.R. Kaback, *Properties of permease dimer, a fusion protein containing two lactose permease molecules from Escherichia coli.* Proc Natl Acad Sci U S A, 1994. **91**(12): p. 5421-5.
43. Kaback, H.R., *A chemiosmotic mechanism of symport.* Proc Natl Acad Sci U S A, 2015. **112**(5): p. 1259-64.
44. Kaczorowski, G.J. and H.R. Kaback, *Mechanism of lactose translocation in membrane vesicles from Escherichia coli. 1. Effect of pH on efflux, exchange, and counterflow.* Biochemistry, 1979. **18**(17): p. 3691-7.
45. Kaczorowski, G.J., D.E. Robertson, and H.R. Kaback, *Mechanism of lactose translocation in membrane vesicles from Escherichia coli. 2. Effect of imposed delata psi, delta pH, and Delta mu H+.* Biochemistry, 1979. **18**(17): p. 3697-704.
46. Calamia, J. and C. Manoil, *lac permease of Escherichia coli: topology and sequence elements promoting membrane insertion.* Proc Natl Acad Sci U S A, 1990. **87**(13): p. 4937-41.
47. Mirza, O., et al., *Structural evidence for induced fit and a mechanism for sugar/H+ symport in LacY.* The EMBO journal, 2006. **25**(6): p. 1177-83.
48. Guan, L., et al., *Structural determination of wild-type lactose permease.* Proc Natl Acad Sci U S A, 2007. **104**(39): p. 15294-8.
49. Chaptal, V., et al., *Crystal structure of lactose permease in complex with an affinity inactivator yields unique insight into sugar recognition.* Proc Natl Acad Sci U S A, 2011. **108**(23): p. 9361-6.
50. Frillingos, S., et al., *Cys-scanning mutagenesis: a novel approach to structure function relationships in polytopic membrane proteins.* FASEB J, 1998. **12**(13): p. 1281-99.
51. Guan, L., Y. Hu, and H.R. Kaback, *Aromatic stacking in the sugar binding site of the lactose permease.* Biochemistry, 2003. **42**(6): p. 1377-82.
52. Jiang, X., et al., *Galactoside-binding site in LacY.* Biochemistry, 2014. **53**(9): p. 1536-43.
53. Roepe, P.D. and H.R. Kaback, *Site-directed mutagenesis of tyrosine residues in the lac permease of Escherichia coli.* Biochemistry, 1989. **28**(14): p. 6127-32.
54. Sandermann, H., Jr., *beta-D-Galactoside transport in Escherichia coli: substrate recognition.* European journal of biochemistry / FEBS, 1977. **80**(2): p. 507-15.
55. Olsen, S.G. and R.J. Brooker, *Analysis of the structural specificity of the lactose permease toward sugars.* The Journal of biological chemistry, 1989. **264**(27): p. 15982-7.

56. Wu, J. and H.R. Kaback, *Cysteine 148 in the lactose permease of Escherichia coli is a component of a substrate binding site. 2. Site-directed fluorescence studies.* Biochemistry, 1994. **33**(40): p. 12166-71.
57. Sahin-Toth, M., et al., *The C-4 hydroxyl group of galactopyranosides is the major determinant for ligand recognition by the lactose permease of Escherichia coli.* Biochemistry, 2001. **40**(43): p. 13015-9.
58. Kumar, H., et al., *Structure of sugar-bound LacY.* Proc Natl Acad Sci U S A, 2014. **111**(5): p. 1784-8.
59. Kumar, H., et al., *Structure of LacY with an alpha-substituted galactoside: Connecting the binding site to the protonation site.* Proc Natl Acad Sci U S A, 2015. **112**(29): p. 9004-9.
60. Carrasco, N., et al., *lac permease of Escherichia coli: histidine-322 and glutamic acid-325 may be components of a charge-relay system.* Biochemistry, 1986. **25**(16): p. 4486-8.
61. Carrasco, N., et al., *Characterization of site-directed mutants in the lac permease of Escherichia coli. 2. Glutamate-325 replacements.* Biochemistry, 1989. **28**(6): p. 2533-9.
62. Smirnova, I.N., V. Kasho, and H.R. Kaback, *Protonation and sugar binding to LacY.* Proc Natl Acad Sci U S A, 2008. **105**(26): p. 8896-901.
63. Smirnova, I., et al., *Residues in the H+ translocation site define the pKa for sugar binding to LacY.* Biochemistry, 2009. **48**(37): p. 8852-60.
64. Smirnova, I., et al., *Role of protons in sugar binding to LacY.* Proc Natl Acad Sci U S A, 2012. **109**(42): p. 16835-40.
65. le Coutre, J., et al., *Fourier transform infrared spectroscopy reveals a rigid alpha-helical assembly for the tetrameric Streptomyces lividans K+ channel.* Proc Natl Acad Sci U S A, 1998. **95**(11): p. 6114-7.
66. Patzlaff, J.S., et al., *Fourier transform infrared analysis of purified lactose permease: a monodisperse lactose permease preparation is stably folded, alpha-helical, and highly accessible to deuterium exchange.* Biochemistry, 1998. **37**(44): p. 15363-75.
67. Sayeed, W.M. and J.E. Baenziger, *Structural characterization of the osmosensor ProP.* Biochim Biophys Acta, 2009. **1788**(5): p. 1108-15.
68. Nie, Y., et al., *Energetics of ligand-induced conformational flexibility in the lactose permease of Escherichia coli.* The Journal of biological chemistry, 2006. **281**(47): p. 35779-84.
69. Smirnova, I., V. Kasho, and H.R. Kaback, *Lactose permease and the alternating access mechanism.* Biochemistry, 2011. **50**(45): p. 9684-93.
70. Wu, J. and H.R. Kaback, *A general method for determining helix packing in membrane proteins in situ: helices I and II are close to helix VII in the lactose permease of Escherichia coli.* Proc Natl Acad Sci U S A, 1996. **93**(25): p. 14498-502.
71. Wu, J. and H.R. Kaback, *Helix proximity and ligand-induced conformational changes in the lactose permease of Escherichia coli determined by site-directed chemical crosslinking.* J Mol Biol, 1997. **270**(2): p. 285-93.

72. Wu, J., D. Hardy, and H.R. Kaback, *Tilting of helix I and ligand-induced changes in the lactose permease determined by site-directed chemical cross-linking in situ.* Biochemistry, 1998. **37**(45): p. 15785-90.
73. Wu, J., D. Hardy, and H.R. Kaback, *Transmembrane helix tilting and ligand-induced conformational changes in the lactose permease determined by site-directed chemical crosslinking in situ.* J Mol Biol, 1998. **282**(5): p. 959-67.
74. Wu, J., D. Hardy, and H.R. Kaback, *Tertiary contacts of helix V in the lactose permease determined by site-directed chemical cross-linking in situ.* Biochemistry, 1999. **38**(8): p. 2320-5.
75. Wu, J., D. Hardy, and H.R. Kaback, *Site-directed chemical cross-linking demonstrates that helix IV is close to helices VII and XI in the lactose permease.* Biochemistry, 1999. **38**(6): p. 1715-20.
76. Sorgen, P.L., et al., *An approach to membrane protein structure without crystals.* Proc Natl Acad Sci U S A, 2002. **99**(22): p. 14037-40.
77. Zhou, Y., et al., *Opening and closing of the periplasmic gate in lactose permease.* Proc Natl Acad Sci U S A, 2008. **105**(10): p. 3774-8.
78. Kaback, H.R., et al., *Site-directed alkylation and the alternating access model for LacY.* Proc Natl Acad Sci U S A, 2007. **104**(2): p. 491-4.
79. Nie, Y., N. Ermolova, and H.R. Kaback, *Site-directed alkylation of LacY: effect of the proton electrochemical gradient.* J Mol Biol, 2007. **374**(2): p. 356-64.
80. Nie, Y., F.E. Sabetfard, and H.R. Kaback, *The Cys154-->Gly mutation in LacY causes constitutive opening of the hydrophilic periplasmic pathway.* J Mol Biol, 2008. **379**(4): p. 695-703.
81. Nie, Y., Y. Zhou, and H.R. Kaback, *Clogging the periplasmic pathway in LacY.* Biochemistry, 2009. **48**(4): p. 738-43.
82. Zhou, Y., Y. Nie, and H.R. Kaback, *Residues gating the periplasmic pathway of LacY.* J Mol Biol, 2009. **394**(2): p. 219-25.
83. Nie, Y. and H.R. Kaback, *Sugar binding induces the same global conformational change in purified LacY as in the native bacterial membrane.* Proc Natl Acad Sci U S A, 2010. **107**(21): p. 9903-8.
84. Majumdar, D.S., et al., *Single-molecule FRET reveals sugar-induced conformational dynamics in LacY.* Proc Natl Acad Sci U S A, 2007. **104**(31): p. 12640-5.
85. Smirnova, I., et al., *Sugar binding induces an outward facing conformation of LacY.* Proc Natl Acad Sci U S A, 2007. **104**(42): p. 16504-9.
86. Smirnova, I., et al., *Opening the periplasmic cavity in lactose permease is the limiting step for sugar binding.* Proc Natl Acad Sci U S A, 2011. **108**(37): p. 15147-51.
87. Smirnova, I., V. Kasho, and H.R. Kaback, *Real-time conformational changes in LacY.* Proc Natl Acad Sci U S A, 2014. **111**(23): p. 8440-5.
88. Smirnova, I., et al., *Probing of the rates of alternating access in LacY with Trp fluorescence.* Proc Natl Acad Sci U S A, 2009. **106**(51): p. 21561-6.
89. Sun, L., et al., *Crystal structure of a bacterial homologue of glucose transporters GLUT1-4.* Nature, 2012. **490**(7420): p. 361-6.

90. Quistgaard, E.M., et al., *Structural basis for substrate transport in the GLUT-homology family of monosaccharide transporters.* Nat Struct Mol Biol, 2013. **20**(6): p. 766-8.
91. Dang, S., et al., *Structure of a fucose transporter in an outward-open conformation.* Nature, 2010. **467**(7316): p. 734-8.
92. Saier, M.H., Jr., *Families of transmembrane sugar transport proteins.* Mol Microbiol, 2000. **35**(4): p. 699-710.
93. Kasho, V.N., I.N. Smirnova, and H.R. Kaback, *Sequence alignment and homology threading reveals prokaryotic and eukaryotic proteins similar to lactose permease.* Journal of molecular biology, 2006. **358**(4): p. 1060-70.
94. Vadyvaloo, V., et al., *Conservation of residues involved in sugar/H(+) symport by the sucrose permease of Escherichia coli relative to lactose permease.* J Mol Biol, 2006. **358**(4): p. 1051-9.
95. Bockmann, J., H. Heuel, and J.W. Lengeler, *Characterization of a chromosomally encoded, non-PTS metabolic pathway for sucrose utilization in Escherichia coli EC3132.* Mol Gen Genet, 1992. **235**(1): p. 22-32.
96. Sahin-Toth, M., et al., *Active transport by the CscB permease in Escherichia coli K-12.* Biochem Biophys Res Commun, 1995. **208**(3): p. 1116-23.
97. Tavoulari, S. and S. Frillingos, *Substrate selectivity of the melibiose permease (MelY) from Enterobacter cloacae.* J Mol Biol, 2008. **376**(3): p. 681-93.
98. Sahin-Toth, M., et al., *The sucrose permease of Escherichia coli: functional significance of cysteine residues and properties of a cysteine-less transporter.* Biochemistry, 2000. **39**(20): p. 6164-9.
99. Sahin-Toth, M. and H.R. Kaback, *Functional conservation in the putative substrate binding site of the sucrose permease from Escherichia coli.* Biochemistry, 2000. **39**(20): p. 6170-5.
100. Robertson, D.E., et al., *Active transport in membrane vesicles from Escherichia coli: the electrochemical proton gradient alters the distribution of the lac carrier between two different kinetic states.* Biochemistry, 1980. **19**(25): p. 5692-702.
101. Sahin-Toth, M., et al., *Ligand recognition by the lactose permease of Escherichia coli: specificity and affinity are defined by distinct structural elements of galactopyranosides.* Biochemistry, 2000. **39**(17): p. 5097-103.
102. Merritt, E.A., et al., *Structural foundation for the design of receptor antagonists targeting Escherichia coli heat-labile enterotoxin.* Structure, 1997. **5**(11): p. 1485-99.
103. Chiou, C.Y., H.H. Wang, and G.C. Shaw, *Identification and characterization of the non-PTS fru locus of Bacillus megaterium ATCC 14581.* Mol Genet Genomics, 2002. **268**(2): p. 240-8.
104. Guan, L. and H.R. Kaback, *Lessons from lactose permease.* Annual review of biophysics and biomolecular structure, 2006. **35**: p. 67-91.
105. Frillingos, S., A. Gonzalez, and H.R. Kaback, *Cysteine-scanning mutagenesis of helix IV and the adjoining loops in the lactose permease of*

Escherichia coli: Glu126 and Arg144 are essential. off. Biochemistry, 1997. **36**(47): p. 14284-90.
106. Venkatesan, P. and H.R. Kaback, *The substrate-binding site in the lactose permease of Escherichia coli.* Proc Natl Acad Sci U S A, 1998. **95**(17): p. 9802-7.
107. Sahin-Toth, M., et al., *Characterization of Glu126 and Arg144, two residues that are indispensable for substrate binding in the lactose permease of Escherichia coli.* Biochemistry, 1999. **38**(2): p. 813-9.
108. Wolin, C.D. and H.R. Kaback, *Thiol cross-linking of transmembrane domains IV and V in the lactose permease of Escherichia coli.* Biochemistry, 2000. **39**(20): p. 6130-5.
109. Franco, P.J. and R.J. Brooker, *Functional roles of Glu-269 and Glu-325 within the lactose permease of Escherichia coli.* J Biol Chem, 1994. **269**(10): p. 7379-86.
110. Ujwal, M.L., et al., *Role of glutamate-269 in the lactose permease of Escherichia coli.* Mol Membr Biol, 1994. **11**(1): p. 9-16.
111. Weinglass, A.B., M. Sondej, and H.R. Kaback, *Manipulating conformational equilibria in the lactose permease of Escherichia coli.* J Mol Biol, 2002. **315**(4): p. 561-71.
112. Vazquez-Ibar, J.L., et al., *Exploiting luminescence spectroscopy to elucidate the interaction between sugar and a tryptophan residue in the lactose permease of Escherichia coli.* Proc Natl Acad Sci U S A, 2003. **100**(22): p. 12706-11.
113. Becker, D.J. and J.B. Lowe, *Fucose: biosynthesis and biological function in mammals.* Glycobiology, 2003. **13**(7): p. 41R-53R.
114. Staudacher, E., et al., *Fucose in N-glycans: from plant to man.* Biochim Biophys Acta, 1999. **1473**(1): p. 216-36.
115. Eagon, R.G., *Bacterial dissimilation of L-fucose and L-rhamnose.* J Bacteriol, 1961. **82**: p. 548-50.
116. Ma, B., J.L. Simala-Grant, and D.E. Taylor, *Fucosylation in prokaryotes and eukaryotes.* Glycobiology, 2006. **16**(12): p. 158R-184R.
117. Bradley, S.A., et al., *Proton-linked L-fucose transport in Escherichia coli.* Biochem J, 1987. **248**(2): p. 495-500.
118. Chen, Y.M., Y. Zhu, and E.C. Lin, *The organization of the fuc regulon specifying L-fucose dissimilation in Escherichia coli K12 as determined by gene cloning.* Mol Gen Genet, 1987. **210**(2): p. 331-7.
119. Lu, Z. and E.C. Lin, *The nucleotide sequence of Escherichia coli genes for L-fucose dissimilation.* Nucleic Acids Res, 1989. **17**(12): p. 4883-4.
120. Gunn, F.J., C.G. Tate, and P.J. Henderson, *Identification of a novel sugar-H+ symport protein, FucP, for transport of L-fucose into Escherichia coli.* Mol Microbiol, 1994. **12**(5): p. 799-809.
121. Gunn, F.J., et al., *Topological analyses of the L-fucose-H+ symport protein, FucP, from Escherichia coli.* Mol Microbiol, 1995. **15**(4): p. 771-83.
122. Rath, A., et al., *Detergent binding explains anomalous SDS-PAGE migration of membrane proteins.* Proc Natl Acad Sci U S A, 2009. **106**(6): p. 1760-5.

123. Smirnova, I., et al., *Trp replacements for tightly interacting Gly-Gly pairs in LacY stabilize an outward-facing conformation.* Proc Natl Acad Sci U S A, 2013. **110**(22): p. 8876-81.
124. Weinglass, A.B., et al., *Elucidation of substrate binding interactions in a membrane transport protein by mass spectrometry.* EMBO J, 2003. **22**(7): p. 1467-77.
125. Smirnova, I.N., V.N. Kasho, and H.R. Kaback, *Direct sugar binding to LacY measured by resonance energy transfer.* Biochemistry, 2006. **45**(51): p. 15279-87.
126. White, S.H. and W.C. Wimley, *Membrane protein folding and stability: physical principles.* Annu Rev Biophys Biomol Struct, 1999. **28**: p. 319-65.
127. Muiry, J.A., et al., *Proton-linked L-rhamnose transport, and its comparison with L-fucose transport in Enterobacteriaceae.* Biochem J, 1993. **290 (Pt 3)**: p. 833-42.
128. Kaback, H.R., M. Sahin-Toth, and A.B. Weinglass, *The kamikaze approach to membrane transport.* Nat Rev Mol Cell Biol, 2001. **2**(8): p. 610-20.
129. Garcia-Celma, J.J., et al., *Electrophysiological characterization of LacY.* Proc Natl Acad Sci U S A, 2009. **106**(18): p. 7373-8.
130. Garcia-Celma, J.J., et al., *Delineating electrogenic reactions during lactose/H+ symport.* Biochemistry, 2010. **49**(29): p. 6115-21.
131. Jiang, X., et al., *Evidence for an intermediate conformational state of LacY.* Proc Natl Acad Sci U S A, 2012. **109**(12): p. E698-704.
132. Carruthers, A. and D.L. Melchior, *Human erythrocyte hexose transporter activity is governed by bilayer lipid composition in reconstituted vesicles.* Biochemistry, 1984. **23**(26): p. 6901-11.
133. Curtis, B.M. and W.A. Catterall, *Purification of the calcium antagonist receptor of the voltage-sensitive calcium channel from skeletal muscle transverse tubules.* Biochemistry, 1984. **23**(10): p. 2113-8.
134. Schmidt, D., Q.X. Jiang, and R. MacKinnon, *Phospholipids and the origin of cationic gating charges in voltage sensors.* Nature, 2006. **444**(7120): p. 775-9.
135. Schmidt, D., S.R. Cross, and R. MacKinnon, *A gating model for the archeal voltage-dependent K(+) channel KvAP in DPhPC and POPE:POPG decane lipid bilayers.* J Mol Biol, 2009. **390**(5): p. 902-12.
136. Bogdanov, M. and W. Dowhan, *Lipid-dependent generation of dual topology for a membrane protein.* J Biol Chem, 2012. **287**(45): p. 37939-48.
137. Bogdanov, M. and W. Dowhan, *Phosphatidylethanolamine is required for in vivo function of the membrane-associated lactose permease of Escherichia coli.* J Biol Chem, 1995. **270**(2): p. 732-9.
138. Bogdanov, M., et al., *A phospholipid acts as a chaperone in assembly of a membrane transport protein.* J Biol Chem, 1996. **271**(20): p. 11615-8.
139. Vitrac, H., M. Bogdanov, and W. Dowhan, *Proper fatty acid composition rather than an ionizable lipid amine is required for full transport function of*

lactose permease from Escherichia coli. J Biol Chem, 2013. **288**(8): p. 5873-85.
140. Fox, C.F. and E.P. Kennedy, *Specific labeling and partial purification of the M protein, a component of the beta-galactoside transport system of Escherichia coli.* Proc Natl Acad Sci U S A, 1965. **54**(3): p. 891-9.
141. Bieseler, B., H. Prinz, and K. Beyreuther, *Topological studies of lactose permease of Escherichia coli by protein sequence analysis.* Ann N Y Acad Sci, 1985. **456**: p. 309-25.
142. Kaback, H.R., *Transport in isolated bacterial membrane vesicles.* Methods Enzymol, 1974. **31**: p. 698-709.
143. Consler, T.G., O. Tsolas, and H.R. Kaback, *Role of proline residues in the structure and function of a membrane transport protein.* Biochemistry, 1991. **30**(5): p. 1291-8.
144. Short, S.A., H.R. Kaback, and L.D. Kohn, *Localization of D-lactate dehydrogenase in native and reconstituted Escherichia coli membrane vesicles.* J Biol Chem, 1975. **250**(11): p. 4291-6.
145. Kaback, H.R., *Bacterial Membranes*, in *Methods in Enzymol*, N.P. Kaplan, W.B. Jakoby, and N.P. Colowick, Editors. 1971, Elsevier: New York. p. 99-120.
146. Wu, J., et al., *Ligand-induced conformational changes in the lactose permease of Escherichia coli: evidence for two binding sites.* Protein science : a publication of the Protein Society, 1994. **3**(12): p. 2294-301.
147. Schwede, T., et al., *SWISS-MODEL: An automated protein homology-modeling server.* Nucleic Acids Res, 2003. **31**(13): p. 3381-5.
148. Ermolova, N.V., et al., *Interhelical packing modulates conformational flexibility in the lactose permease of Escherichia coli.* Biochemistry, 2005. **44**(21): p. 7669-77.
149. Jiang, X., Y. Nie, and H.R. Kaback, *Site-directed alkylation studies with LacY provide evidence for the alternating access model of transport.* Biochemistry, 2011. **50**(10): p. 1634-40.